COMPARATIVE BONE HISTOLOGY OF *STIGMOCHELYS PARDALIS* (LEOPARD TORTOISE), WITH SPECIFIC REFERENCE TO ONTOGENY AND BIOMECHANICS.

By

ALEXANDER EDWARD BOTHA

Submitted in fulfilment of the requirements for the degree

MAGISTER SCIENTIAE (ZOOLOGY)

In the Faculty of Natural and Agricultural Sciences

Department of Zoology and Entomology

University of the Free State

Bloemfontein

Supervisor: Dr Jennifer Botha-Brink

January 2017

DECLARATION

I, the undersigned, hereby declare that the work contained in this dissertation is my own original wok and that I have not previously in its entirety or in part submitted it at any university for a degree. I further more cede copyright of the dissertation in favour of the University of the Free State.

Signature:…….

Date:…….

LIST OF FIGURES

LIST OF TABLES

ABSTRACT

Testudines are a group of reptiles characterised by the presence of a shell comprised of bony shields. *Stigmochelys pardalis* is the most widely distributed terrestrial testudine in southern Africa. Although relatively common with some life history traits (e.g. lifestyle, reproduction, longevity) being well known, the growth of this species has yet to be studied in any detail. This study is the first to use bone histology and microanatomy to examine the growth and biomechanics in an ontogenetic series of *S.pardalis.* The study also indicates clear short-comings in the determination of lifestyle using a single section on the diaphysis in *S. pardalis* and possibly in other testudines.

The bone microanatomy of this clade differs from that found in other amniotes. In other amniotes, aquatic species tend to display large osteoporotic bone with large infilled medullary cavities and thin cortices. Semi-aquatic species have thick bone walls with small or no medullary cavities whereas terrestrial species tend to have thinner bone walls, open medullary cavities and a sharp transition from cancellous to compact bone.

A detailed histological analysis of the limb bones of *S.pardalis* reveals extensive variation through ontogeny. Cortical bone becomes increasingly thicker through ontogeny and is finally resorbed in the late sub-adult stage, resulting in a thin cortex and a large infilled medullary cavity. The predominant bone tissues are parallel-fibred and lamellar-zonal for forelimb and hind limbs respectively. In certain cases parallel fibred bone tissue transitions to lamellar-zonal bone tissue later in ontogeny. A few older individuals exhibit and External Fundamental System indicating that the growth rate had decreased substantially by this stage. However, these individuals are between 56% and 60% maximum known size indicating that this slow growing species takes many more years to reach its maximum body size.

Inter-elemental variability is most prevalent between the forelimb and hind limb. Forelimb elements exhibit characteristics such as faster growing parallel-fibred bone tissue, slightly higher vascularisation and a predominance of annuli over Lines of Arrested Growth compared to the hind limb which exhibits poorly vascularised, slower growing lamellar zonal-bone interrupted by LAGs. These differences indicate that the forelimb grew more rapidly than the hind limb, possibly due to the method of locomotion typical in chelonians.

Lifestyle inferences using Bone Profiler indicate an aquatic lifestyle for this species despite it being clearly terrestrial. Sections from individuals of various ontogenetic stages were tested and although the microanatomy of the bone changes dramatically with age, the lifestyle readings remained inaccurate. The extensive bone resorption that occurs from the early sub-adult stage destroys much of the primary cortex, thus destroying the ecological signal. This supports the results from other studies that have found that using bone microanatomy to determine lifestyle in testudines is inaccurate.

ACKNOWLEDGEMENTS

I thank my supervisor, Dr Jennifer Botha-Brink for her tireless assistance, advice and guidance, without her this project would not have been possible.

I would like to thank to thank the Mammology Department and the Karoo Vertebrate Palaeontology at the National Museum, Bloemfontein for the use of their facilities and equipment. I am thankful for the material supplied by Dr Jackie Codron and Sharon Stone.

I am indebted to Bobby Eloff for her constant assistance with the practical aspect of the project.

I am grateful to the Council and Director of the National Museum, Bloemfontein for their support of the study and the National Research foundation for their funding of this project as well as the University of the Free State for the use of their facilities.

I would in particular like to thank my mom and dad for their support during these two years and always believing in me and my ambitions. I would also like to thank my friends for their encouragement and in particular Gerhard de Jager, for his moral support and guidance.

TABLE OF CONTENTS

1. INTRODUCTION

Background

General information and classification

Testudines (Chelonia) are one of the oldest living groups of reptiles. The clade falls within Reptilia and is comprised of three subgroups, namely tortoises, terrapins and turtles (Schmidt & Inger 1957). These sub-groups are further divided according to a number of different features including morphological characteristics, reproduction, feeding behaviour and distribution although all, to some extent, have a protective encasing, formed from interlocking plates that act as armour (Rose 1950).

Testudines have several features that separate them from other groups within Reptilia including a shell covered with horny shields, distinct digits with four or five claws and pectoral shields separated from the marginal bones by infra-marginals. Within Testudines, various characteristics separate the families and allow for easier practical identification of individuals (See Table 1 for classification of focus species). Although no longer used frequently in classification studies, Testudines' are also classified as anapsid reptiles, i.e. the absence of any temporal fenestrae in the skull. This feature is another characteristic that separates Testudines' from other extant reptiles (and birds) that are classified as diapsids based on the presence of two temporal fenestrae in the skull (Zardoya & Meyer 2001).

Table 1: Taxonomic classification of *Stigmochelys pardalis*.

Kingdom:	Animalia
Phylum:	Chordata
Class:	Reptilia
Order:	Testudines/Chelonia
Family:	Testudinidae
Genus:	*Stigmochelys* (Formerly *Geochelone*)
Species:	*pardalis*

Biology and ecology

South Africa contains the highest diversity of land tortoises in the world (Testudinidae) (Branch 1998; McMaster & Downs 2006; Daniels *et al.* 2010) and despite being listed under the IUCN Appendix II list (McMaster & Downs 2009), little research has been done on the biology of this group. Several studies have examined the molecular systematics (Daniels *et al.* 2010), ecology (Branch 1984; McMaster 2001; McMaster & Downs 2006), biomechanics (Erickson *et al.* 2002), vision (Simang *et al.* 2010) and evolutionary history (Lyson *et al*. 2010; Lyson *et al*. 2011; Lyson *et al*. 2013) of this group. Furthermore, given their longevity, ontogenetic and reproductive studies are also limited. This is problematic because this information is important in the understanding the ontogeny, demography, adaptive and evolutionary processes within a group or singular organism (Castanet 1994). Moreover, the use of captive specimens (Patterson *et al.* 1989) may negatively impact results because the lack of environmental fluctuations in an artificial environment influences the ecology, physiology and various behavioural mechanisms of the animal (Seebacher *et al.* 2004; McMaster Downs 2006). Captive specimens may even reach sexual maturity faster and grow to maximum size more quickly than wild individuals (Furrer *et al*. 2004), suggesting that the conditions under which organisms are studied influences their metabolic activity.

However, despite various constraints, information regarding the southern African leopard tortoise *S. pardalis*, has been successfully been collected in several studies that reveal important information ranging from habitat and ecology to reproductive maturity and longevity. This makes it an ideal species for testing theories related to testudine growth.

Stigmochelys pardalis is the most widely distributed species of tortoise in southern Africa (Fritz *et al.* 2010). Its distribution ranges from southern to eastern Africa (McMaster & Downs 2006) and it occupies various habitats including arid, semi-arid, grassland, savannah, tropical woodland (Boycott and Bourquin 2000; McMaster & Downs 2006) and valley thicket (Mason & Weatherby 1995). Within this wide distribution there exists different shell shapes, colour-morphs and patterns (Fritz *et al.* 2010), body sizes (McMaster & Downs 2009; Fritz *et al.* 2010), population densities (McMaster & Downs 2009), gender ratios (McMaster & Downs 2006) and food preferences (Simang *et al.* 2010).

The leopard tortoise, like most other reptiles is oviparous. The number, size and shape of the eggs differ between species. According to Orenstein (2012), leopard tortoises lay approximately five clutches per nesting season with roughly 10 to 12 eggs per clutch. Tortoises lay eggs all year round and are buried in a hole, covered in sand and in certain cases the mother will flatten the soil above the hole by raising herself above the area as high as possible and dropping herself until the soil is flat. Developing eggs are protected for 12 to 14 months and will only emerge when rain comes into contact with them (Rose 1950). Environmental conditions influence the sex of the offspring and (with some exceptions) females are formed at higher temperatures and males at lower temperatures (Miller & Fowler 2015). Individuals reach sexual maturity within approximately 15 years and may live as long as 75 years (Orenstein 2012).

Challenges in turtle bone microanatomy

The internal architecture of bones, or bone microanatomy, varies with changes in ontogeny, ecology and biomechanics and may provide insight into the relationship between an element's internal structure and an animal's lifestyle. In order to assess differences in bone microanatomy in vertebrates with diverse lifestyles, various features such as thickness of the compact bone wall (cortex), structure of the bony trabeculae in and around the medullary cavity and ratio between compact and spongy bone, must be examined.

Laurin has been the most prominent researcher in studying the bone microanatomy of various amphibian and amniote limb bones (e.g. Germain & Laurin 2005; Kriloff *et al*. 2008; Canoville & Laurin 2009; Laurin *et al*. 2011). Results generally show that the bones of animals with an aquatic pelagic lifestyle (e.g. dolphins, whales) have osteoporotic bones that comprise mostly spongy bone with a gradual transition from the medullary cavity to outer cortex. The medullary cavity is generally completely infilled by bone trabeculae (spongy bone). This is thought to improve diving capabilities by decreasing the weight of the bones. In contrast, species that live in shallow water (e.g. manatees) tend to have pachyostotic bones that are highly compact and have no or tiny medullary cavities. These features are thought to aid in counter-acting buoyancy while in the water. Terrestrial animals tend to have thinner bone walls compared to aquatic species, clear medullary cavities and a sharp transition from medullary cavity to cortex. However, Laurin and colleagues found that Testudines do not always follow these patterns, but instead, contradict the pattern found in other

amniotes. Freshwater aquatic Testudines' tend to exhibit more compact bone, marine aquatic species tend to exhibit large regions of spongy bone (in some cases to the extent where the cortical bone cannot be distinguished) whereas terrestrial species have smaller medullary cavities with a large proportion of compact cortical bone (Laurin *et al*. 2011).

Laurin and colleagues standardize their method by comparing the mid-diaphysis of the limb bones of sub-adult or fully grown individuals (Germain & Laurin 2005). This region is generally the most appropriate as it should exhibit the strongest ecological signal because it preserves the thickest compact cortex and least secondary remodelling. Secondary remodelling is a process that alters the thickness of the bone wall via resorption and redeposition of bone. A potential problem with this method is that the mid-diaphysis is assumed to represent the thickest part of the mid-shaft and this may not always be the case. In a study by Nakajima *et al*. (2014) on the compactness of turtle humeri, it became clear that the growth centre (the point from where bone growth originates) and thus, thickest compact cortex, is not necessarily located in the mid-point of the diaphysis in Testudines. The growth centre shifts as the organism develops.

Moreover, Testudines experience a distinctive limb bone loading during terrestrial locomotion due to the orientation of bending and high degree of torsion (twisting) (Butcher & Blob 2008). Limb bone loads might be expected to be low in terrestrial Testudines because of their slow walking speed, but the orientation of the limb in a sprawling position increases the loading. The most noteworthy feature of turtle limb bones is the oddly shaped humerus, which experiences a remarkably high degree of torsion. This feature changes the mechanical property of the bone and influences the microanatomy of the element, thus potentially affecting data used to predict lifestyle.

To date, no study has tested the viability of using the mid-diaphysis in terrestrial Testudines to assess lifestyle, nor the effect of ontogeny on the microanatomy of the limb bones. Given their distinctive locomotion and failure of the microanatomy to fall within the pattern of other terrestrial amniotes, these factors should be assessed to test the validity of the findings obtained in previous studies.

Skeletochronology and histological analysis

Skeletochronology is a technique used to determine the age of vertebrates using histological information gathered from long bones (Klein *et al*. 2009). This technique has been used in numerous studies (e.g.: de Buffrènil & Castanet 2000; Guarino *et al*. 2003; Misawa & Matsui 2009; Chinsamy & Valenzuela 2008) and involves counting the number of growth marks to determine the developmental age of an organism (Klein *et al*. 2009). These marks are referred to as annuli or Lines of Arrested Growth (LAGs) and are located in the compact bone. However, these rings are influenced by bone remodelling during growth, bone plasticity and inconsistent deposition of bone. The deposition of LAGs is also not constant. Padian *et al.* (2004) suggested that juvenile turtles do not always display annual LAGs. Furthermore, disease may result in the deposition of two LAGs in a single year (Klein *et al*. 2009) and Tucker (1997) suggested that egg laying females exhibit increased bone remodelling which destroys the growth rings. Furthermore, Klein *et al* (2009) suggested that female osteoderms act as calcium stores during oogenesis which could result in difficulties when counting growth marks.

Histological analysis is a complicated process that requires the use of specialised equipment to determine various characteristics of bone including morphology, cell structure, bone matrix type and arrangement of various cells within the matrix (An & Martin 2003). These characteristics include a variety of different aspects of the bone tissue but for this study will include the following:

Cortical thickness and medullary cavity analysis: The relationship between cancellous and compact bone and how changes through ontogeny influence this relationship.

Bone matrix analysis: The type and structure of bone matrices and how they differ between elements and through ontogeny.

Vascular canals analysis: The orientation, size, arrangement, placement and quantity of the vascular canals in the primary cortex and how these features differ between elements and ontogenetic stages. .

Secondary osteon and resorption cavity analysis: The size, quantity, position and influence of secondary osteons between elements and different ontogenetic stages.

Growth marks: The type of growth marks and differences between elements and ontogenetic stages.

Sharpey's fibres: The presence and depth of the fibres indicating regions of tendinous or ligamentous insertion into the bone tissues and variation between elements and ontogenetic stages.

Aims and hypotheses

Aim: To assess the effects of growth and biomechanics on the ecological signal exhibited in the bone histology and microanatomy of *Stigmochelys pardalis*.

Objectives:

1. Assess changes in growth through ontogeny
2. Assess inter-elemental variation in bone tissues and microanatomy
3. Assess the influence of intra-elemental variation on microanatomy interpretations.

Hypothesis: Ontogeny and biomechanics do not destroy the ecological signal in the bone microstructure of *Stigmochelys pardalis*.

2. LITERATURE REVIEW

Detailed evolutionary history

The presence of a shell and distinctive body plan makes Testudines one of the most recognisable groups in nature, but these features are also responsible for the controversy regarding the phylogenetic relationships of this clade (Lee 1997). The origin and placement of Testudines has fascinated zoologists for many years (Reisz & Laurin 1991; Lee 2013; Lyson *et al.* 2013; Shaffer *et al.* 2013), this uniqueness is important for identifying the structural and developmental evolution in turtles (Lyson *et al.* 2014) both on a molecular and morphological scale (Hill 2005). The difficulties in understanding the origin of these distinctive features has caused one of the most intensive debates in the field of macroevolution (Lee 2013).

Although Reisz and Laurin (1991) agreed that Testudines were parareptiles, they proposed a closer affinity to procolophonids, based on the discovery of *Owenetta* from South Africa. They focused on similarities in the postcranial skeleton because information regarding changes in the skeleton have resulted in the differing opinions regarding testudine evolution. They suggested that procolophonids and turtles were a monophyletic group due to similar derived characteristics that are still in primitive form in other Palaeozoic reptiles. These characteristics include “a great reduction in the length of the cultriform processes, the loss of replacement teeth on the transverse flange of the pterygoid and replacement with a ventral ridge, a distinct anterodorsal expansion of the maxilla formed directly posterior to the external naris, a close contact between the prefrontal and palatine, lateral exposure of the dorsal process of the quadrate, and the squamosal and the enlarged quadratojugal forming the edge of a well-developed tympanic notch. The slender stapes has lost both its dorsal process and foramen, the distinctly shaped anterior edge of the splenial on the lower jaw is excluded from the symphysis, the dorsal surface of the retro-articular process is wide and concave and is formed by a minimum of three bones (articular, angular and prearticular), the post-parietal is greatly reduced or completely lost and the entepicondylar foramen of the humerus is lost” (Taken directly from Reisz & Laurin 1991).

Another theory on testudine relationships was proposed by Rieppel and deBraga (1996). They suggested that the closest relatives of turtles are the sauropterygians,

an extinct group of aquatic reptiles. The theory is based on the similarity between various synapomorphies. These include the formation of a choana, constriction of the parasphenoid, the angle of the external edge of the transverse flange, a mineralized sternum, a coracoid foramen, humeral torsion, femoral condyles for the crus, number of pedal centralia and the limb morphology. Although the results of this study indicated some similarity between the diapsid sauropterygians and turtles, Testudines do not display any of the basal diapsid characteristics, which raises questions about the validity of results

Lee (1997) later concluded that pareiasaurs were monophyletic with turtles. These taxa share characteristics that not only suggest pareiasaurs are the closest relatives of Testudines, but that pareiasaurs may be their ancestors with the most closely related genus being *Pumilionpareia*. Lee (1997) also indicated that the evolution towards extant Testudines' occurred in a number of separate (possibly linked) steps over millions of years. He came to his conclusions based on various synapomorphies of Pareiasauria and Testudines. These characteristics include: pleurosphenoid ossification, a prefrontal-postfrontal contact, fused basicranial articulation, thick braincase floor, reduced presacral count, an acromion process on the scapula, four sacral ribs and dermal armour. This study also suggested that the turtle shell, one of Testudines most distinctive characteristics, was not the first to evolve, but might have been a result of modifications in other parts of the body.

Hill (2005) conducted a phylogenetic analysis using morphological and histological characters of the skin and osteology as well as behavioural characters together. He concluded that turtles are the most closely related to Lepidosauromorpha (Diapsida) and based his findings on the broad spectrum of characteristics used in their comparison (a large character and taxonomic data set). The findings, however, suggest a "de-evolution" from Diapsida (two temporal fenestra) back to Anapsida (one temporal fenestra) together with other various other characters that are shared between Testudines and Parareptilia. This theory is viable due to this phenomenon occurring in other taxa, such as in Araroscelidia, Acleistorhinidae, Crocodylomorpha and Dinosauria (Hill 2005).

Evidence collected by Crawford *et al.* (2012) suggests an archosaur (birds and crocodiles) and turtle relationship. A genomic phylogenetic analysis of 1145 nuclear loci was completed using DNA from a tuatara and two species of crocodilians,

squamates and turtles. They also emphasised the importance of using tuatara in their analysis and elaborated further on why using micro-RNA revealed a close relationship between lepidosaurs and turtles in other studies and not between archosaurs and turtles.

Lee (2013) then proposed that turtles fall within Parareptilia and are most closely related to the relatively newly discovered fossil, *Eunotosaurus*. The use of morphological characters combined with molecular information from extant turtles showed that they are most closely related to extant archosaurs. This study showed the importance of large samples because their large data set showed that turtles and *Eunotosaurus* fall within Parareptilia. Additionally, in the anapsid based analysis, turtles were originally placed with ankyromorphs (pareiasaurs and procolophonids) within Parareptilia, but with the use of extra characters, turtles grouped with *Eunotosaurus.* These results support recent comparative studies on the ventilator apparatus (Lyson *et al.* 2014) and lifestyle (Lyson *et al.* 2016) of extant turtles and Eunotosaurus.

As seen above, the evolutionary debate regarding the origin and relationships of Testudines' is ongoing. Technological advancements have resulted in increased use of molecular work but the importance of morphological comparisons continues to be as important in classification studies. The discovery of new fossils such as *Eunotosaurus* has led to new opinions and classification methods, as well as more comprehensive analyses of similar characteristics. Furthermore several studies have emphasised how the character base for comparison influences the results and how results vary between the use of soft tissues and hard tissues and in certain cases, the use of RNA instead of DNA.

Bone Histology

Bone is a complex connective tissue composed of cells (osteocytes) and extra-cellular matrix and is formed via osteogenesis, the histo-cytological process of bone formation. It corresponds to the secretion and spatial arrangement of collagenous and non-collagenous matrix by osteoblasts and the mineralization of calcium phosphate that gives it its stiffness (Ross & Pawlina 2011). Bone, however, is not a static system, but is comprised of various components that interact, change and transform throughout development. These characteristics make it possible for researchers to study

numerous aspects of the biology and ecology of vertebrates in terms of lifestyle, habitat and ecology (Canoville & Laurin 2009) mechanical properties (Currey 1984; Carter *et al*. 1996), morphological modifications and adaptations (Canoville & Laurin 2009), various ontogenetic changes (De Boef & Larsson 2007) and the nature and structure of bone tissues in modern material and fossilised bone (Scheyer *et al.* 2007).

Amprino (1947) was the first to suggest a relationship between bone growth and the degree of vascularisation in cortical bone. This relationship has since been quantified by de Margerie *et al.* (2002) who proposed that the most accurate method for quantifying bone growth is measuring it in the cortical bone as demarcated by vascular orientation. Bone histological analysis also reveals information regarding growth of an individual through the technique known as skeletochronology. This technique examines interruptions in growth (i.e. growth marks - annuli or LAGs) within cortical bone and uses these interruptions to determine the approximate ontogenetic age of an individual.

Organisms occupy numerous ecological niches. Various lifestyles result in distinctive morphological adaptations (Houssaye 2012), such as modification of the limbs into paddles for living in an aquatic environment (Canoville & Laurin 2009) or the lightening and lengthening of the forelimb in flying birds (Currey 2003). However, modifications also occur on a microstructural scale. These modifications influence biomechanics, ontogeny (Kriloff *et al.* 2008) and energy expenditure during movement (de Ricqlès 1983).

It has been noted in previous publications (Wall 1983, Scheyer & Sander 2007, Canoville & Laurin 2009; Kriloff *et al.* 2008) that there are numerous differences in the bone microstructure of terrestrial, semi-aquatic and aquatic species. Shallow aquatic species tend to have a small medullary cavity and larger areas of compact bone to reduce buoyancy whereas the bones of pelagic species tend to be almost completely cancellous with very little compact bone. Terrestrial species have a larger, more open medullary region and smaller areas of cortical compact bone compared to shallow water species (Canoville & Laurin 2009). Additionally, semi-aquatic species often have thickened bone walls (pachyostosis) as an evolutionary adaptation to reduce buoyancy (Taylor 2000).

Girondot & Laurin (2003) developed a method for quantifying the compactness of bones to compare different species and their lifestyles. This method uses a software programme, Bone Profiler, and allows for the accurate comparison of modern material as well as fossilised material. However, it was observed in Canoville & Laurin (2010) and noted in Nakajima *et al.* (2014) that the global compactness (Cg, the estimation of the compactness using the bone centre as a pivotal point (Girondot & Laurin 2003) of Testudines yields a poor ecological signal because of overlaps in the results of terrestrial and aquatic species. It was also noted that there is a reversed relationship in Testudines in that both terrestrial species and aquatic species exhibit very spongy bones and terrestrial species tend to have broad transition zones between spongiosa and compact bone, which is generally only seen in aquatic taxa (Nakajima *et al*. 2014). Nakajima *et al*. (2014) also suggested that the inability to predict the correct lifestyle using turtle microanatomy was due to poor sampling methods and found that differentiation using a humeral cross-section did not yield enough information to distinguish between lifestyles.

Nakajima *et al.* (2014) showed, in a comprehensive bone histological study comparing a diverse group of terrestrial, semi-aquatic and aquatic turtles (marine and non-marine) that the growth centre of the focus species in this study (*S. pardalis*) is two-thirds from the distal humeral head and the cancellous bone is in a columnar pattern with a large open medullary cavity. There are sparsely distributed cavities towards the exterior of the cross-section. However, it was noted in their study that as the size (length and thickness) of an element increased (older individuals), the percentage of cancellous bone increased.

Ontogenetic influence on bone histology

Ontogenetic studies are important for determining the evolutionary history of an organism. Nagashima *et al*. (2007) and Sheamran & Burke (2009) suggested that by studying the ontogenetic changes in Testudines, important information regarding its body plan can be obtained. The growth of an animal affects its ability to reproduce, its chances of survival and its metabolic requirements (Brown *et al*. 2005). However, growth can be energetically costly. Growth and development require new biomass which by itself, results in extra risk during feeding, extra energy for thermoregulation and digestion, as well as various social interactions that may result in harm. Therefore growth is not an independent factor. Growth is also influenced by a number of different

environmental variables such as habitat quality. For example, Aresco & Guyer (1999) found that tortoises occupying unsatisfactory conditions experienced slower growth rates, which ultimately affected the time it took to reach sexual maturity. In a study conducted by Brown *et al*. (2005) it was also found that younger tortoises have higher energy demands than adults due to rapid growth during the juvenile stage.

Ontogenetic variation results in morphological and physiological changes that can be observed macroscopically, but also on a microscopic level. Bone modelling and remodeling results in various changes that influence the organism despite Brown *et al*. (2005) suggesting that micro-evolutionary changes in Testudines are slow compared to other vertebrates.

3. MATERIAL AND METHODS

Material

Specimens were collected from various sites in the Free State and Northern Cape provinces, South Africa between 2000 and 2015. Bones were collected from a farm near Jacobsdal, a site near Quaggasfontein in the Free State Province as well as from a farm (Platberg, Koppieskraal) near Fraserburg, Northern Cape Province.

Macro-measurements

Soft tissue was removed and disposed of in an appropriate manner. Elements were degreased in a sunlight liquid solution for approximately two weeks in glass containers that were covered, but not completely sealed off. Elements were photographed and the measurements (total lengths, mid-shaft diameter, proximal and distal widths) were recorded into a database with details concerning species, age, locality and anatomical features of the bones. A humerus (MNHN-ZA-AC 2010-2) from Nakajima *et al*. (2014) is the largest recorded element of *S. pardalis* and was used to calculate all the % adult values for the elements in this study. This was possible because different elements belonged to the same individual. Age classes were categorized according to the following: juvenile, 0-20% of the maximum known size; early sub-adult, 21 – 49% of maximum size; late sub-adult, 50-79% of the maximum size; adult, 80-100% of the maximum size (Table 2). For brevity, % of the maximum known size for each element is referred to as % adult as humerus MNHN-ZA-AC 2010-2 is considered to be 100% adult (maximum adult size).

Table 2: The complete set of specimens used in this study with information on element type, bone length, mid-shaft diameter, % adult and ontogenetic status (approximate age class). (J - Juvenile; ESA - Early sub-adult; LSA - Late sub-adult: A- Adult). Data from an adult humerus (MNHN-ZA-AC 2010-2) was taken from Nakajima *et al.* (2014).

Accession #	Element	Bone length (mm)	Midshaft Diameter (mm)	% Adult	Age Class
MVD-R 12b	Humerus	8.1	0.97	5.21	J
MVD-R 12a	Humerus	8.21	0.98	5.28	J
MVD-R 11b	Humerus	9.5	1.24	6.11	J
MVD-R 11a	Humerus	9.61	1.19	6.18	J
MVD-R 10a	Humerus	45.89	8.56	29.51	ESA
MVD-R 9	Humerus	60.37	7.26	38.82	ESA
MVD-R 8	Humerus	60.89	6.18	39.16	ESA
MVD-R 7	Humerus	68.8	7.78	44.24	ESA
MVD-R 6	Humerus	73.44	8.59	47.23	ESA
MVD-R 5	Humerus	81.2	9.61	52.22	LSA
MVD-R 4	Humerus	81.43	9.81	52.37	LSA
MVD-R 3	Humerus	87.3	10.29	56.14	LSA
MVD-R 2a	Humerus	94.47	11.64	60.75	LSA
MVD-R 1	Humerus	97.93	10.28	62.98	LSA
MNHN-ZA-AC 2010-2	Humerus	155.5	-	100.00	A
MVD-R 12c	Radius	4.91	0.37	5.29	J
MVD-R 18a	Radius	12.21	0.95	13.17	J
MVD-R 17	Radius	42.35	4.77	45.67	ESA
MVD-R 16	Radius	50.08	4.99	54.00	LSA
MVD-R 15	Radius	51.69	5.65	55.74	LSA
MVD-R 14	Radius	52.48	6.36	56.59	LSA
MVD-R 13	Radius	54.27	6.09	58.52	LSA
MVD-R 2b	Radius	56.34	6.35	60.75	LSA
MVD-R 12e	Ulna	4.67	0.44	4.40	J
MVD-R 12d	Ulna	4.93	0.45	4.65	J
MVD-R 18b	Ulna	12.48	0.91	11.76	J
MVD-R 10b	Ulna	31.84	3.04	30.00	ESA
MVD-R 23	Ulna	39.81	3.04	37.51	ESA
MVD-R 22	Ulna	47.76	4.12	45.01	ESA
MVD-R 21	Ulna	53.93	4.72	50.82	LSA
MVD-R 20	Ulna	55.22	5.12	52.04	LSA
MVD-R 19	Ulna	62.73	5.63	59.11	LSA
MVD-R 2c	Ulna	64.47	6	60.75	LSA

Table 2 continued: The complete set of specimens used in this study with information on element type, bone length, mid-shaft diameter, % adult and ontogenetic status (approximate age class). (J - Juvenile; ESA - Early sub-adult; LSA - Late sub-adult: A- Adult). Data from an adult humerus (MNHN-ZA-AC 2010-2) was taken from Nakajima *et al.* (2014).

Accession #	Element	Bone length (mm)	Midshaft Diameter (mm)	% Adult	Age Class
MVD-R 12g	Femur	7.2	0.76	5.07	J
MVD-R 12f	Femur	7.41	0.73	5.22	J
MVD-R 11c	Femur	11.47	1.04	8.08	J
MVD-R 10c	Femur	41.54	4.17	29.23	ESA
MVD-R 28	Femur	49.17	4.57	34.63	ESA
MVD-R 27	Femur	73.58	8.68	51.82	LSA
MVD-R 26	Femur	73.88	8.18	52.03	LSA
MVD-R 25	Femur	84.29	8.41	59.36	LSA
MVD-R 24	Femur	85.84	9.76	60.45	LSA
MVD-R 2d	Femur	86.26	8.56	60.75	LSA
MVD-R 12i	Tibia	6.15	0.56	6.03	J
MVD-R 12h	Tibia	6.18	0.56	6.06	J
MVD-R 11e	Tibia	8.3	0.77	8.14	J
MVD-R 11d	Tibia	8.91	0.72	8.73	J
MVD-R 11e	Tibia	43.79	5.06	42.93	ESA
MVD-R 11e	Tibia	53.32	6.32	52.27	LSA
MVD-R 11e	Tibia	56.25	6.68	55.14	LSA
MVD-R 11e	Tibia	56.58	6.45	55.47	LSA
MVD-R 11e	Tibia	61.97	7.6	60.75	LSA
MVD-R 11e	Tibia	63.37	7.71	62.12	LSA
MVD-R 12k	Fibula	6.03	0.35	5.80	J
MVD-R 12j	Fibula	6.13	0.34	5.90	J
MVD-R 11f	Fibula	7.84	0.54	7.54	J
MVD-R 36	Fibula	46.65	3.69	44.89	ESA
MVD-R 31b	Fibula	54.25	4.41	52.20	LSA
MVD-R 35	Fibula	55.51	4.42	53.42	LSA
MVD-R 34	Fibula	61.98	3.97	59.64	LSA
MVD-R 2f	Fibula	63.13	6.01	60.75	LSA

Bone Histology

Pre-treatment

Pre-treatment was divided into three steps, namely: fixation, dehydration and clearing. However, before preparation, all elements were cut into smaller sections to allow for successful penetration of the various agents as well as successful implementation of the embedding process.

Pre-treatment took place over seven days. All specimens were fixated in 10% non-buffered formalin for 48 hours (with one change) to preserve the bone tissues. To remove excess water, they were then placed in 70% ethanol for 48 hours (with a single change) and 96% ethanol for 24 hours (with one change). The bones were then soaked in the clearing agent xylene for 24 hours and left to air dry on paper towels for approximately 24 hours.

Thin sectioning

Specimens were glued onto the base of plastic containers (using superglue) to prevent movement during embedding. An Epoxy Techno-resin was mixed with its corresponding catalyst in a 12:1 ratio and placed in a Struers CitoVac vacuum chamber to remove air bubbles. The resin container was then removed and replaced with the container holding the specimen, which was then filled with resin under vacuum. The containers were left for 10 minutes in the vacuum chamber and then removed and left to air-dry for approximately two days.

Cross-sections of approximately 1.8mm of the diaphysis and 1.8mm longitudinal sections of the epiphyses were cut using a diamond tipped cutting blade in the cutting and grinding thin sectioning machine, the Accutom-50. Thereafter, these sections were rinsed in acetone to remove any excess moisture and then placed in a desiccation chamber overnight. An Epolam 2022 industrial glue was mixed with its corresponding catalyst in a 2:1 ratio and placed into the vacuum chamber for 10 minutes to remove any excess bubbles. The sections were then glued to frosted glass slides using the mixed glue. Specimens were clamped together with their corresponding slide and left to dry in a desiccation chamber overnight. Specimens were then ground (course and fine) to approximately 150 µm using a diamond tipped grinding cup-wheel in the Accutom-50. Specimens were finally sanded down using a

fine sand-paper and polished using a Struers LaboPol-5 polishing machine where necessary.

A few problems were encountered where, due to the spongy nature of the bone, sections separated from the glass slides and resulted in poor quality images. Together with this, uneven grinding occurred during a series of mechanical faults with the Accutom-50 resulting in uneven sections making the histological analysis difficult in certain cases.

Analysis

Sections were viewed using a Nikon DS-FI1 polarising petrographic microscope. High magnification images (4X) were rendered together (in normal and cross-polarised light with lambda compensator) to form images of whole cross-sections for the analysis of the microanatomy and 10X magnification images were captured for analysing the bone histology. Images were captured using a DS-F1 digital camera mounted on the microscope and saved using the computer program, NIS-Elements D 3.

The quantitative analysis was divided into three main sections: 1: the extent of vascularisation in the cortical region of the bone; 2: the degree of compactness of diaphyseal sections and lifestyle predictions using Bone Profiler for Windows (Girondot and Laurin 2003) together with a Wilcoxon rank sum test with continuity correction and 3: Growth mark counts. This information was used to describe the osteohistological changes through different ontogenetic stages.

1. The degree of vascularisation was determined through the analysis of high-magnification images using Image J 1.50i. Images of the compact cortex were captured at 10X magnification around the whole cross-section of each bone. The degree of vascularisation was determined by tracing the perimeter of all the vascular canals in a given field of view, calculating the area occupied by the canals and dividing it by the total area of the field of view. The area occupied by the canals was expressed as a percentage.

2. Compactness was quantified by comparing the extent of cortical (solid bone) and spongy bone (medullary cavity). This analysis was done at the middle of the diaphysis. Sections were converted into binary black and white images using Corel Photo Paint X4 and a Genius Drawing Pad where bone is black and the cavities

white (see Appendix 3). The extent of compactness was then determined using Bone Profiler for Windows V4.5.8 (Girondot & Laurin 2003) and further information regarding Min, Max, S and P values were also obtained. These values were used to predict lifestyle for the humerus (Canoville & Laurin 2010), radius (Laurin *et al*. 2011) and tibia (Kriloff *et al.* 2008). The lifestyles readings of the ulnae and fibulae were not determined as a result of no formulas to predict lifestyle in these bones. The lifestyle of the femora (Quemeneur *et al*. 2013) was not completed because certain variables used in the determination of lifestyle could not be obtained. The R/t value, where R is the outer radius of the bone and t the thickness of the cortical wall was also recorded as this provides an indication of the thickness of the cortical bone wall (Currey & Alexander 1985). These values were converted to K which is the ratio of the internal diameter to the outer diameter of the bone according to the formula outlined in Currey and Alexander (1985). This was done for easy comparison as most studies present K and not the original R/t values. A Wilcoxon sum test with continuity correction was performed to determine the differences between elements by testing the similarity between their K values and a separate test to test the similarity between their global compactness values (Cg).

3. Growth marks were counted using rendered normal and cross polarised light images and then recorded into a database.

Together with the quantitative analysis mentioned above, a histological analysis was conducted. This included:

1. The determination of bone type which together with vascularisation and growth marks was used to determine growth rates.
2. The extent of resorption and presence of resorption cavities and secondary osteons in the cortical bone.
3. The presence of Sharpey's fibres using high magnification images in normal and cross polarised light.

4. RESULTS

4.1 Bone histology

4.1.1 Humeri

4.1.1.1 Juveniles

Juveniles have almost, if not completely, open medullary cavities. Medullary cavities are circular in shape and almost centrally placed. The medullary cavities in comparison to the size of the bone, are large. A number of smaller openings where bone had yet to form are situated in the cortex. The size and quantity of these smaller cavities differs between specimens. MVD-R12a (Figure 1) and MVD-R12b have smaller, more numerous cavities distributed throughout the cortex. MVD-R11a (Figure 2) and MVD-R11b have larger, but fewer, cavities that are divided from the main cavity via bony trabeculae.

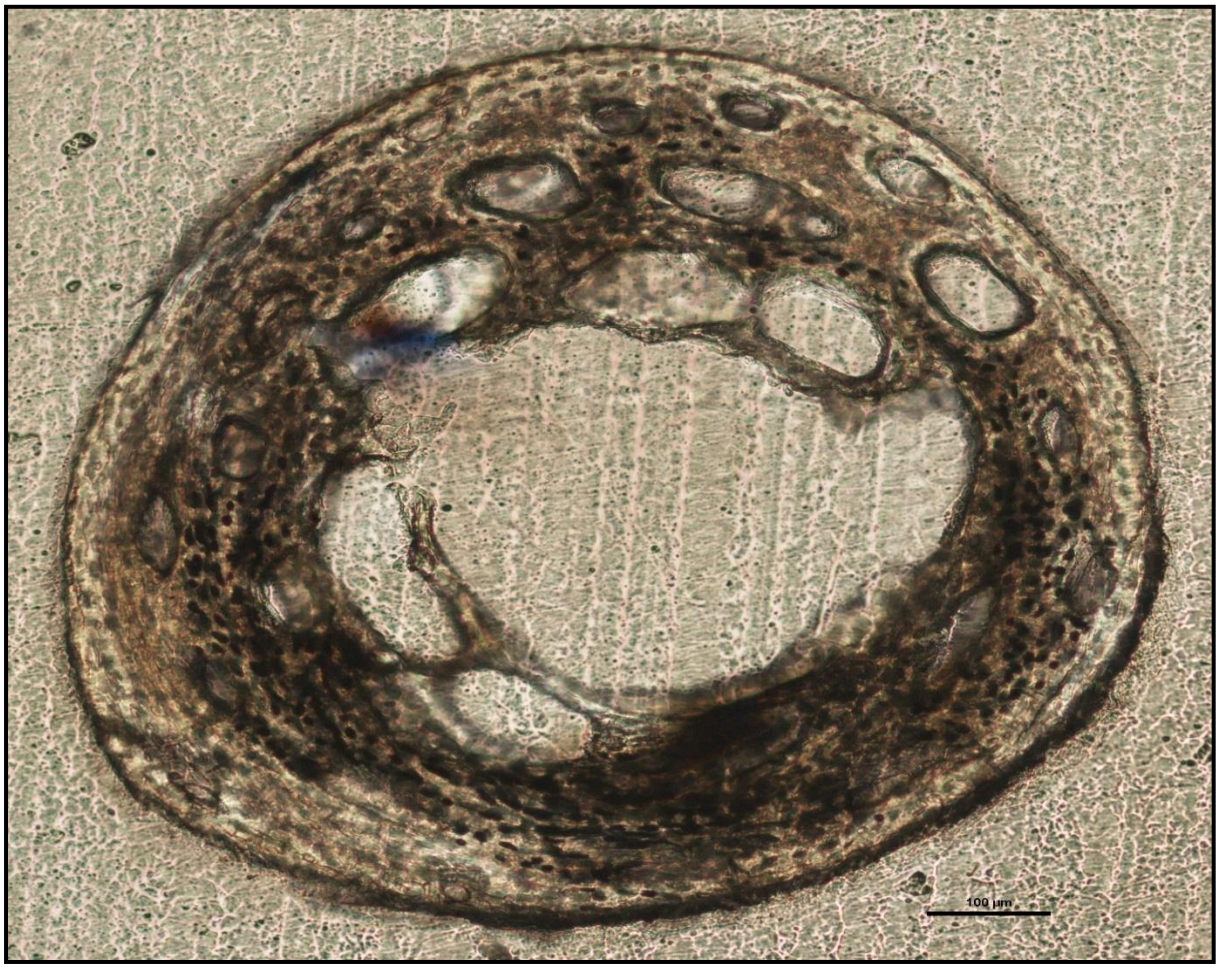

Figure 1: Juvenile humerus MVD-R 12a, depicting the large medullary cavity and small cortical cavities where bone had yet to be deposited.

As a result of a centrally placed medullary cavity, the cortices maintain the same thickness throughout majority of the section with slight deviations at the periphery where the bone is clearly still actively growing. However, despite the relatively thin cortices (average K value of 0.6) (Table 3), their compactness is relatively high. The average global compactness (Cg) is 0.733 (Table 3). These results, like other juveniles, are more influenced by the section of the bone sampled as a result of the small size and the likelihood of sampling parts of the metaphysis.

Figure 2: Whole cross-section of juvenile humerus MVD-R 11a displaying a large medullary cavity with numerous smaller cavities in the peri-medullary region. A few large bony trabeculae traverse the medullary cavity.

The bones of the juvenile humeri contain numerous, large, globular randomly distributed osteocyte lacunae. The collagen fibres cannot be detected making it difficult to classify the bone matrix. However, given the size, shape and abundance of osteocytes, the bone matrix is most likely woven fibred. This is typical of embryos and juveniles. Primary osteons had yet to develop but the cortical cavities are large

resulting in an average vascularisation of 3.5% for individual MVD-R 11 (left and right humeri) and MVD-R 12 averaged 6% (left and right humeri) (Table 3). Secondary osteons are absent from all the juvenile humeri. There are no growth marks. Sharpey's fibres, indicating areas of muscle insertions were not observed.

Table 3: The percentage vascularisation, global compactness (Cg) and corresponding R/t (R is the outer radius of the bone, and t is the thickness of the wall) and K (ratio of the internal diameter to the outer diameter) values. Note how the k values are substantially lower and Cg values higher in early sub-adults compared to other ontogenetic groups.

Accession #	Element	Age Class	% Vascularisation	C	R/t	K
MVD-R 12b	Humerus	J	4.89	0.694	2.057	0.514
MVD-R 12a	Humerus	J	7.23	0.658	2.828	0.646
MVD-R 11b	Humerus	J	3.47	0.853	2.269	0.559
MVD-R 11a	Humerus	J	3.73	0.726	3.246	0.692
MVD-R 10a	Humerus	ESA	0.17	0.963	1.301	0.231
MVD-R 9	Humerus	ESA	0.18	0.974	1.788	0.441
MVD-R 8	Humerus	ESA	0.24	0.96	1.118	0.106
MVD-R 7	Humerus	ESA	0.09	0.961	1.657	0.396
MVD-R 6	Humerus	ESA	0.11	0.933	1.130	0.115
MVD-R 5	Humerus	LSA	0.282	0.914	1.772	0.436
MVD-R 4	Humerus	LSA	0.19	0.917	1.685	0.407
MVD-R 3	Humerus	LSA	0.068	0.824	2.328	0.570
MVD-R 2a	Humerus	LSA	0.15	0.847	2.764	0.638
MVD-R 1	Humerus	LSA	0.1	0.906	1.747	0.428
MNHN-ZA-AC 2010-2	Humerus	A	-	0.799	1.746	0.427
MVD-R 12c	Radius	J	-	0.424	4.059	0.754
MVD-R 18a	Radius	J	0.42	0.809	2.443	0.591
MVD-R 17	Radius	ESA	0.65	0.989	1.037	0.036
MVD-R 16	Radius	LSA	0.09	0.939	1.475	0.322
MVD-R 15	Radius	LSA	0.16	0.965	1.135	0.119
MVD-R 14	Radius	LSA	0.077	0.912	1.888	0.470
MVD-R 13	Radius	LSA	0.13	0.894	1.992	0.498
MVD-R 2b	Radius	LSA	0.085	0.894	1.827	0.453
MVD-R 12e	Ulna	J	2.68	0.524	3.068	0.674
MVD-R 12d	Ulna	J	2.46	0.677	2.259	0.557
MVD-R 18b	Ulna	J	0.39	0.834	1.923	0.480
MVD-R 10b	Ulna	ESA	0.18	0.95	1.274	0.215
MVD-R 23	Ulna	ESA	0.11	0.924	1.111	0.100
MVD-R 22	Ulna	ESA	0.18	0.954	1.981	0.495
MVD-R 21	Ulna	LSA	0.071	0.889	2.067	0.516
MVD-R 20	Ulna	LSA	0.13	0.961	3.434	0.709
MVD-R 19	Ulna	LSA	0.13	0.842	4.304	0.768
MVD-R 2c	Ulna	LSA	4.46	0.804	3.348	0.701

Table 3: The percentage vascularisation, global compactness (Cg) and corresponding R/t (R is the outer radius of the bone, and t is the thickness of the wall) and K (ratio of the internal diameter to the outer diameter) values. Note how the k values are substantially lower and Cg values higher in early sub-adults compared to other ontogenetic groups.

Accession #	Element	Age Class	% Vascularisation	C	R/t	K
MVD-R 12g	Femur	J	1.95	0.805	1.714	0.416
MVD-R 12f	Femur	J	4.8	0.605	2.531	0.605
MVD-R 11c	Femur	J	0.29	0.822	1.719	0.418
MVD-R 10c	Femur	ESA	0.09	0.973	1.136	0.119
MVD-R 28	Femur	ESA	0.051	0.959	1.608	0.378
MVD-R 27	Femur	LSA	0.12	0.786	3.395	0.705
MVD-R 26	Femur	LSA	0.14	0.908	2.458	0.593
MVD-R 25	Femur	LSA	0.13	0.781	3.457	0.711
MVD-R 24	Femur	LSA	0.071	0.798	2.795	0.642
MVD-R 2d	Femur	LSA	0.12	0.746	3.055	0.673
MVD-R 12i	Tibia	J	0.78	0.494	3.396	0.706
MVD-R 12h	Tibia	J	3.1	0.78	1.792	0.442
MVD-R 11f	Tibia	J	1.6	0.556	3.690	0.729
MVD-R 11e	Tibia	J	0.52	0.729	4.056	0.753
MVD-R 33	Tibia	ESA	0.057	0.987	1.168	0.144
MVD-R 32	Tibia	LSA	0.08	0.89	1.675	0.403
MVD-R 31a	Tibia	LSA	0.086	0.915	1.230	0.187
MVD-R 30	Tibia	LSA	0.11	0.953	1.334	0.251
MVD-R 2e	Tibia	LSA	0.11	0.884	2.762	0.638
MVD-R 29	Tibia	LSA	0.079	0.908	2.476	0.596
MVD-R 12k	Fibula	J	0.87	0.723	2.829	0.647
MVD-R 12j	Fibula	J	-	0.521	3.188	0.686
MVD-R 11f	Fibula	J	-	0.89	1.490	0.329
MVD-R 36	Fibula	ESA	0.066	0.957	1.169	0.145
MVD-R 31b	Fibula	LSA	0.13	0.916	1.283	0.221
MVD-R 35	Fibula	LSA	0.079	0.925	1.860	0.462
MVD-R 34	Fibula	LSA	0.062	0.936	1.171	0.146
MVD-R 2f	Fibula	LSA	0.065	0.822	2.220	0.550

4.1.1.2 Early sub-adults

Early sub-adults have smaller medullary cavities that are completely infilled with bony trabeculae. Cavities are generally consistently sized, but in MVD-R 10a there are larger cavities and a few smaller cavities surrounding the larger ones. MVD-R6 and MVD-R-9 have similar medullary regions that exhibit larger cavities towards the centre and smaller cavities at the periphery of the medullary cavity, resulting in a gradual transition zone. These medullary cavities took on a variety of shapes from oval to completely irregular, which is probably a result of the twisted nature of the bone due to torsion. Cortical drift appears to be prominent in the humeri as the medullary cavities tend to drift towards the posterior side of the bone and are not centrally placed. As the bones undergo more torsion with age, the placement of the medullary cavity becomes increasingly asymmetrical (Figure 3).

Early sub-adults are clearly noticeable by their thicker cortices (Average K value of 0.26). The cortex is also not consistently thick, but has more visible regions of active growth (where the vascular canals are larger and more abundant). All early sub-adults have a Cg above 0.93 (Table 3), indicative of their small medullary cavities and thick cortices. It is also noteworthy, that in certain early sub-adults (MVD-R 6; MVD-R 7; MVD-R 10a) there are clear signs of recently deposited bone as well as instances where the bone is still forming at the periphery. Older individuals (MVD-R 6 and MVD-R 7) have extensively resorbed areas surrounding the medullary cavity within the peri-medullary region.

Early sub-adults have a predominantly parallel-fibred bone matrix. They contain many flattened and randomly distributed osteocyte lacunae, but clusters of larger circular lacunae are also observed in the inner cortex. MVD-R 7 differs from the other early sub-adults in containing lamellar zonal-bone tissue in the outer cortex. All specimens in this category exhibit several growth marks. Specimens have growth marks that range from two single annuli (MVD-R 6) to four single annuli and a double LAG (at the periphery) (MVD-R7) (Figure 4). Given the onset of slowly forming lamellar-zonal bone and presence of a double LAG in this specimen, MVD-R 7 might be slightly ontogenetically older than the other early sub-adults (See Appendix 1 for details). Evidence of muscle insertions is visible by the presence of Sharpey's fibres within the cortex of MVD-R 8 on the dorsal side of the bone.

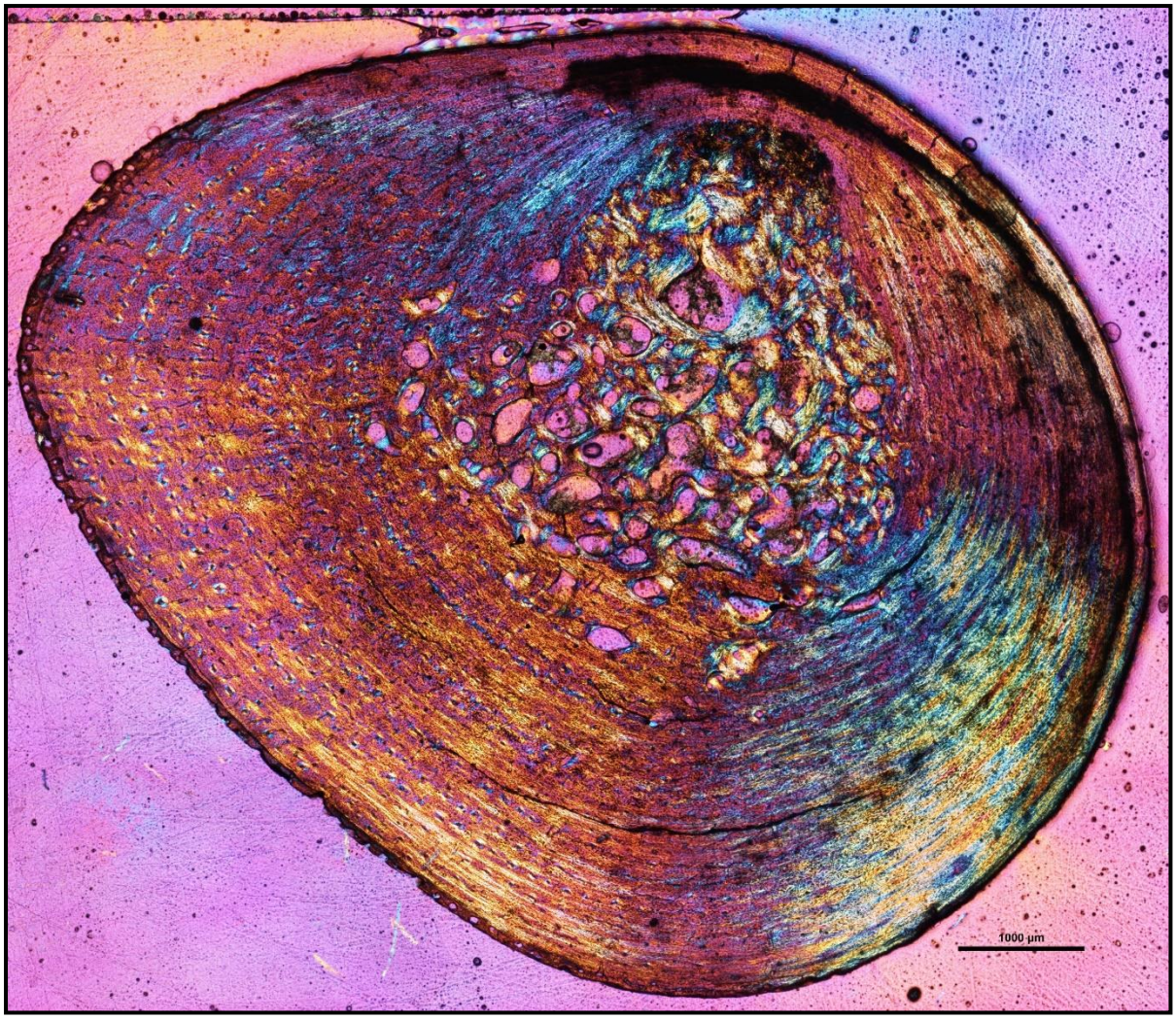

Figure 3: Whole cross-section of early sub-adult humerus MVD-R 7 in cross polarised light, showing the asymmetry of the medullary cavity due to bone drift.

The type and pattern of vascular canals differed between specimens. MVD-R 6 has predominantly simple canals whereas MVD-R7 has many longitudinally-orientated primary osteons distributed throughout the cortex. MVD-R 8 and MVD-R 9 have many primary and simple canals. Vascularisation is much lower compared to the juveniles, ranging from 0.24% in MVD-R 8 to as little as 0.09% in MVD-R 7 (Table 3). MVD-R10a differs substantially from the rest of the early sub-adults as it contains many branched vascular canals forming a sub-plexiform arrangement (Figure 5). The surface on the anterior side of the bone is also uneven with clear active bone growth in this region (with some short radiating canals in this area as well). Figure 4 also indicates active growth in MVD-R 7 by the presence of large cavities at the periphery of the bone.

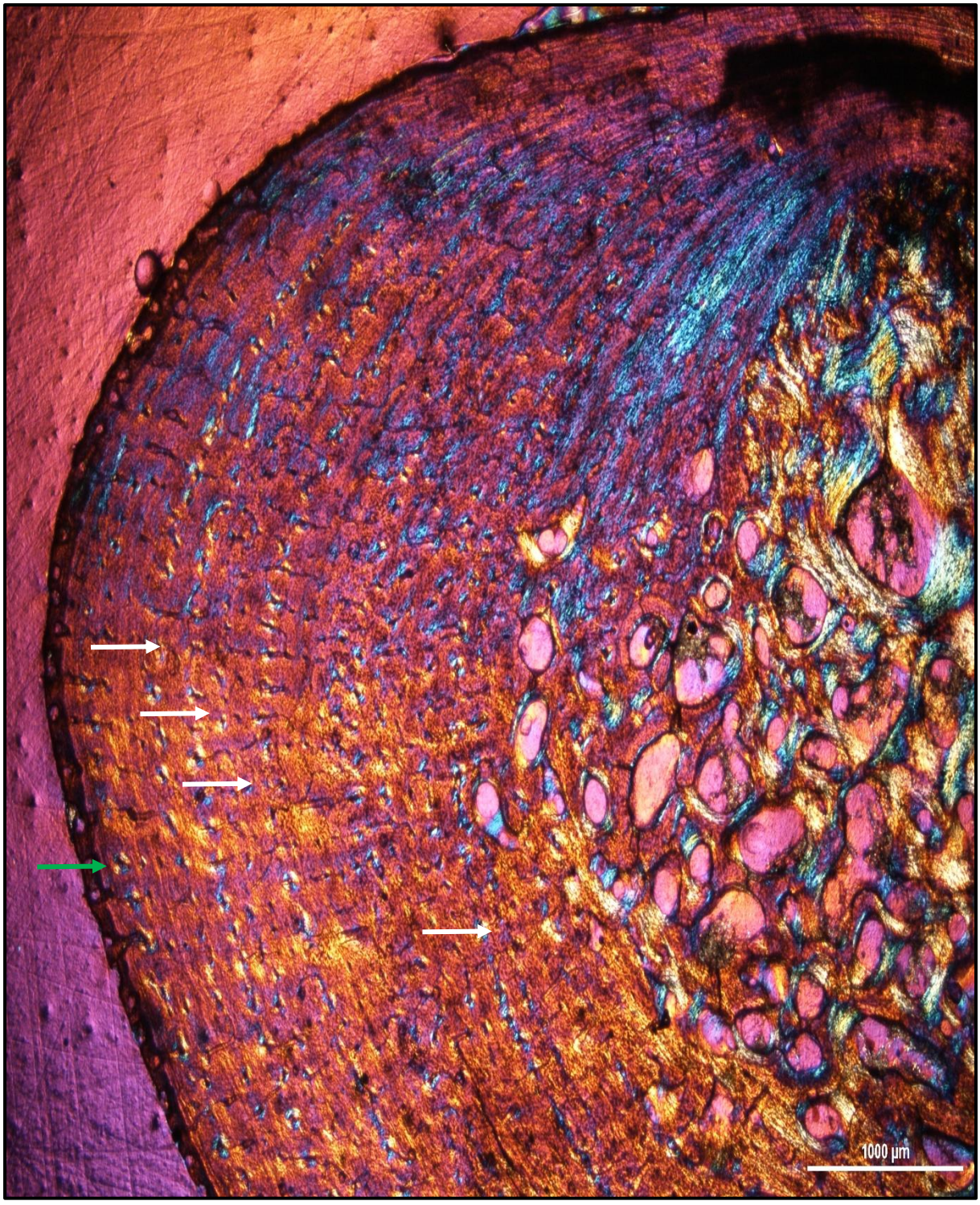

Figure 4: A close up of early sub-adult humerus MVD-R 7 showing the annuli (white arrows) and a double LAG (green arrow). Note the large cavities at the periphery, indicating active growth.

Figure 5: Whole cross-section of early sub-adult humerus MVD-R 10a showing a sub-plexiform vascular arrangement indicating a relatively rapid growth rate.

4.1.1.3 Late sub-adults

The late sub-adult specimens show a clear increase in the size of the medullary cavity especially in older specimens (MVD-R 1; 2a; 3). MVD-R 5 and MVD-R 4 are very similar to the early sub-adults in the size and shape of the medullary cavities. In the older individuals (MVD-R 1; 2a; 3), however, the medullary cavities tend to be more rounded and are more centrally placed (Figure 6). The medullary cavities are

completely infilled with fine bony trabeculae resulting in a relatively gradual transition zone.

The cortices of the late sub-adults have undergone extensive resorption and as a result, the compact cortices are thinner than the early sub-adults (average K value of 0.49), particularly in the oldest individual (MVD-R 1) (Table 3). However, the extensive bony trabeculae in the medullary cavity still result in a high compactness in all late sub-adult specimens. The late sub-adults, MVD-R4 and MVD-R 5 have a higher Cg of 0.917 and 0.914 respectively, due to the retention of various characteristics (smaller medullary cavities, thicker cortices) seen in the earlier sub-adults. In contrast, the older individuals such as MVD-R 2a and MVD-R 3, have lower Cg values of 0.847 and 0.824 respectively which is expected considering the extensive resorption of primary cortical bone seen in these individuals (Figure 6). The resorption cavities in these older individuals extend into the mid cortex, leaving very little of the primary compact cortex. Secondary osteons are concentrated in the peri-medullary region. This is particularly clear in MVD-R5 where there are numerous secondary osteons as well as isolated ones in the thickest part of the cortex. Larger sub-adults have fewer secondary osteons over all but still contain them within their peri-medullary region. The size of the secondary osteons increases with age while the younger individuals' osteons are mostly smaller.

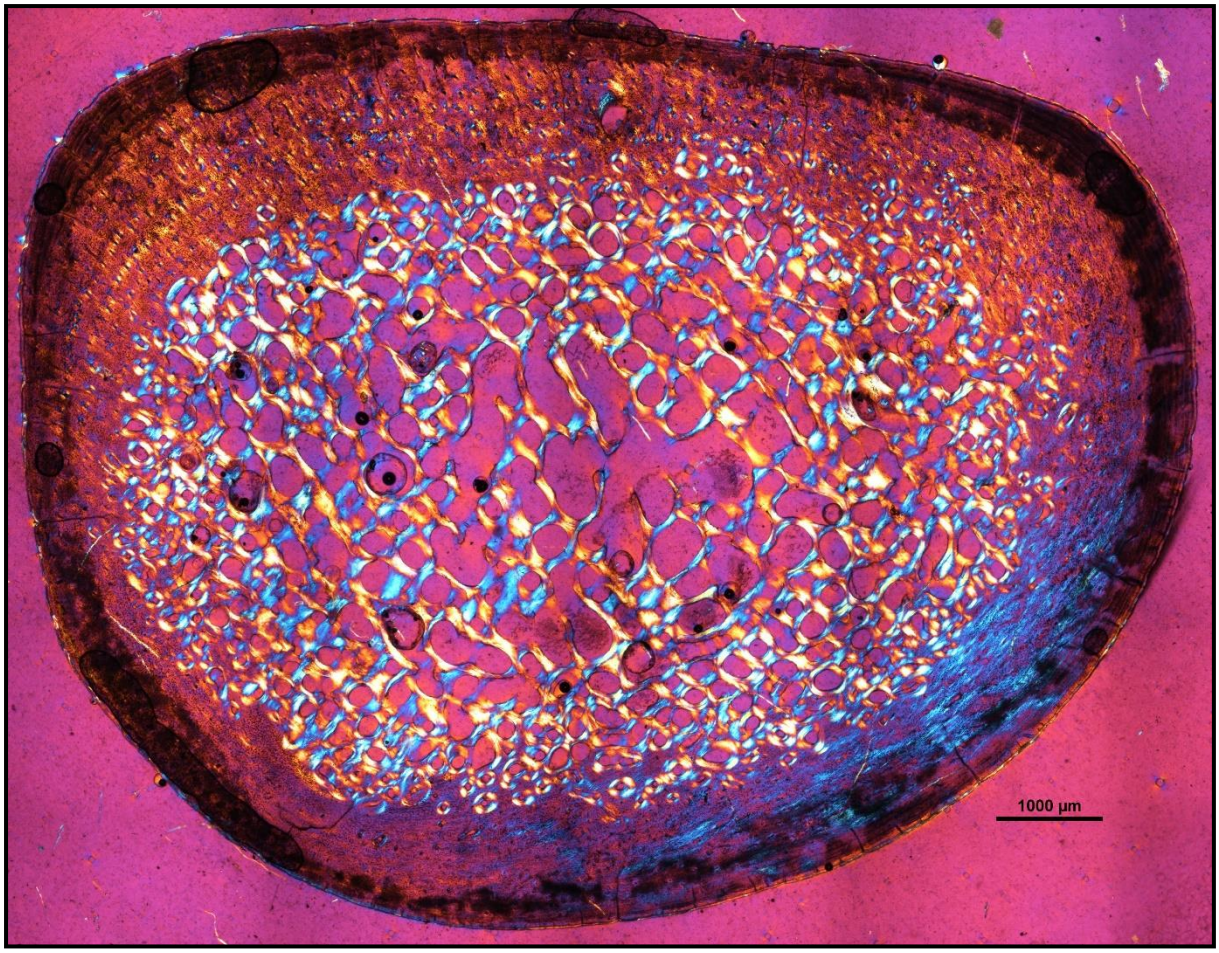

Figure 6: Extensive secondary resorption and slow growing bone tissues in late sub-adult humerus MVD-R 3 support an ontogenetically older status. Note the rounded centrally placed medullary cavity.

The bone tissues of late sub-adults are mostly parallel-fibred with a mixture of flattened and oval osteocyte lacunae distributed throughout the cortex. However, MVD-R 5 has a lamellar-zonal bone matrix with organised flattened osteocyte lacunae throughout most of the section, but a parallel fibred bone matrix with round osteocyte lacunae was observed in the inner-cortex. MVD-R 3 and MVD-R 1 are predominantly parallel fibred with clear lamellar zonal bone on the periphery of the bone, possibly indicating the development of an External Fundamental System (EFS). Late sub-adults are similar to the early sub-adults in that they also contain longitudinally-orientated primary osteons in circular rows. However, the less developed late sub-adults (MVD-R4 and MVD-R 5) have more rows as less of the primary cortex has been resorbed (Figure 7). The cortices are very poorly vascularised with an average of 0.16%. MVD-R 5 has the highest vascularisation (0.28%) whereas MVD-R 3 (0.07%) (Table 3). Simple

canals are mostly small longitudinally-orientated and unbranched, with a few having short anastomoses. Vascularisation decreases substantially towards the periphery in some parts of the bone indicating a decrease in growth rate.

Growth marks are visible in all of the late sub-adult specimens. The type of growth mark as well as the number in each specimen differed. Nine annuli as well as one LAG were observed in MVD-R 5 (Figure 7), whereas several closely spaced LAGs were observed at the periphery of MVD-R 3, indicating the presence of an EFS on its periphery and that bone growth had decreased substantially at the time of death (Figure 8). Sharpey's fibres were observed in MVD-R 1, indicating the attachment of muscles on the anterodorsal side of the bone (Figure 9).

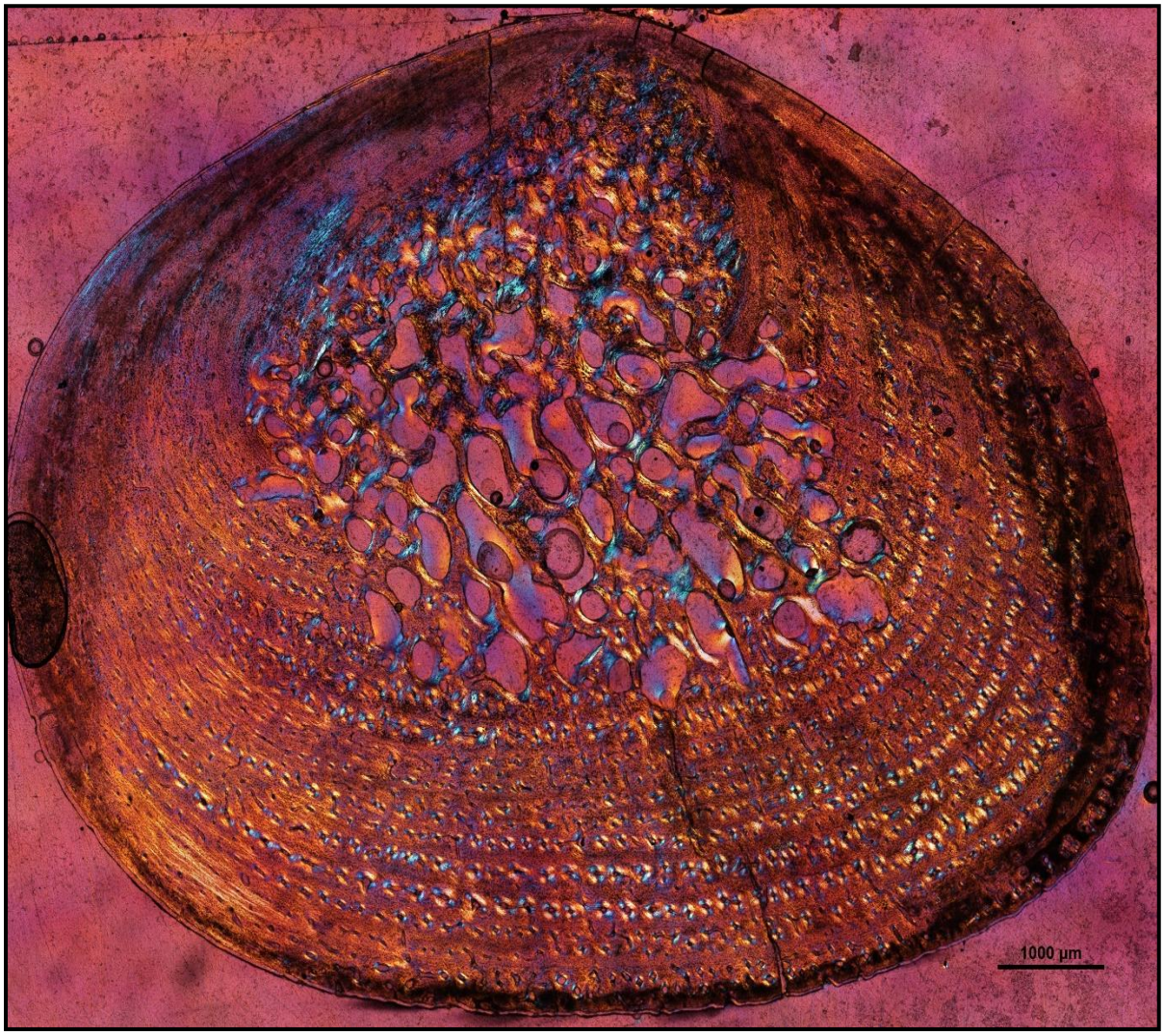

Figure 7: Growth marks and circular rows of primary osteons visible in the thickest part of the cortex in late sub-adult humerus MVD-R 5.

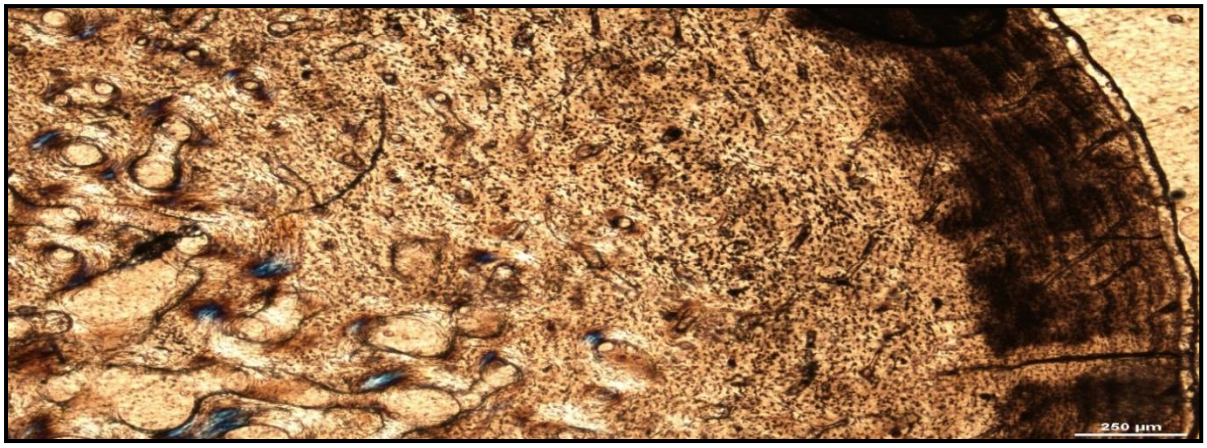

Figure 8: Late sub-adult humerus MVD-R 3 showing lamellar-zonal bone with numerous closely spaced LAGs at the periphery indicating the presence of an External Fundamental System.

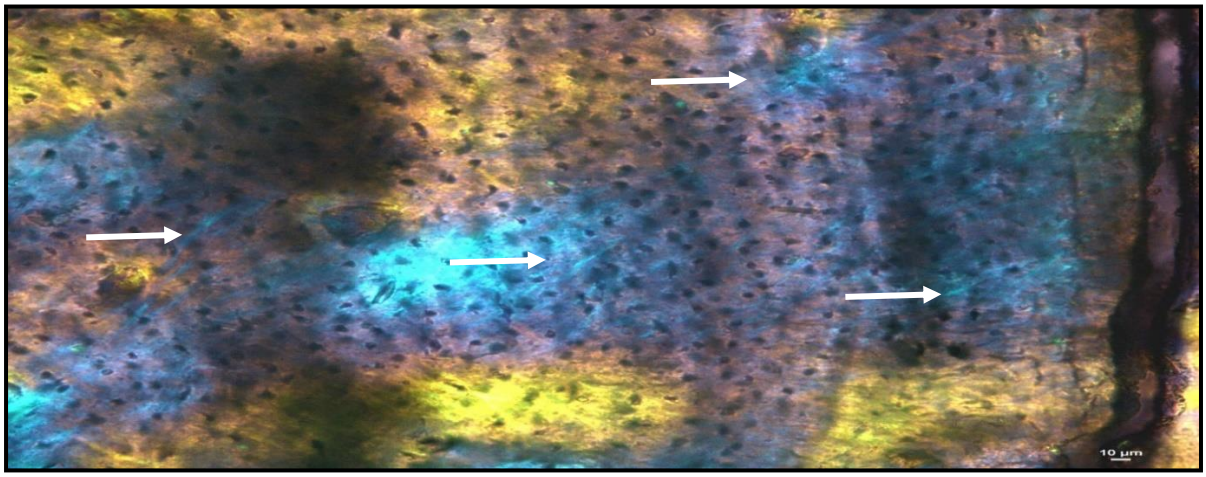

Figure 9: Sharpey's fibres indicate an area of muscle attachment in late sub-adult humerus MVD-R 1 (arrows).

4.1.2 Radii

4.1.2.1 Juveniles

The juvenile radii contain a centrally placed oval medullary cavity with a few bony trabeculae traversing it. There are smaller cavities surrounding the large cavity where bone has yet to form. MVD-R 18a has a high Cg of 0.809 (Table 3) probably because the bony trabeculae traversing the medullary cavity are relatively thick, so increasing the overall compactness of the bone (Figure 10). The cortex also has relatively few cortical cavities. The Cg of juvenile MVD-R 12c is lower (0.424), but the section is from

the metaphysis where the compact cortex is narrower, as seen in Figure 11. This is also noticeable in the different K values of MVD-R 12c (0.754) and MVD-R 18a (0.591).

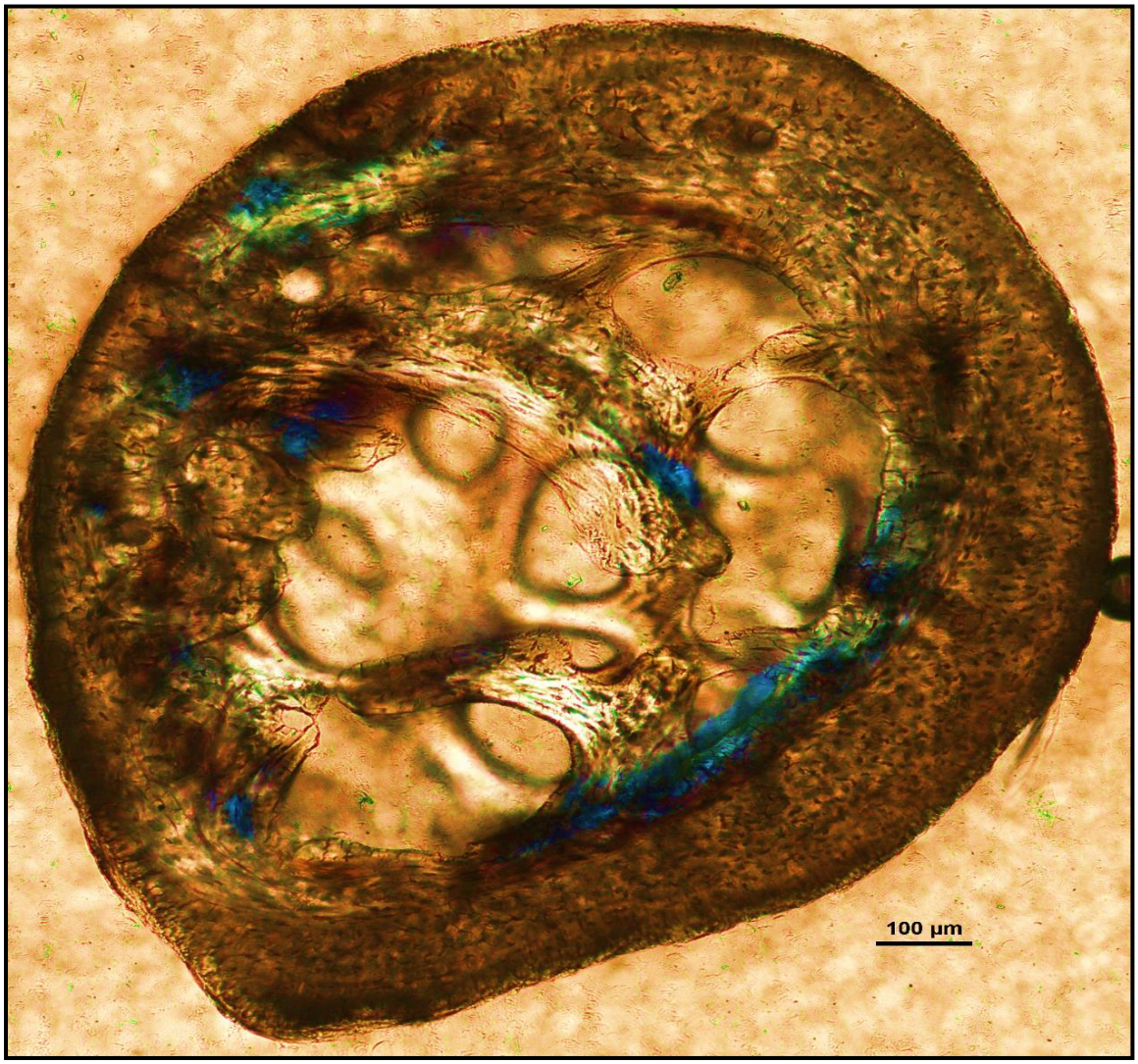

Figure 10: Juvenile radius MVD-R 18a with thick bony trabeculae traversing the medullary cavity.

It is difficult to observe the orientation of the collagen fibres and therefore identifying the bone matrix is problematic. However, the presence of abundant, randomly distributed oval osteocyte lacunae is suggestive of a woven-fibred bone matrix. There are also patches of more organised osteocyte lacunae however, suggesting that the bone comprises a mixture of woven and parallel-fibred bone. Primary osteons are absent and vascularisation is low with an average of 0.42. There are no growth marks. Sharpey's fibres were also not observed in either juvenile.

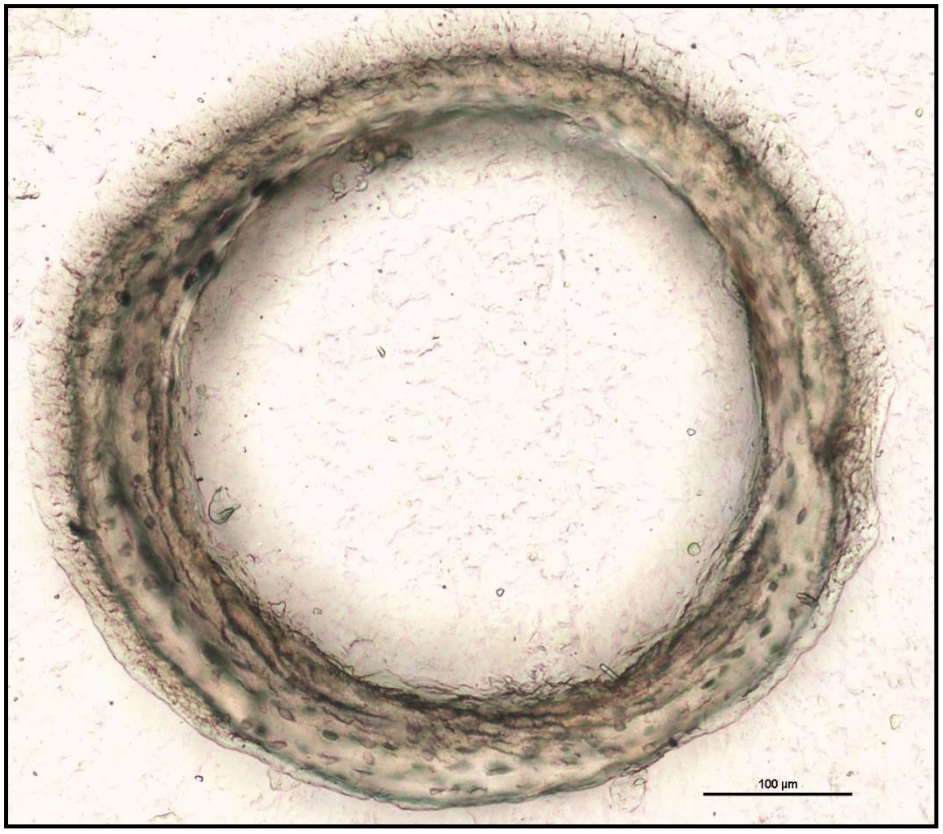

Figure 11: Juvenile radius MVD-R 12c taken slightly off the mid-diaphysis level. The osteocyte lacunae are numerous and oval in shape.

4.1.2.2 Early sub-adults

There is only one early sub-adult radius available for study, MVD-R 17. This bone has a tiny central area with four cavities just off-centre. There is no single, large main medullary cavity in this element.

MVD-R 17 shows clear changes in its cortical microstructure compared to the juveniles. The cortex is extremely thick (K = 0.036) and comprises most of the bone (Cg = 0.989). There are no established secondary osteons.

The bone tissue in the inner cortex is parallel-fibred and the osteocyte lacunae are more rounded in this region. The bone transitions into more slowly forming lamellar-zonal bone in the mid-cortex where the osteocyte lacunae become flattened and highly organised (Figure 12). The bone tissue contains a few small, longitudinally orientated simple vascular canals distributed throughout the cortex and there are a few primary osteons resulting in avascularisation of 0.65% (Table 3). There is a clear decrease in vascularisation towards the periphery indicating a decrease in growth rate.

Annuli in the inner cortex become LAGs (sometimes double) towards the periphery. Prominent deep (almost to the mid cortex) Sharpey's fibres on one side of the bone were observed (Figure 13 and Figure 14).

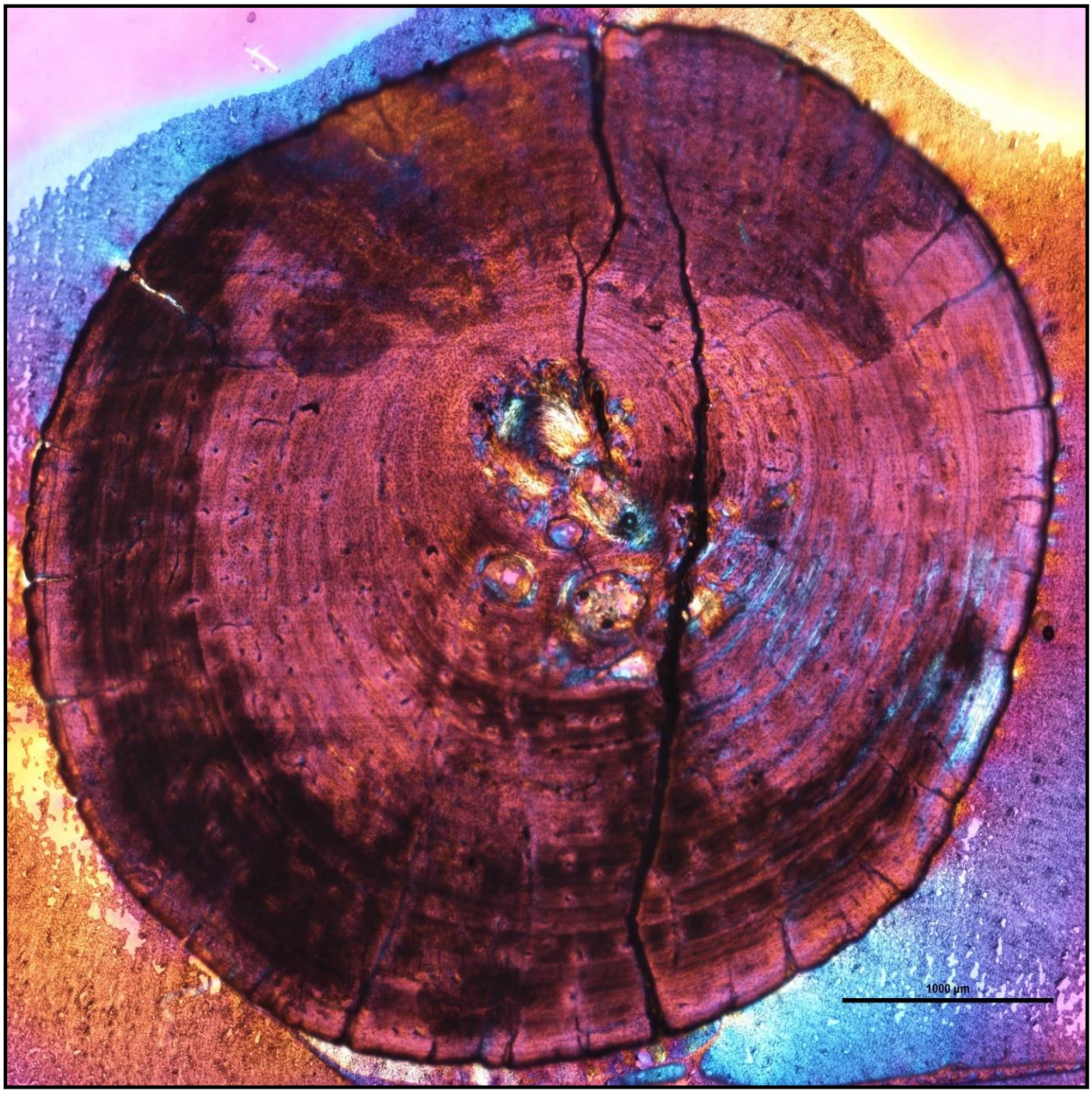

Figure 12: Early sub-adult radius MVD-R 17 showing a tiny medullary cavity and notably thick compact cortex. Note the presence of lamellar-zonal bone and progressively fewer vascular canals towards the periphery, indicating a steadily decreasing growth rate.

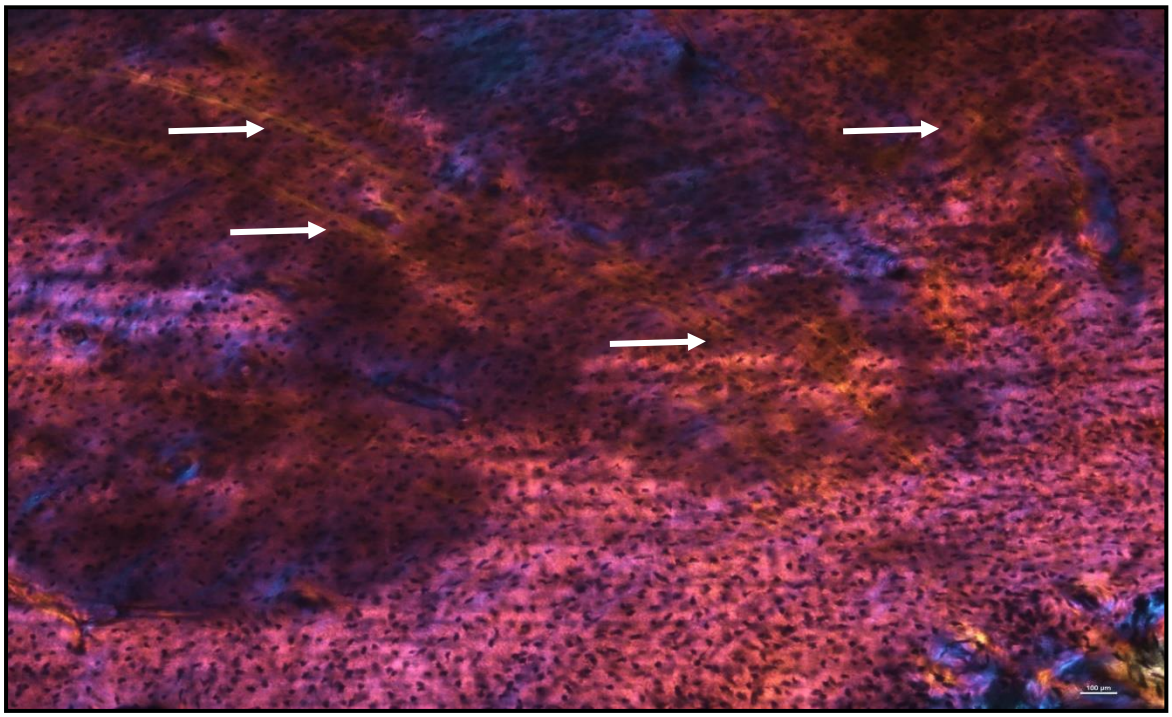

Figure 13: Deep Sharpey's fibres seen in the early sub-adult radius MVD-R 17.

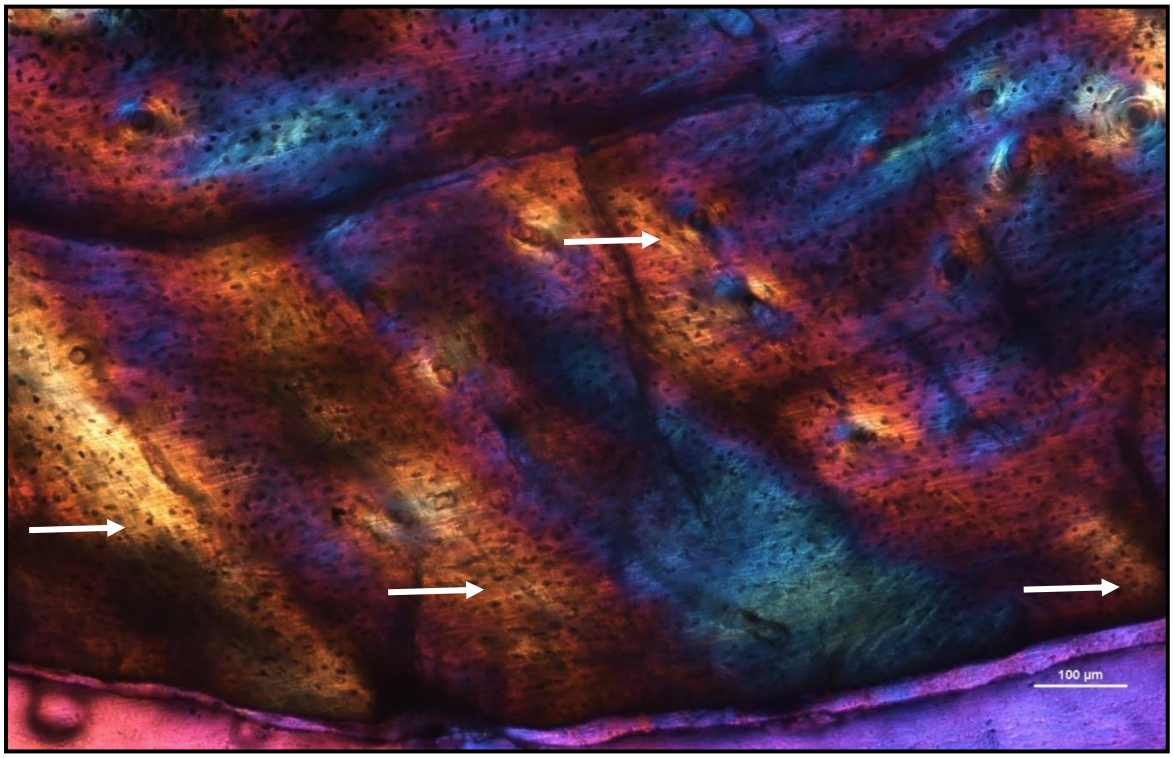

Figure 14: Sharpey's fibres seen at the periphery of the cortex in early sub-adult radius MVD-R 17.

4.1.2.3 Late sub-adults

The medullary cavities of the late sub-adults are larger than early sub-adult MVD-R 17 due to the primary bone tissue being more heavily resorbed. The transition zone from cancellous to compact bone is more gradual in older late sub-adults MVD-R 2b, MVD-R 13 and MVD-R 14 compared to younger late sub-adults MVD-R 15 and MVD-R 16 that have rapid transitions similar to early sub-adult MVD-R 17.

Younger individuals in this age class (MVD-R15 and MVD-R16) show similar characteristics to those of the early sub-adult and have an average Cg of 0.952. The older individuals (MVD-R13; MVD-R14 and MVD-R2b) have larger medullary cavities and as a result, thinner cortices but the average global compactness remains high at 0.9 (Table 3). The late sub-adults, as a result of continued resorption and growth, have numerous randomly distributed secondary osteons and resorption cavities ranging in size. Secondary osteons are distributed throughout the cortex in between circular rows of primary osteons. Secondary remodelling is concentrated in the peri-medullary region and various parts of the inner cortex, but it does extend to the periphery in MVD-R 15 where a number of secondary osteons are situated in between the circular row of primary osteons and isolated on the periphery of the bone.

The bones of the late sub-adults contain a mixture of randomly distributed oval osteocyte lacunae and more organised, flattened osteocyte lacunae. MVD-R 15 has numerous primary osteons that are randomly distributed, but in some cases, arranged in circular rows in the inner and mid-cortex (Figure 15). Very few primary osteons are present in MVD-R 13 and MVD-R 14, which mostly contain longitudinally-orientated simple vascular canals resulting in an average vascularisation 0.11% (Table 3). The bone tissues are, mostly parallel fibred, but, some specimens exhibit the more slowly forming lamellar-zonal bone. The youngest individual of this age class (MVD-R 16) exhibits lamellar-zonal bone throughout its cortex except in zones with longitudinally-orientated primary osteons in circular rows where thick parallel-fibred bone is present. Older individuals (MVD-R 2b, MVD-R 13 and MVD-R 14) transition from parallel-fibred bone into lamellar-zonal bone in the outer cortex and retain this to the periphery and together with a low vascularisation, indicate a decrease in growth rate.

Five LAGs were observed in MVD-R 16 whereas has four wide annuli and a possible LAG within the inner two annuli were observed in MVD-R 15. Four closely spaced

LAGs at the periphery of MVD-R 14 indicate the presence of an EFS, indicating that bone growth had reached an asymptote.

Sharpey's fibres were visible in a number of the late sub-adults. MVD-R 2b and MVD-R 16 have shallow Sharpey's fibres in the outer cortex and periphery. Younger individual MVD-R 16 has deep Sharpey's fibres (Figure 16) extending into the inner-cortex of the bone.

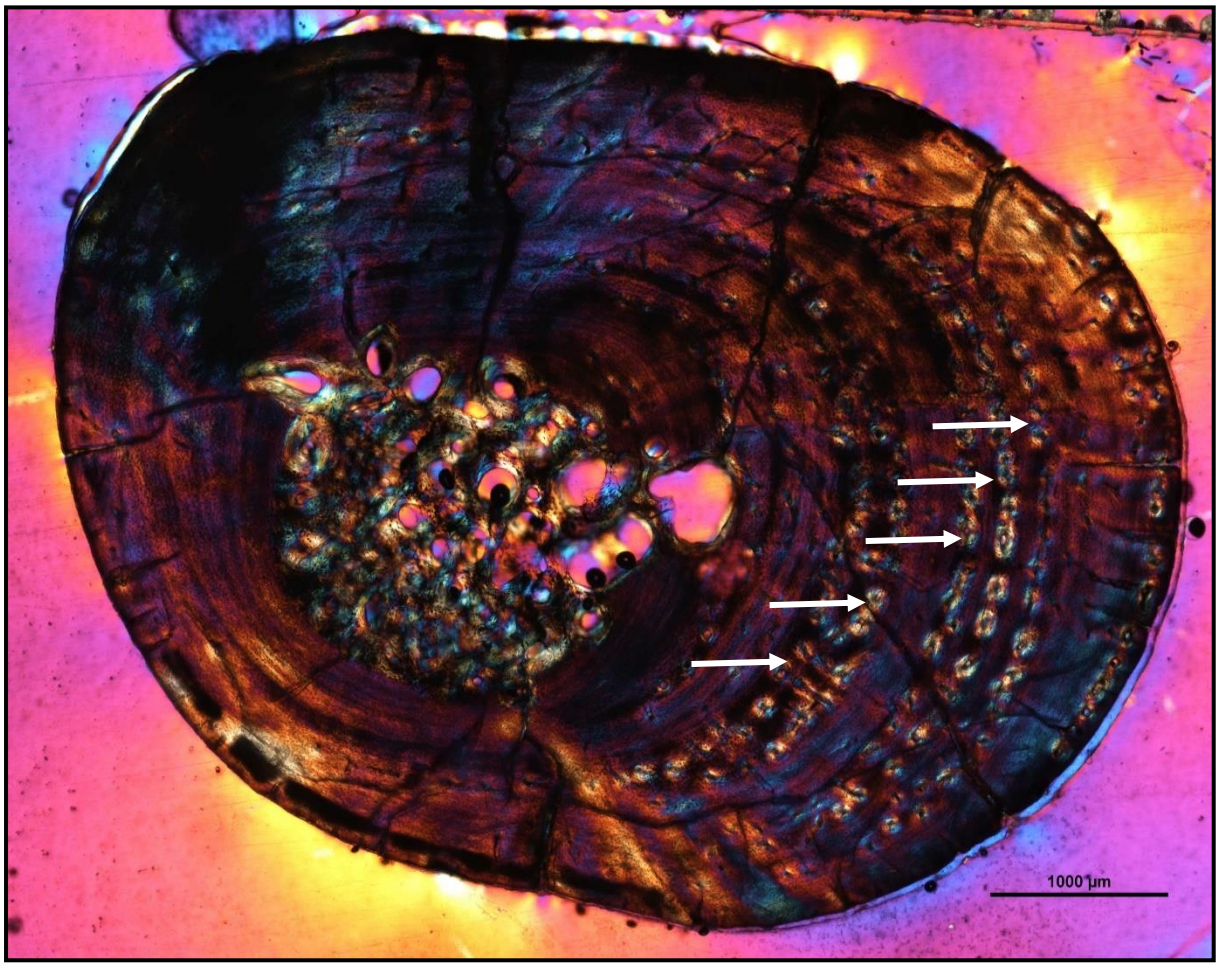

Figure 15: Late sub-adult radius MVD-R 15 showing thick regions of parallel-fibred bone interspersed with longitudinally-orientated primary osteons in circular rows indicating regions faster growth.

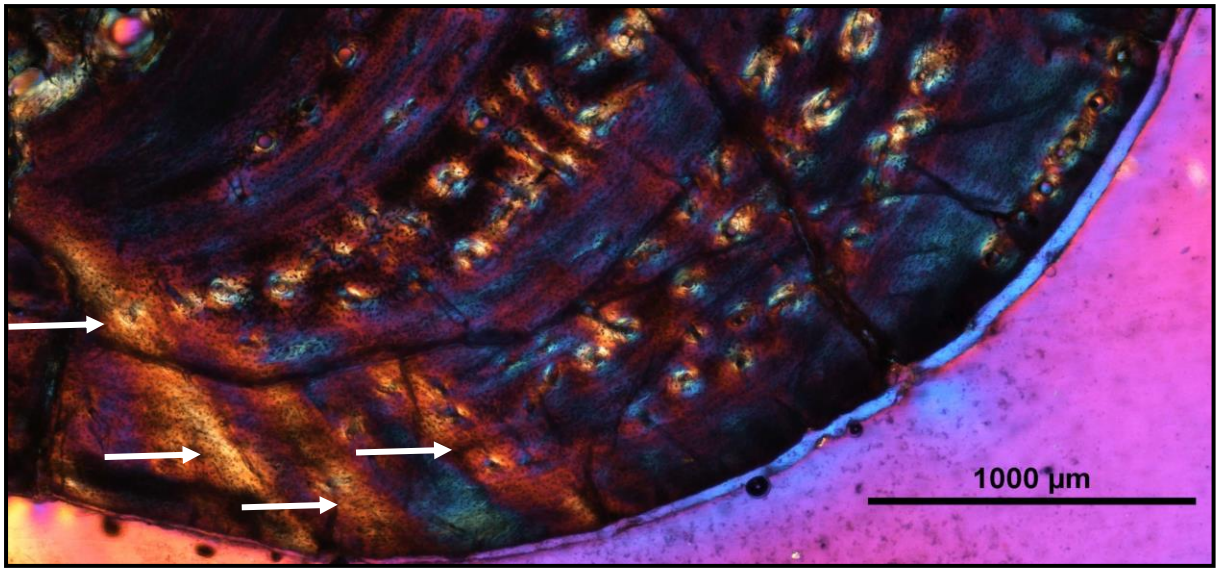

Figure 16: Sharpey's fibres indicating strong muscle insertions in late sub-adult radius MVD-R 15.

4.1.3 Ulnae

4.1.3.1 Juveniles

Medullary cavities are approximately centrally placed and are large with either completely open (MVD-R 12d and MVD-R 12e) or are traversed by one or two thick bony trabeculae seen in MVD-R 18b (Figure 17).

Figure 17: Juvenile ulna MVD-R 18b indicating a relatively thick primary cortex and centrally placed medullary cavity with a few trabeculae traversing the medullary cavity.

The cortex retains its thickness with slight deviations resulting in thicker areas in certain parts of the bone seen in MVD-R 18b (K = 0.480 in MVD-R 18b) compared to an average of 0.62 for MVD-R 12). The youngest individual (MVD-R 12e) has a relaltively low Cg of 0.524 compared to older individuals but this could be a result of the small size of the bone as a deviation in a single cross section could result in the analysis of a region closer to the epihpyses of the bone. The oldest individual of this age class, MVD-R 18b, has a higher Cg of 0.834, similar to older individuals of different age classes.

The bones of the juveniles contain numerous, large globular and oblong osteocyte lacunae (Figure 18). They are generally evenly distributed throughout the bone matrix, but appear more random in the inner cortex and arranged in parallel towards the outer cortex, suggesting an initial deposition of a woven-fibred bone matrix and then a transition to parallel-fibred bone. There are no growth marks in any of the bones. Primary and secondary osteons are absent from all individuals, but the bone contains a few large cavities in the cortex for vascular canals. Vascularisation is relatively low, ranging from 0.39% to 2.68% (Table 3).

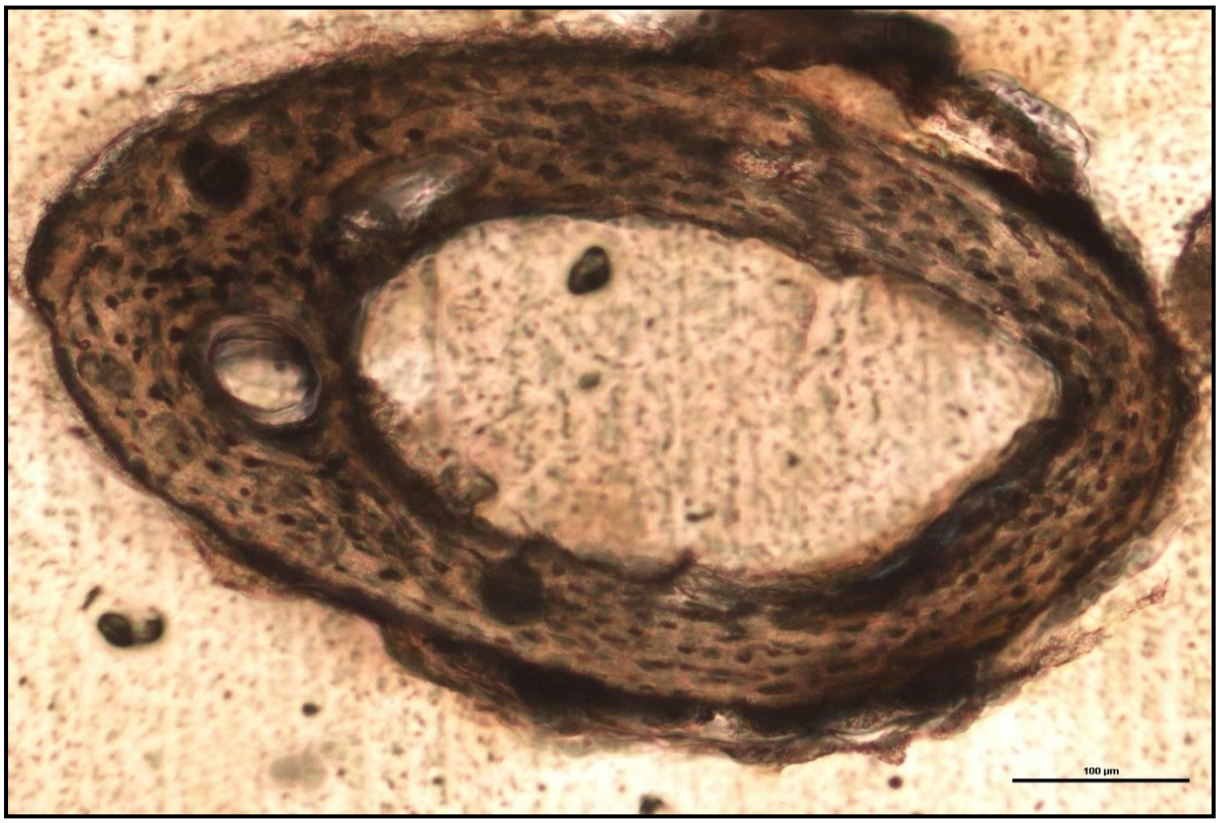

Figure 18: Juvenile ulna MVD-R 12d showing a large open medullary cavity and numerous large globular osteocyte lacunae indicating rapid growth.

4.1.3.2 Early sub-adults

Early sub-adults show a substantial decrease in the size of the medullary cavity. MVD-R 10b, MVD-R 22 and MVD-R 23 have small medullary cavities that are slightly shifted from the centre of the bone. MVD-R 22 and MVD-R 23 have a number of large cavities comprising the entire medullary cavity with a few smaller cavities. The ontogenetic or growth centre is almost completely infilled with bone apart from a small cavity. There is no single large medullary cavity, but instead there are several large resorption cavities beside the ontogenetic centre extending towards the postero/dorsal side of the bone. MVD-R 10b contains a single large cavity near the centre of the bone and a few smaller surrounding cavities. The medullary cavities of the early sub-adults are either circular in shape or resembled the shape of the ulna itself resulting in a “boomerang” shape.

The early sub-adult stage is characterised by thicker cortices (average k = 0.16) and more bone resorption (in the form of resorption cavities and secondary osteons) in the peri-medullary region. These thicker cortices, as seen in MVD-R 22 (Figure 19), and absence of completely open medullary regions (compared to juveniles) results in a higher degree of compactness (Table 3). Early sub-adult specimens have a Cg ranging from 0.924 (MVD-R 23) to 0.954 (MVD-R 22), a clear increase in comparison to juveniles (Table 3). Early sub-adults show clear signs of secondary osteons and resorption cavities.

Figure 19: Early sub-adult ulna MVD-R 22 showing a notably thick cortex and off centred medullary cavity. Note the radiating canals on the anteroventral side of the bone indicating rapid growth in this region.

The bone matrix is predominantly parallel-fibred with randomly distributed small round/oval osteocyte lacunae, but MVD-R 22 and MVD-R 23 display regions of more organised lamellar-zonal bone, particularly towards the periphery of the bone and regions where circular rows and/or radiating canals are present.

There are a few longitudinally orientated primary osteons limited to the inner and mid-cortex, but most of the vascular canals are simple. In certain areas of the thickest part of the cortex radiating canals were observed (Figure 19), indicating more active growth in these regions of the bone (Figure 20). Vascularisation decreases substantially towards the periphery and as a result, early sub-adults average 0.15% (Table 3). Growth marks are present in the form of annuli and LAGs. Three thin closely spaced inner annuli and two outer LAGs were observed in MVD-R 22 whereas five clear annuli WERE OBSERVED IN MVD-R 23. The growth marks were unclear in MVD-R 10b, but at least one annulus was observed.

Sharpey's fibres are present in specimens MVD-R 10b and MVD-R 23 on the ventral side of the bones.

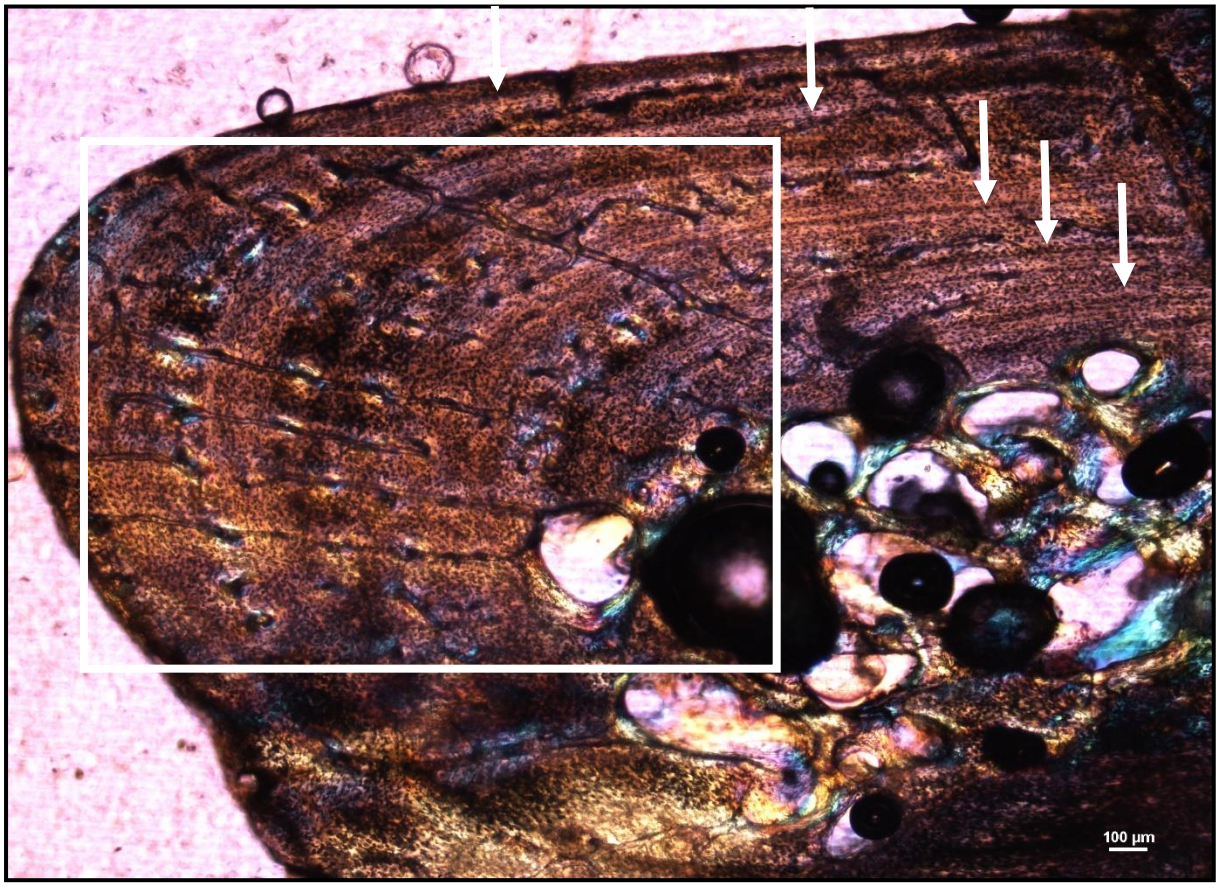

Figure 20: Early sub-adult ulna MVD-R 23 showing radiating vascular canals (square) and five annuli (arrows).

4.1.3.3 Late sub-adults

The medullary cavities of late sub-adults are circular "boomerang'' shaped resembling the shape of the ulna itself. Certain late sub-adults (MVD-R 20 and MVD-R 21) showed a slight increase in the size of the medullary cavity but are otherwise similar to the early sub-adults in regard to the medullary cavity size, shape and placement. Larger late sub-adults (MVD-R 19; MVD-R 2c) have much larger medullary cavities that occupy a larger percentage of the entire bone, leaving very little of the primary cortex intact. Larger cavities are concentrated towards the centre (with exceptions) smaller cavities are found dispersed between them and at the periphery of the medullary region, creating a gradual transition from cancellous to compact bone (Figure 21).

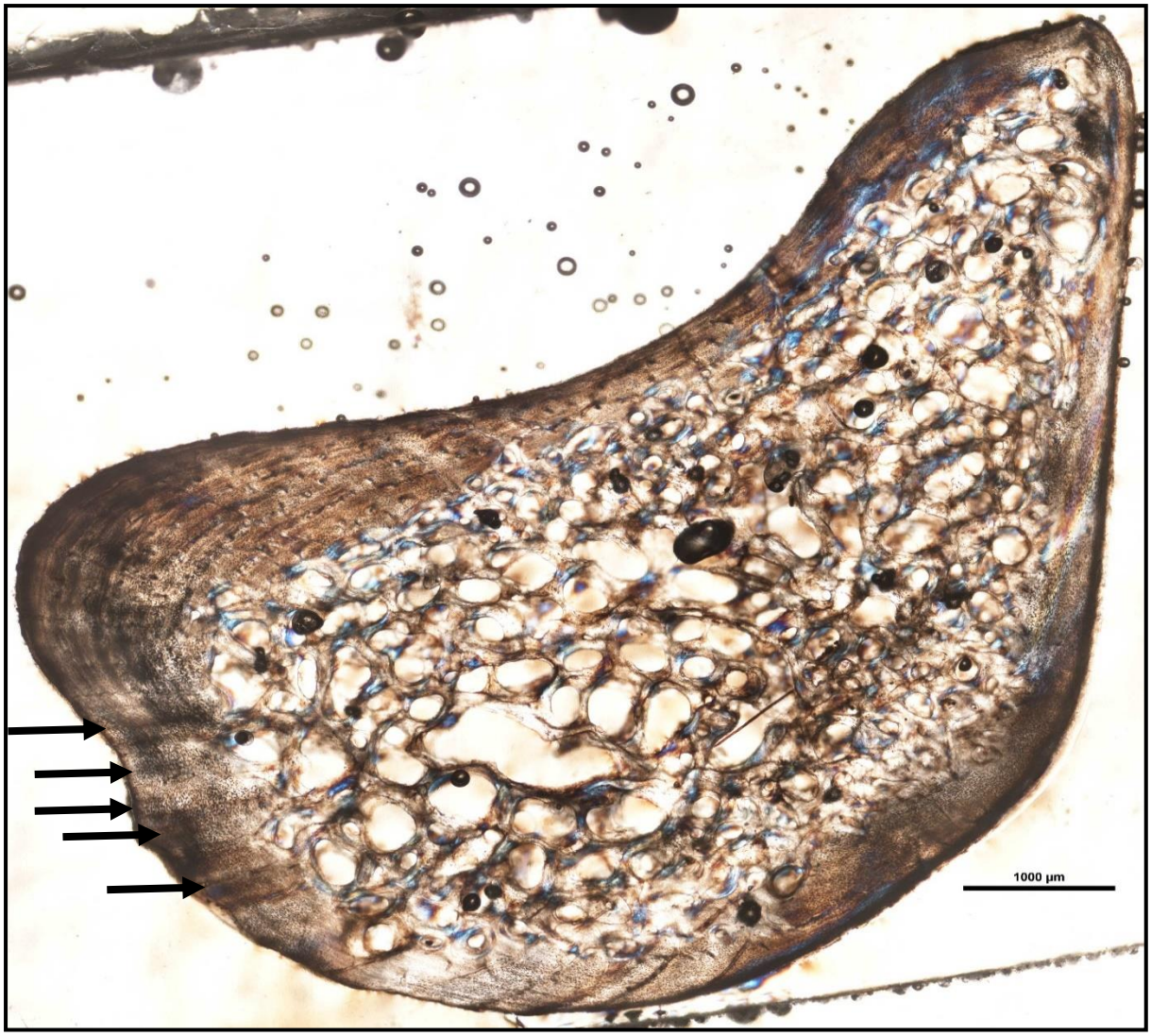

Figure 21: Late sub-adult ulna MVD-R 19 showing extensive resorption of the compact cortex. Note the extensive Sharpey's fibres (arrows) on the ventral side of the bone.

The size of the medullary cavity increases significantly in later developmental stages and as a result, a substantial decrease in the thickness of the cortex is noticeable by the average K value of 0.67 compared to 0.16 seen in early sub-adults. However, as a result of numerous bony trabeculae occupying the medullary cavity, Cg is still high, ranging from 0.804 (MVD-R 2c) to 0.961 (MVD-R 20). Secondary osteons are mainly limited to the peri-medullary region with a few in the surrounding inner-cortex.

The bone matrix is predominantly parallel-fibred with some specimens showing a transition to slower growing lamellae-zonal bone from the mid to outer cortices in regions where circular rows of primary osteons are present. Osteocyte lacunae are flattened and oval, randomly distributed and less organised in the peri-medullary region and in regions where circular rows are not present. Growth marks differed

significantly between specimens. For example: in MVD-R 2c (oldest specimen) only two annuli and one LAG were observed whereas in MVD-R 20 seven annuli were observed. Sharpey's fibres are present in MVD-R 2c (Figure 22), MVD-R 19 (Figure 21), MVD-R 20 and MVD-R 21.

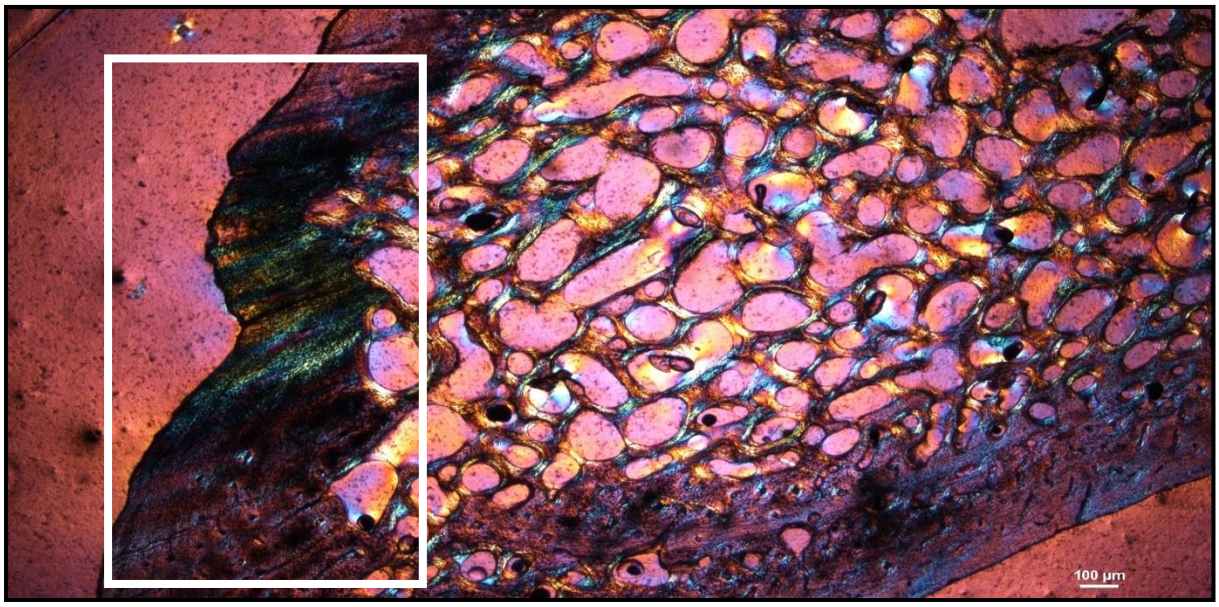

Figure 22: Site of muscle attachment indicated by the presence of Sharpey's fibres in late sub-adult ulna MVD-R 2c.

The late sub-adults have small primary osteons and few simple vascular canals resulting in a poor vascularisation of 0197% (Table 3). Circular rows of longitudinally-orientated primary osteons are also present in these specimens, similar to that seen in the earl sub-adults and other elements. Radiating canals in some specimens such as MVD-R 20 show a regional increase in bone growth and found in areas where the cortex is thicker (Figure 23). Vascularisation is generally consistent but decreases substantially at the periphery of the bone.

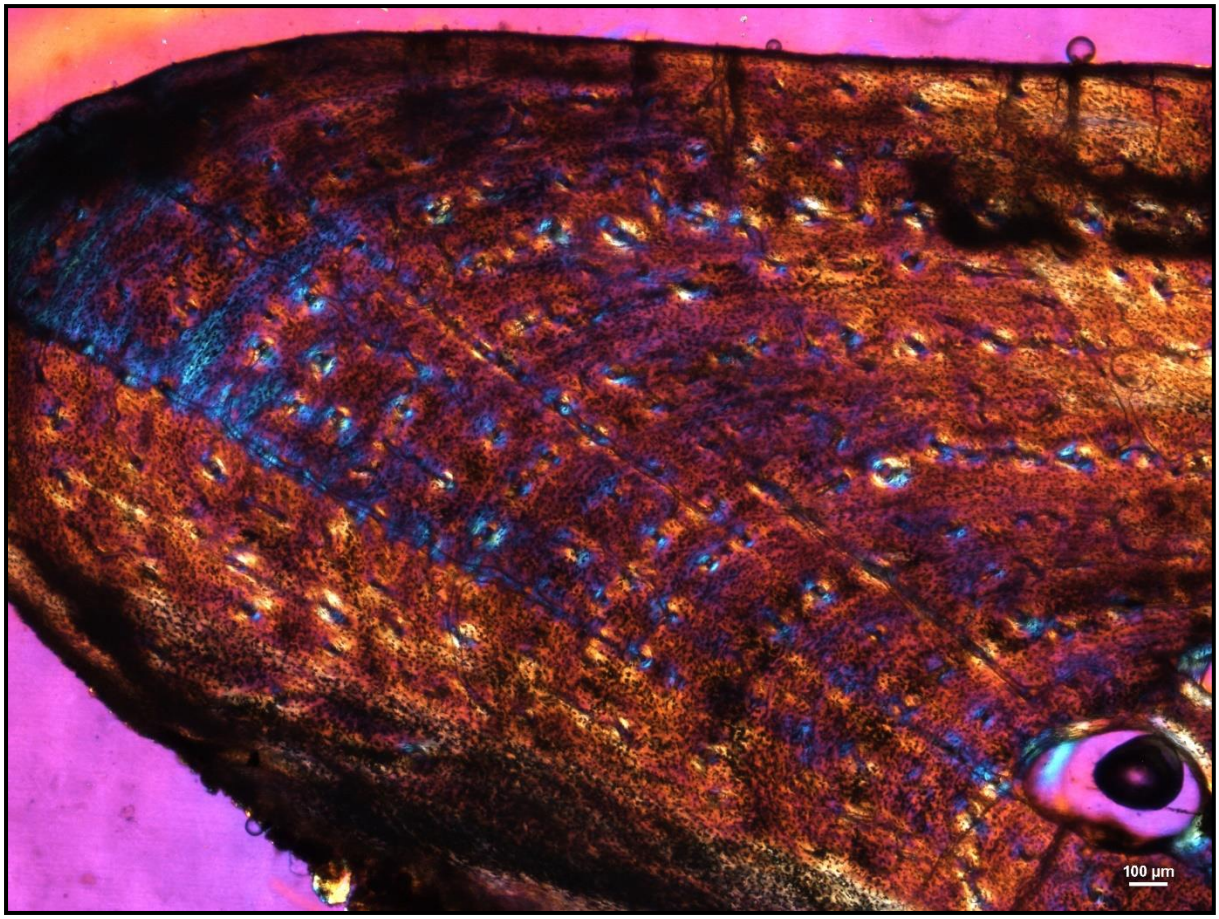

Figure 23: Late sub-adult ulna MVD-R 20 showing circular rows of longitudinally orientated primary osteons. Also note the radiating vascular canals indicating rapid growth in the thickest part of the bone.

4.1.4 Femora

4.1.4.1 Juveniles

Juvenile specimens have circular, centrally placed medullary cavities. MVD-R 12 and MVD-R 11c have open medullary cavities with no bony trabeculae. However, MVD-R 11c also has smaller cavities surrounding the main opening.

Cortices are moderately thick and consistently maintain this thickness around the medullary cavity (average K = of 0.48). Mid-cortical openings are limited but in MVD-R 12f and 12g, there are numerous cavities resulting in an average Cg of 0.71 (Table 3). This value is lower than MVD-R 11c (0.82), which has only a few small openings in the inner cortex. Secondary osteons are not present.

Osteocyte lacunae vary from flat to oval and are generally relatively large, but MVD-R 11c has smaller flattened lacunae that are more neatly arranged compared to MVD-R 12f. The random distribution of osteocyte lacunae in MVD-R 12 suggests the presence of a woven-fibred bone matrix, which is typical of very young individuals. However, the more organised nature of the osteocyte lacunae in MVD-R 11 suggests that the bone matrix is more parallel-fibred. Growth marks are absent except for a possible faint annulus in the mid-cortex of MVD-R 11c (Figure 24). This individual is very young (approximately a few weeks old, based on body size). Thus, it either hatched during an unfavourable growing season and its growth slowed very soon after birth, or the feature represents a hatchling line. Hatchling lines (also known as neonatal lines) are deposited during birth and represent a particularly stressful time in an individuals life (de Buffrénil *et al.* 2008; de Buffrénil & Castanet 2000). They are generally in the form of a LAG that differs from annual LAGs in that it is more pronounced. The annulus in MVD-R 11c is indistinct and cannot be followed around the whole cortex, thus it is unclear at this stage if it does represent a hatchling line. Vascularisation ranges from 0.29% to relatively high at 4.8%. A prominent patch of Sharpey's fibres was observed in MVD-R 11c (Figure 24).

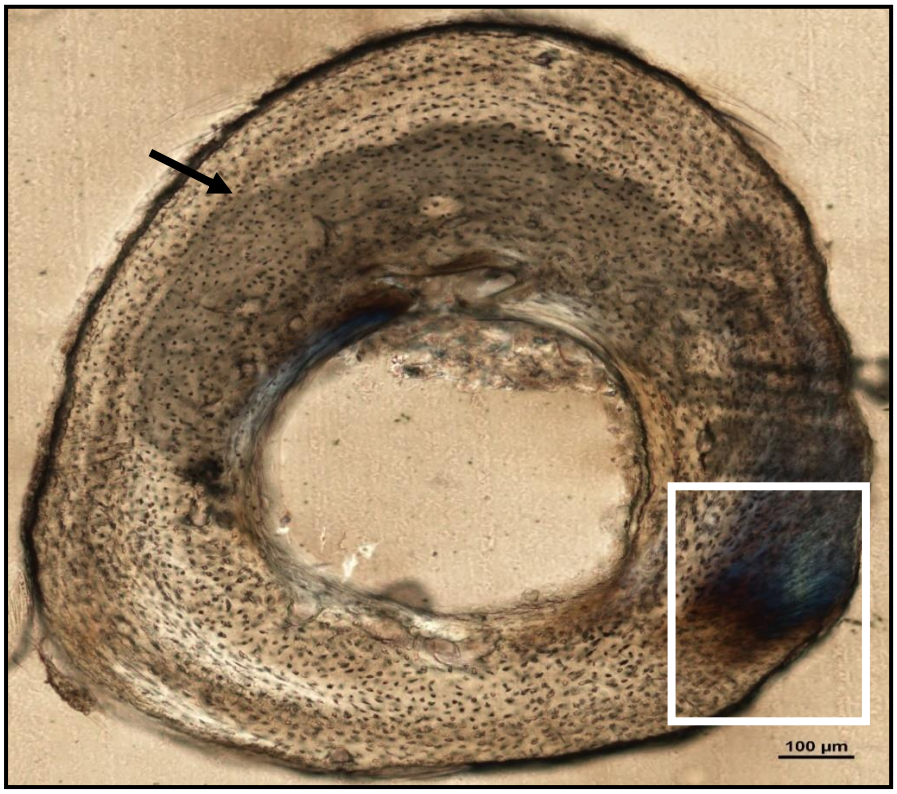

Figure 24: Juvenile femur MVD-R 11c indicating a site of muscle attachment (square) and a possible hatching line (arrow).

4.1.4.2 Early sub-adults

The early sub-adults are limited to two specimens, MVD-R 10c and MVD-R 28. These specimens both have tiny open medullary cavities situated approximately at the centre of the section and are surrounded by smaller cavities, which tend to extend towards the ventral side of the bone. As a result of limited cavities surrounding the main opening, there is a relatively rapid transition from cancellous to compact bone. However, MVD-R 28 shows clear signs of resorption taking place in parts of the cortex that will eventually form part of the medullary cavity (Figure 25).

The cortices of both early sub-adult specimens are thick (average K = 0.25). The thickness is approximately consistent throughout the cortex. Global compactness is high, averaging 0.966 (Table 3). Secondary osteons are extremely limited within both specimens, but there are numerous resorption cavities surrounding the main opening in both MVD-R 10c and MVD-R 28 and as seen in MVD-R 28 a number of cavities extending into the mid and outer cortices.

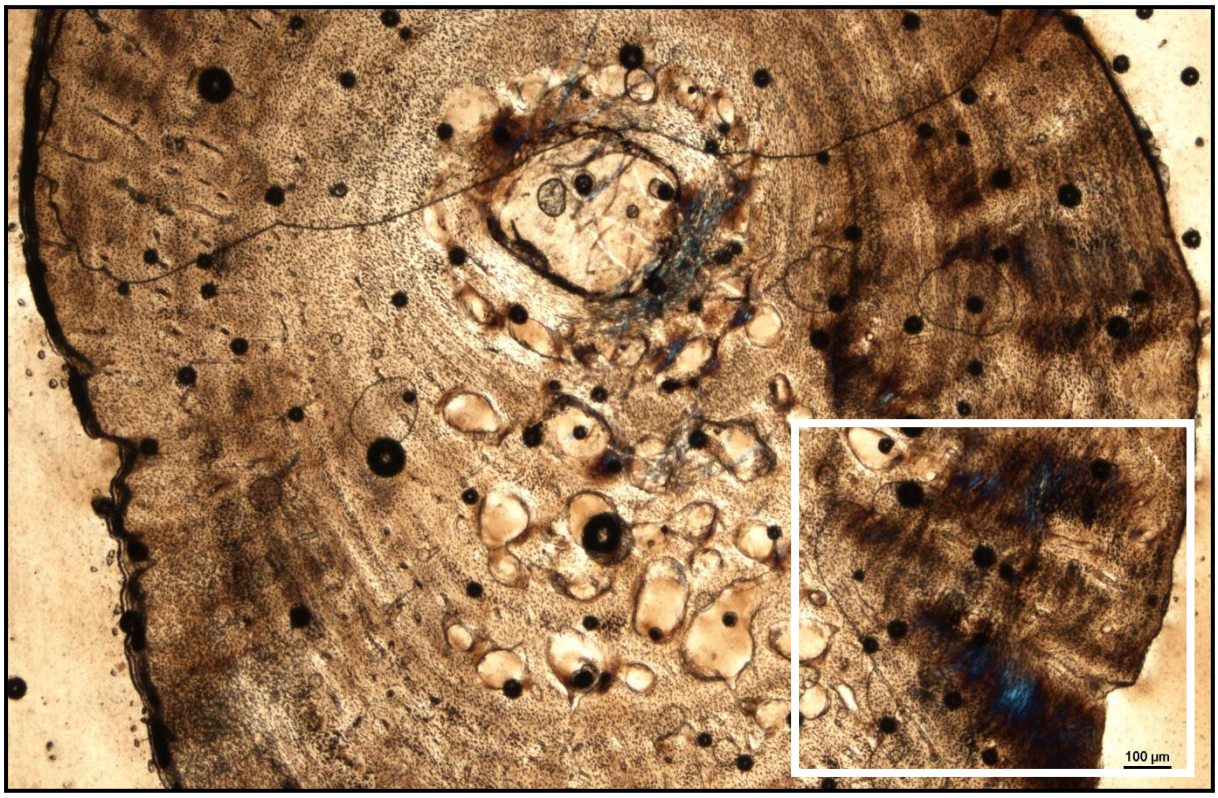

Figure 25: Early sub-adult femur MVD-R 28 showing large resorption cavities extending into the mid-cortex and Sharpey's fibres within the compact cortex.

Both specimens have a parallel-fibred bone matrix with predominantly flattened/oval osteocyte lacunae. However, MVD-R 10c still shows signs of active growth as seen by the uneven, newly deposited bone surface (Figure 26). MVD-R 28 transitions from parallel-fibred bone to lamellar-zonal bone towards the periphery. Vascularisation is similar between specimens. MVD-R 10c has both branched radiating and unbranched simple canals whereas MVD-R 28 shows predominantly unbranched, longitudinally-orientated canals distributed throughout the cortex. Primary osteons are mainly randomly distributed throughout the cortex, but there is at least one circular row of longitudinally-orientated primary osteons present in each specimen. However, as a result of the small size of the vascular canals, vascularisation in the early sub-adults is very low at 0.079% (Table 3). LAGs were observed in both MVD-R 10c and MVD-R 28, with six double LAGs and two LAGs respectively. Sharpey's fibres are prominent in areas of muscle attachment (Figure 25).

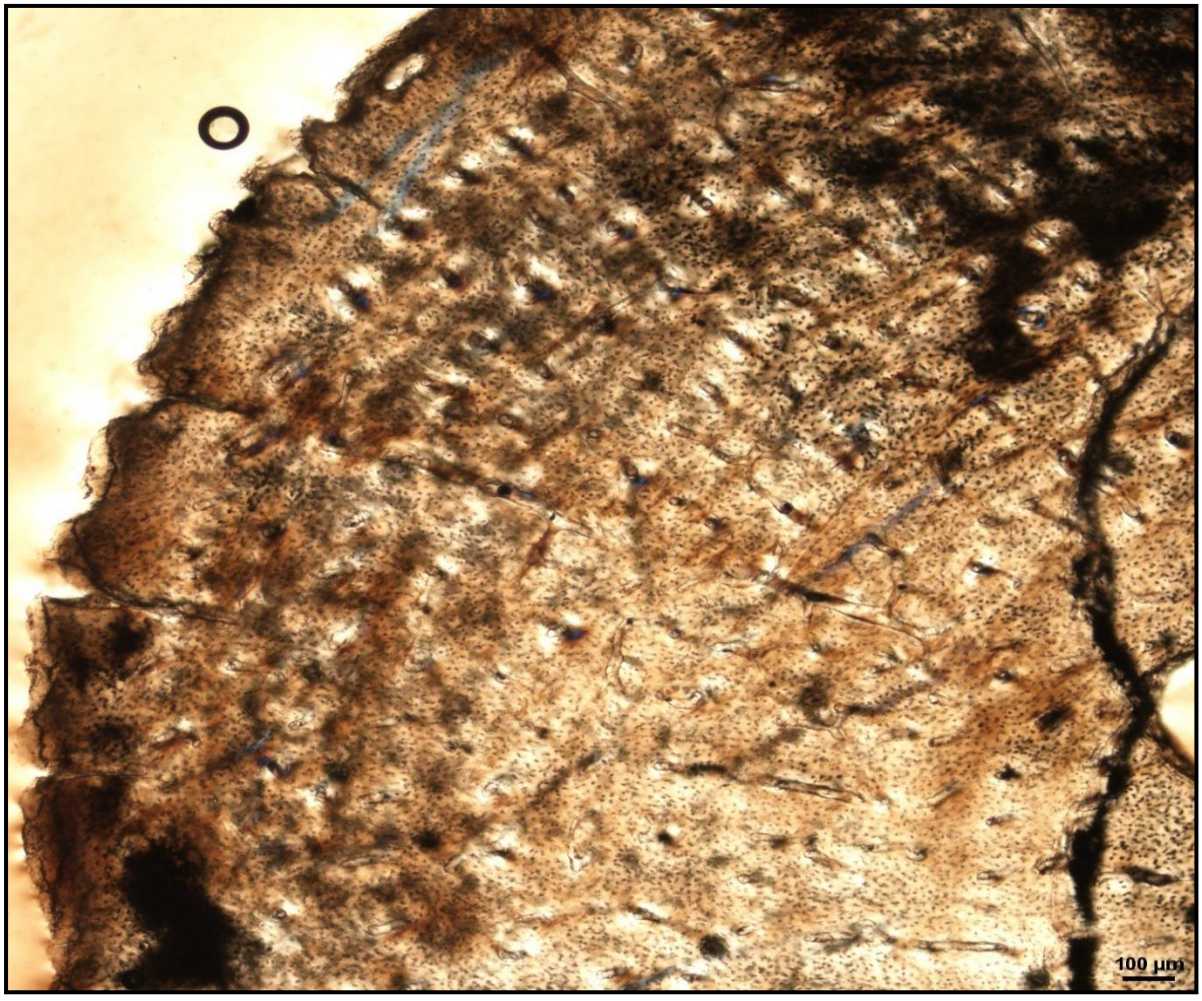

Figure 26: Early sub-adult femur MVD-R 10c showing abundant vascular canals including a few radiating canals. Note the irregular bone surface indicating active bone growth.

4.1.4.3 Late sub-adults

Much of the primary cortex has been resorbed in the late sub-adults. Medullary cavities are filled in with fine bony trabeculae forming cavities throughout the medullary region. Larger cavities are concentrated towards the centre whereas smaller cavities are found closer to the periphery, creating a gradual transition zone (Figure 27). The medullary cavities are circular or oval in shape, with the exception of MVD-R 24 that resembles a square. This difference could be the result of the shape of the bone in a specific region of the mid-shaft.

The cortical regions of late sub-adults are relatively thin compared to early sub-adults (average K = 0.65). Global compactness is moderate to high, ranging from 0.746 (MVD-R 2d) to 0.91 (MVD-R 26) (Table 3). Secondary osteons are few and found mainly within the peri-medullary region

Figure 27: Late sub-adult MVD-R 25 showing a heavily resorbed bone with a large completely infilled medullary cavity. Note the gradual transiton zone.

There is great variation in the type of bone tissue amongst the late sub-adults. The bones of MVD-R 2d, MVD-R 24 and MVD-R 25 are comprised of lamellar-zonal bone

with small flattened osteocytes. MVD-R 26 differs from the other specimens in having a mixture of bone tissues. Organised osteocyte lacunae indicate the presence of parallel-fibred bone, but there are alsdo patches of woven fibred bone as seen by clumps of osteocytes, possibly indicating static osteogenesis. MVD-R 26 appears to have grown more rapidly than the other late sub-adults, which is not unexpected given that it falls within the lower size range of this age class (Figure 26).

Vascularisation is generally extremely limited (0.07-0.13%) as a result of the small, sparse vascular canals. There are mainly unbranched canals, but in MVD-R 2d and MVD-R 24, there are a number of branched canals with short anastomoses. Primary osteons are small, longitudinally-orientated and randomly distributed throughout the cortex. However, MVD-R 26 and MVD-R 2d have circular rows of primary osteons within the cortex.

Growth marks are generally in the form of LAGs, four annuli were observed in MVD-R 26, indicating that growth did not cease completely during the unfavourable growing season. This further supports the evidence noted above that it grew more quickly than the other late sub-adults. There is evidence of muscle attachment in MVD-R 25 and MVD-R 26, in the form of Sharpey's fibres within its cortical bone.

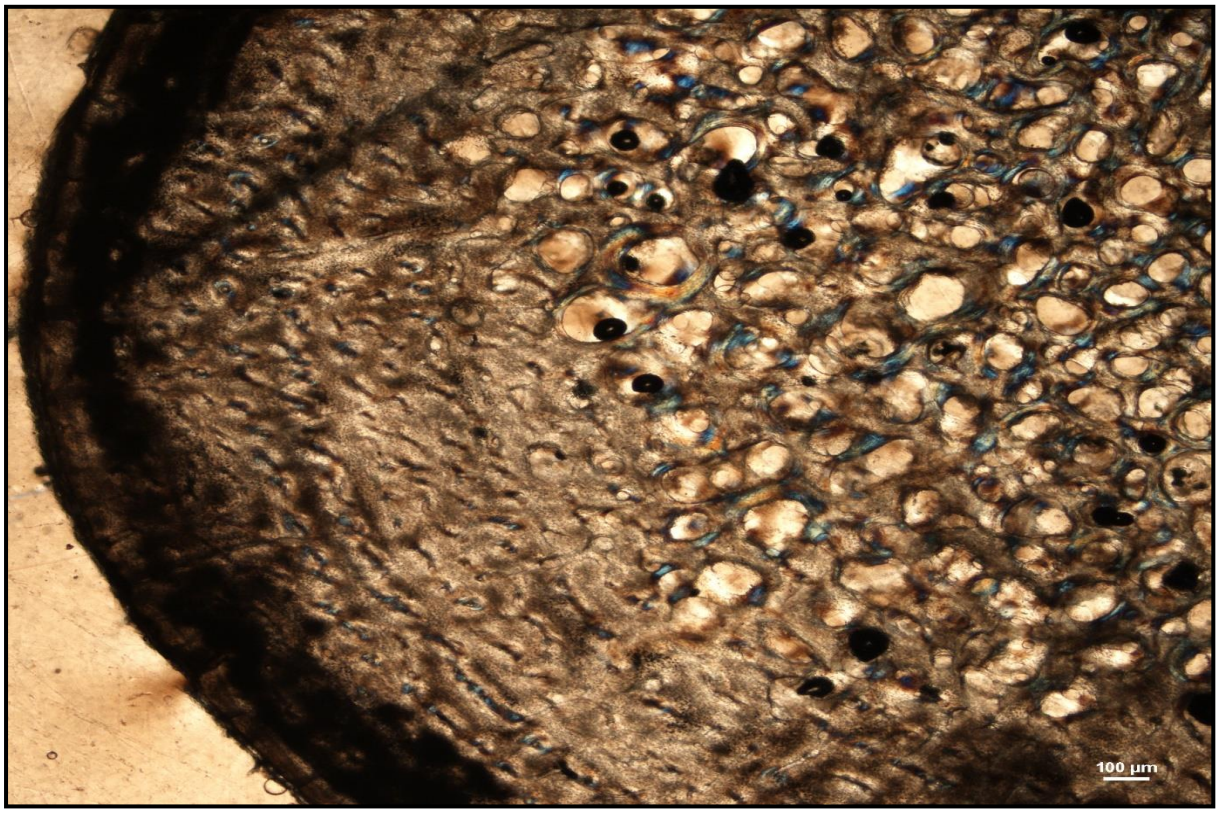

Figure 28: Late sub-adult femur MVD-R 26 showing a sub-reticular vascular arrangement.

4.1.5 Tibiae

4.1.5.1 Juveniles

The medullary cavities of the tibiae of the juvenile specimens all differ from one another. The medullary cavity of MVD-R 12 is open, almost centrally placed and circular (Figure 29) whereas MVD-R 11 has a larger medullary cavity that is partially filled in with bony trabeculae resulting in smaller cavities. However, this, once again, could be a result of the small size of the bones and the major differences along the small diaphysis.

Figure 29: Juvenile tibia MVD-R 12h showing an open medullary cavity. Cortical cavities indicate passage for vascular canals.

The cortical regions of the juvenile specimens also differ quite notably. MVD-R 11 has an average K value of 0.74 whereas MVD-R 12 has an average K value of 0.57. MVD-R 11 has a thin medullary cavity that varies in thickness in different regions of the bone resulting in an average Cg of 0.645. MVD-R 12 has a relatively low average Cg of 0.635 (See Table 3 for different Cg values). However, these differences could be due to the small size of the bones resulting in major differences between close.

The osteocyte lacunae in the juveniles range in shape from flattened to oval. They are generally evenly distributed throughout the cortex. The bone matrix is parallel-fibred. Vascular canals are not particularly abundant (average vascularisation 1.5%) and are

in a form of simple longitudinally-orientated canals (Figure 29); primary osteons have yet to form. Growth marks are absent.

4.1.5.2 Early sub-adults

Early sub-adults are limited to a single specimen, MVD-R 33. The ontogenetic centre is similar to that seen in the early sub-adult ulnae in that it is almost completely infilled with bone and only a few small resorption cavities are present beside it. Secondary osteons are sparse and limited to the medullary region. This results in an extremely thick cortex (Figure 30) with a K value of 0.14 and a high Cg of 0.987.

Figure 30: Early sub-adult tibia MVD-R 33 showing a tiny medullary cavity and extremely thick compact cortex.

The bone tissue is lamellar-zonal with dense, organised and flattened osteocyte lacunae. Five LAGs were observed in the cortex (Figure 31). The simple vascular canals are mostly simple, branched and unbranched, with a few very small primary osteons (vascularisation 0.06%). However, there are also thin radiating canals within the thickest part of the cortex (Figure 32). Vascularisation decreases slightly at the periphery.

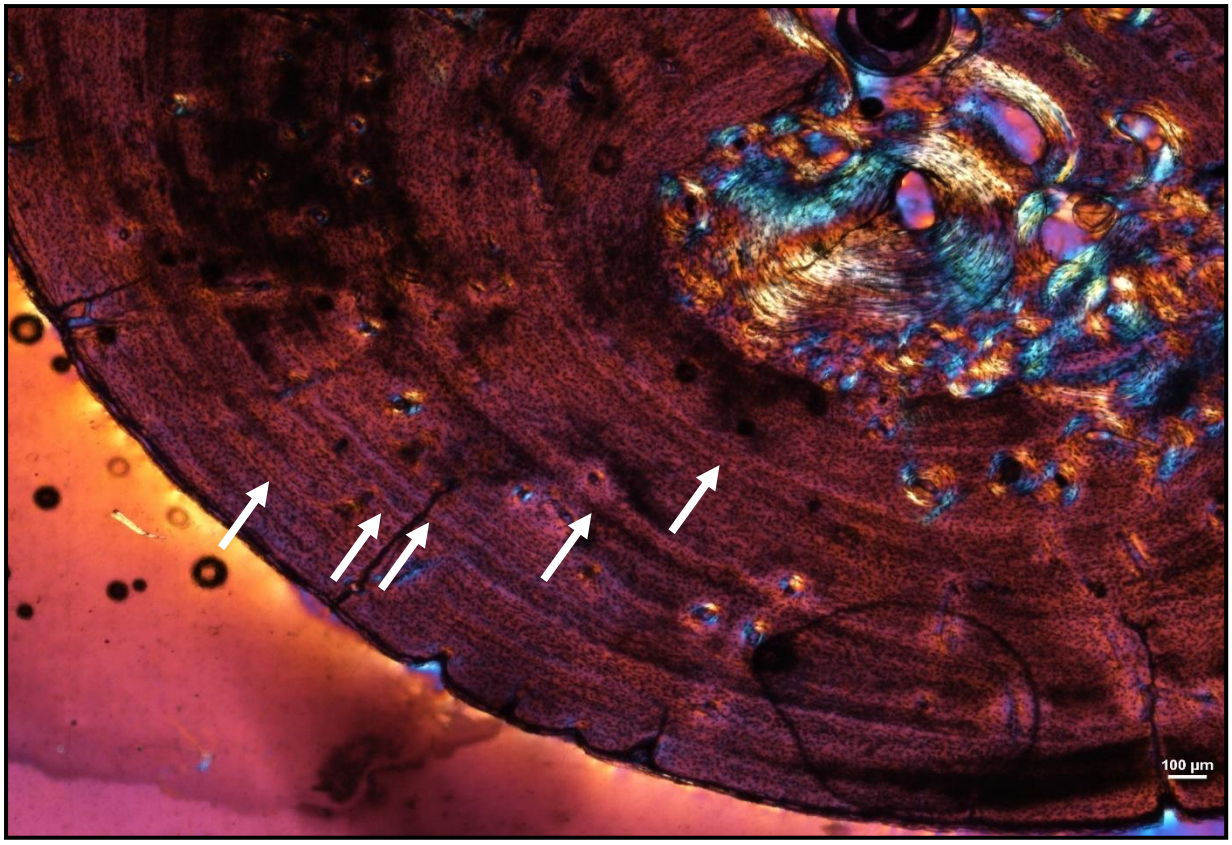

Figure 31: Early late sub-adult tibia MVD-R 33 showing slowly growing lamellar-zonal bone. Arrows indicate growth marks.

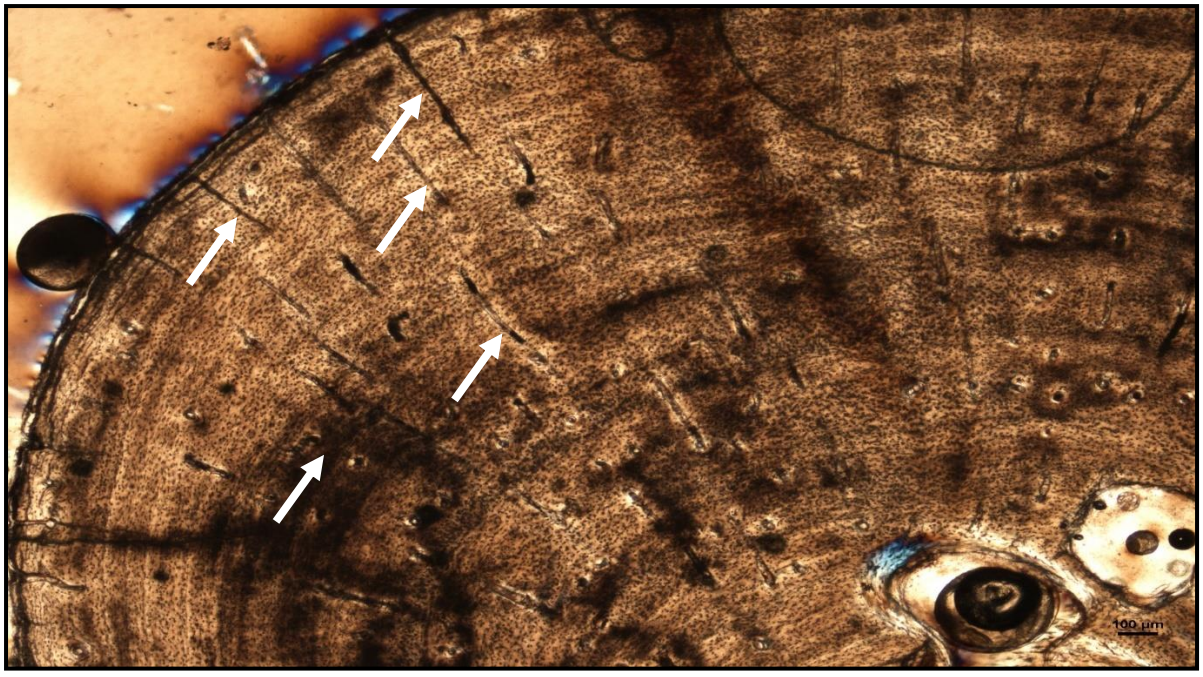

Figure 32: A region of early sub-adult tibia MVD-R 33 with a few radiating simple vascular canals in an otherwise slowly forming lamellar-zonal bone tissue.

4.1.5.3 Late sub-adults

The medullary cavities of the late sub-adults are small, approximately centrally placed and filled in with bony trabeculae. Cavities are relatively large throughout the medullary cavity but there are a number of smaller cavities towards the inner cortex creating a slightly gradual transition zone. Medullary cavities of older specimens (MVD-R 2e and MVD-R 29) are larger compared to younger specimens (MVD-R 30, MVD-R 31a and MVD-R 32). Most medullary cavities are circular/oval in shape but MVD-R 30 has a more triangular-shaped cavity.

The cortices of MVD-R 30, MVD-R 31a (Figure 33) and MVD-R 32 are thick and remain so throughout the section (average K = 0.28). In contrast, the ontogenetically older MVD-R 2e and MVD-R 29 have thinner cortices, which vary in thickness around the bone (average K value of 0.62). Despite this, Cg is approximately constant amongst the various specimens with an average of 0.91 (Table 3). Secondary osteons and resorption cavities are numerous in the inner cortex as well as in the peri-medullary region. Secondary osteons are also more abundant in the younger compared to older individuals (note the row of secondary osteons in MVD-R 31a as seen in Figure 33).

The bones of the late sub-adults are comprised of lamellar-zonal-bone tissue with highly organised flattened/oval osteocyte lacunae in parallel rows throughout the cortex. There are slight deviations in MVD-R 30 and MVD-R 31a (Figure 33), where parallel-fibred bone tissue is present in the inner cortex of the bone. Vascular canals are small and mainly unbranched in all specimens. However, there are a number of branched simple canals with short anastomoses. Primary osteons are small, sparse, longitudinally-orientated and randomly distributed throughout the cortex. However, there are a number of circular rows in MVD-R 30 and MVD-R 2e whereas MVD-R 29 shows signs of circular rows but as a result of resorption, these are rare. As a result of the small size and limited number of canals and primary osteons, vascularisation is poor in all specimens, ranging from 0.079% (MVD-R 29) to 0.11% (MVD-R 2e and MVD-R 30) (Table 3).

Growth marks differ between specimens, but in most of the specimens there is a combination of both LAGs and annuli within the cortex. In MVD-R 31a a triple annulus, two single annuli and two double LAGs were observed, but in MVD-R 29 six LAGs and

MVD-R 32 five annuli. There are Sharpey's fibres present in MVD-R 30, MVD-R 31a (Figure 33) and MVD-R 32.

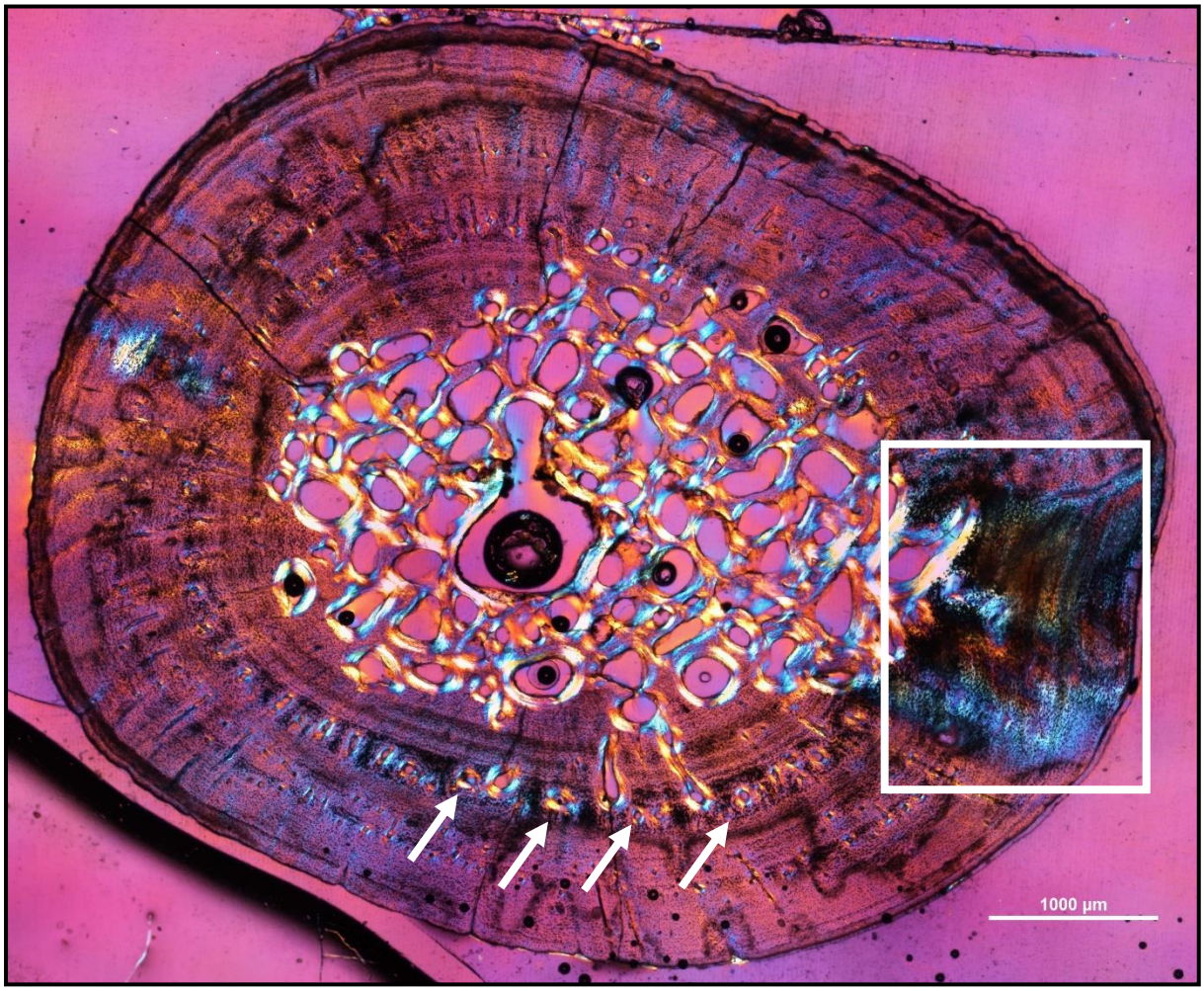

Figure 33: Late sub-adult tibia MVD-R 31a showing a lamellar-zonal bone tissue and large medullary cavity completely infilled with fine bony trabeculae and Sharpey's fibres indicating muscle attachment (square).

4.1.6 Fibulae

4.1.6.1 Juveniles

The medullary cavities of the juveniles are open except for MVD-R 12k, which has small bony trabeculae separating the medullary cavity into five cavities. MVD-R 12j and MVD-R 11f have similar cavities but MVD-R 11f has a centred, single, circular medullary cavity (Figure 34) and MVD-R 12k has an oval medullary cavity comprising a number of cavities.

MVD-R 12k and MVD-R 12j have thin cortices (average = 0.67) with constant thickness almost throughout the section, possibly due to the section including part of the metaphysis (due to the tiny size of the bones, it was difficult to obtain the perfect cross-section through the mid-diaphysis). MVD-R 11f has a thick cortex (K = 0.33) and provides a good representation of the bone histology of the juvenile fibula and will be the focus of the description here. As a result of this noted above, MVD-R 11f has a high Cg of 0.89 and MVD-R 12k and MVD-R 12j average a Cg of 0.62 (Table 3).

The osteocyte lacunae range from flattened to globular, but all are generally aligned roughly parallel to one another, indicating a parallel-fibred bone matrix. Vascularisation is either absent or very low (MVD-R 12k, 0.87%) suggesting a relatively slow growth rate (Table 3). There are no growth marks present in any of the juvenile specimens. MVD-R 11f shows a small region in cross polarised light (Figure 34) that appears to be Sharpey's fibres and may represent a site of muscle attachment. This differs from all (except juvenile femur MVD-R 11c, see Figure 24) juvenile bones where Sharpey's fibres were not observed.

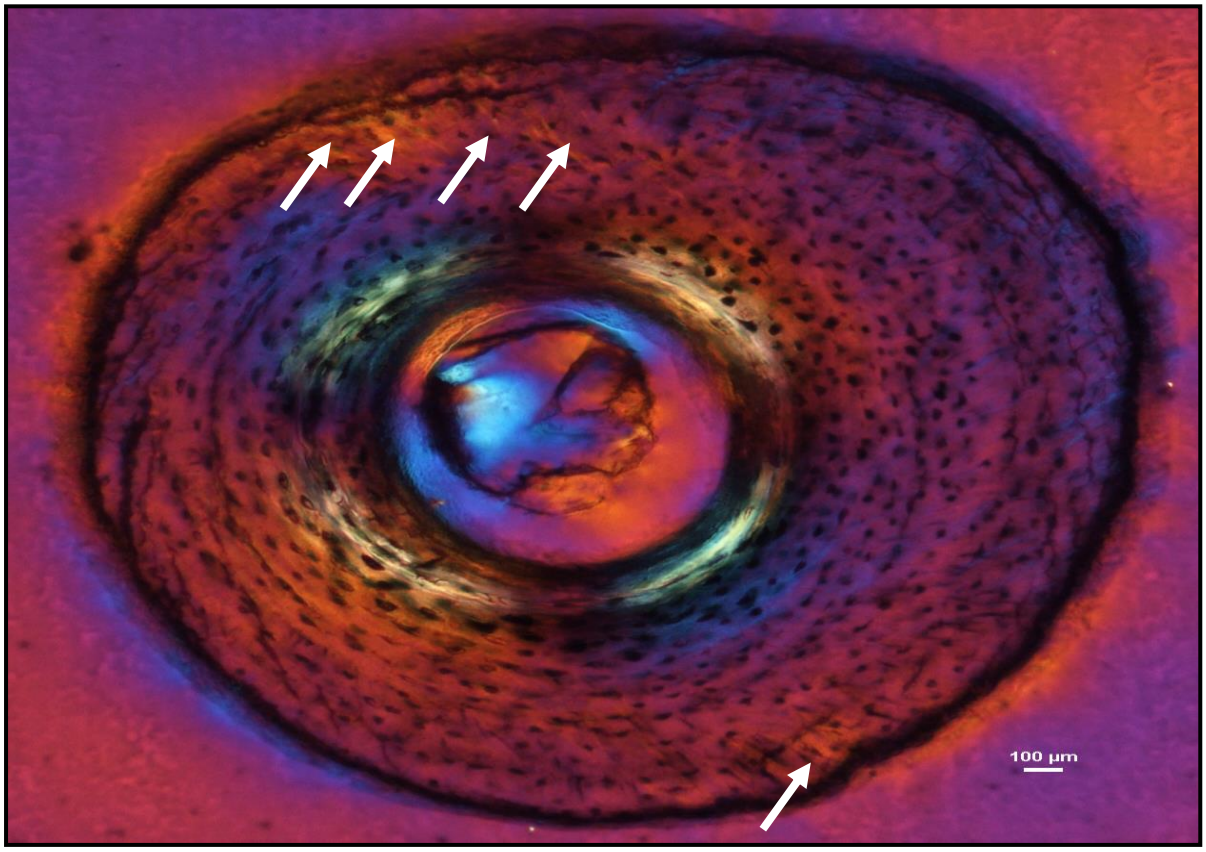

Figure 34: Juvenile fibula MVD-R 11f showing a relatively thick cortex and open medullary cavity. Arrows indicate Sharpey's fibres for muscle attachment.

4.1.6.2 Early sub-adults

Early sub-adults are limited to a single specimen, MVD-R 36. MVD-R 36 has a filled in circular medullary cavity. The cavity is surrounded by a number of smaller cavities, but the transition between compact and cancellous bone is still sharp. The cortex is thick throughout the section with a k value of 0.15 and a Cg of 0.957 (Table 3).

The bone tissue is lamellar-zonal-bone with dense flattened osteocyte lacunae that neatly organised in parallel rows and in certain areas, randomly distributed (Figure 35).

Simple vascular canals are both branched and unbranched and randomly distributed throughout the cortex with a number of thin radiating canals in the thickest part of the cortex. There are few small primary osteons, but they are rare and limited to the inner cortex. Vascularisation is very low (0.07%) and further decreases towards the periphery indicating an overall decrease in bone growth (Table 3). Six LAGs were observed (five single LAGs and one double LAG) (Figure 35).

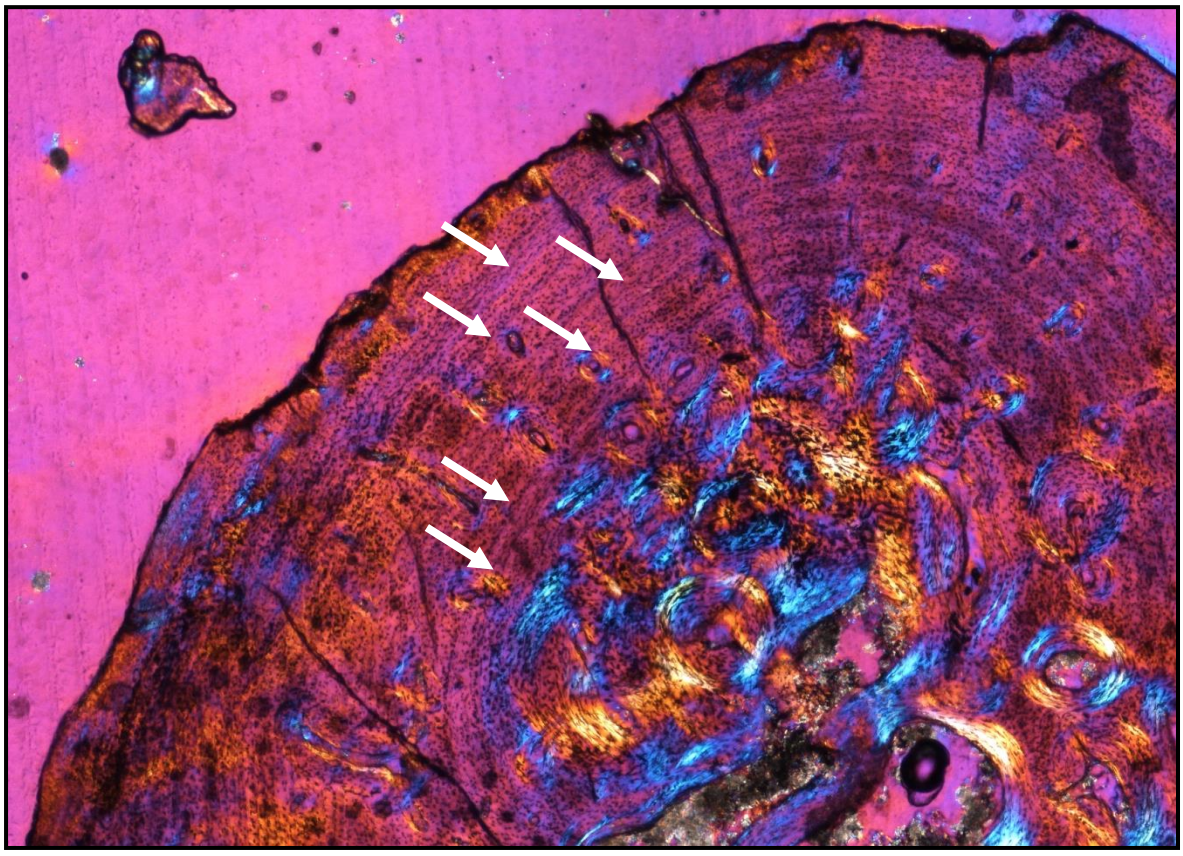

Figure 35: Early sub-adult fibula MVD-R 36 showing poorly vascularised slowly forming lamellar-zonal bone tissue. Arrows indicate growth marks.

4.1.6.3 Late sub-adults

The medullary cavities are all centrally placed and exhibit a variety of different shapes. MVD-R 31b resembles a diamond, MVD-R 35 is rectangular whereas MVD-R 34 and MVD-R 2f are oval. Medullary cavities are all infilled with bony trabeculae. Larger cavities are concentrated towards the centre and cavities decrease in size towards the periphery, creating a gradual transition zone.

Cortices are thick (average K = 0.28) in the younger late sub-adults (MVD-R 31b, MVD-R 34 and MVD-R 35) but the cortex is thinner in MVD-R 2f (K value = 0.550). As a result, MVD-R 2f has the lowest Cg of 0.822 compared to 0.936 in MVD-R 34 (Table 3). Secondary osteons are rare but resorption cavities are numerous and concentrated in the peri-medullary region and inner cortex.

All specimens have a lamellar-zonal-bone tissue with flat and oval osteocyte lacunae that are distributed in a relatively orderly fashion throughout the cortex. Growth marks are present on all of the late sub-adult specimens but as a result of dense osteocyte lacunae obscuring them, the accuracy of these counts may prove to be low. Despite this, a number of growth marks are worth mentioning. MVD-R 35 has approximately 10 LAGs that are observable whereas MVD-R 34 and MVD-R 2f both have an EFS at their periphery (Figure 36). Sharpey's fibres are present in all late sub-adult specimens (MVD-R 35, Figure 37).

Vascular canals are predominantly simple, small and unbranched and show a substantial decrease towards the periphery. As a result, vascularisation is low, ranging from 0.062% MVD-R 34) to 0.13% (MVD-R 31b) (Table 3). A few longitudinally-orientated primary osteons are present, and in MVD-R 35, are arranged in circular rows.

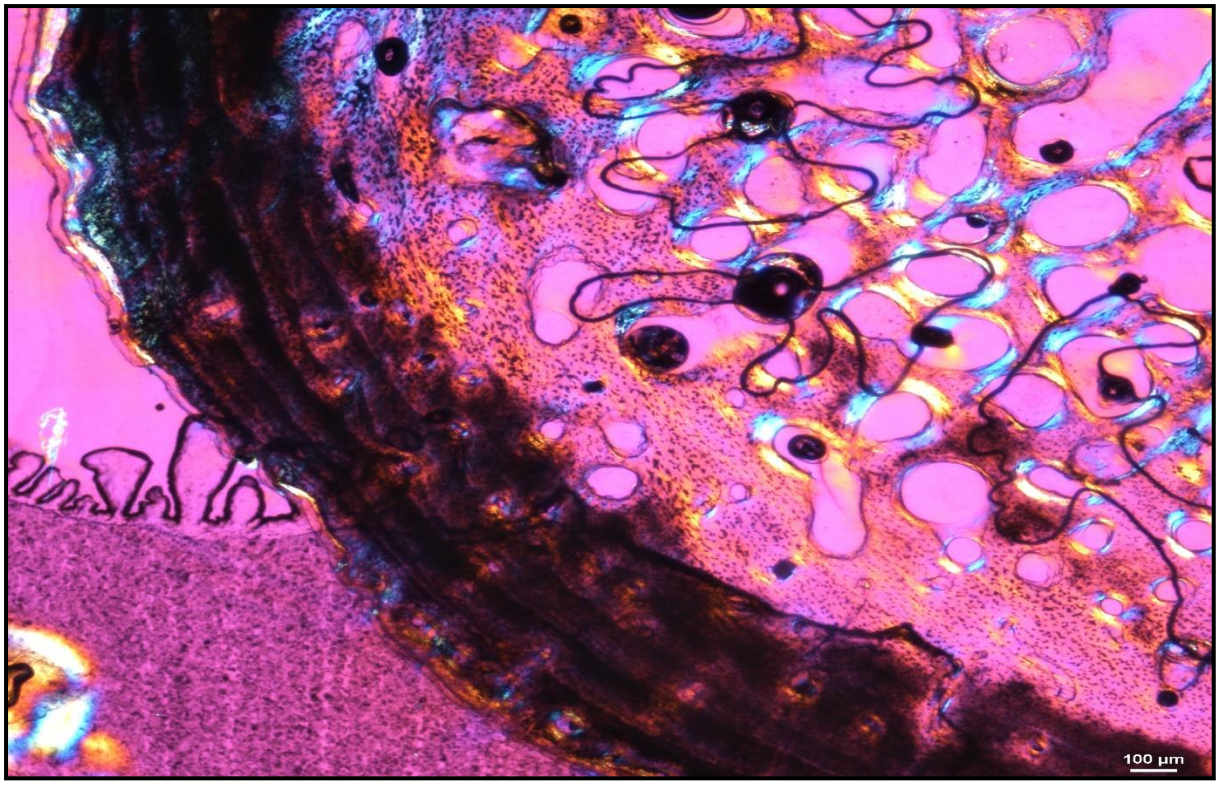

Figure 36: Late sub-adult fibula MVD-R 2f showing peripheral closely spaced LAGs indicative of an EFS.

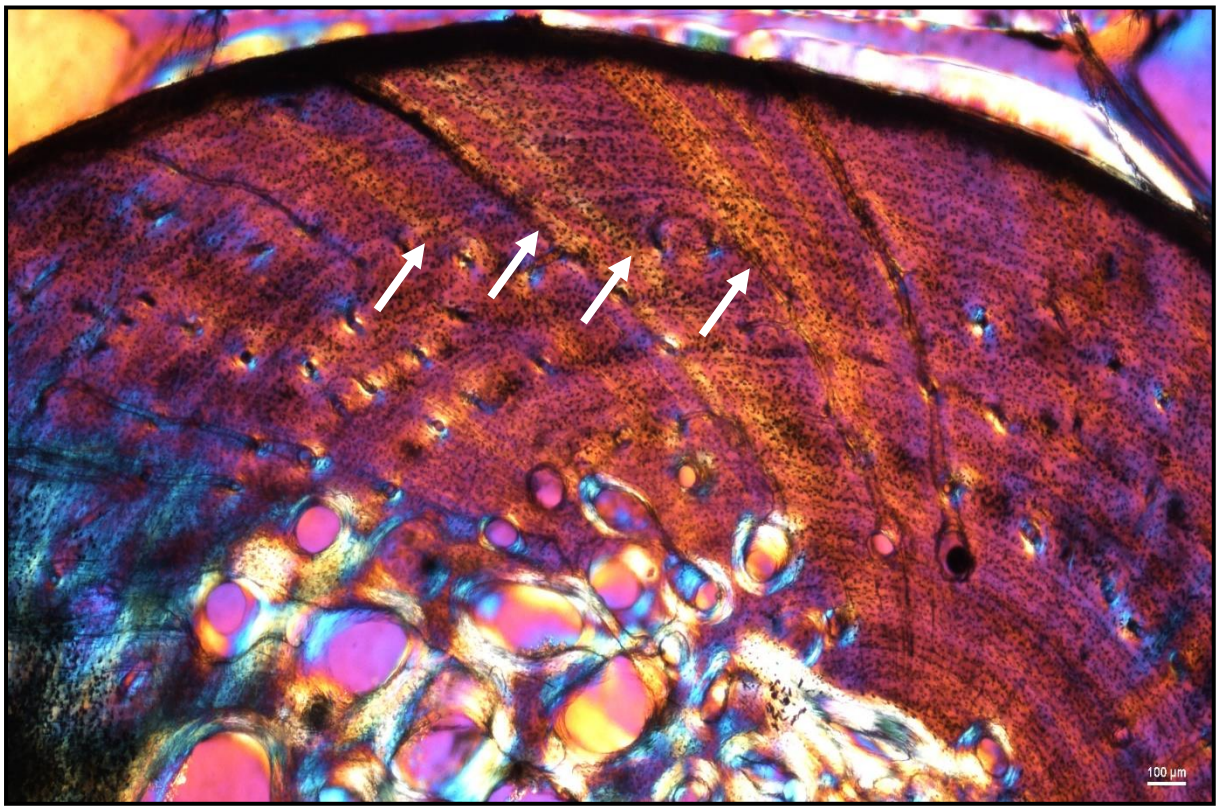

Figure 37: Sharpey's fibres in the late sub-adult fibula MVD-R 35 extending deep into the cortex indicating a strong muscle attachment.

4.2 Lifestyle

Together with the above mentioned histological analysis, a lifestyle analysis was done using Bone Profiler for Windows V 4.5.8 (Girondot & Laurin 2003) where values for Min (representative value for the minimum compactness), Max (representative value for the maximum compactness), S (the value proportional to the width of the transition zone between the medullary cavity and cortex) and P (the materialised value of the transition area between the medullary cavity and compact cortex) (Quemeneur *et al.* 2013) were inserted into supplementary files, together with global compactness and bone diameter, from Germain & Laurin (2005) to determine lifestyle readings. However, formulas have only been developed for certain bones (humerus, radius and tibia and femur) and as a result, the lifestyle for the fibula and ulna were excluded. Also, certain variables could not be obtained to produce a lifestyle reading for he femora.

Lifestyle readings remained constant throughout all early sub-adult and late sub-adult specimens. These readings suggested that *Stigmochelys pardalis* was an aquatic species which is clearly incorrect However *Nakajima et al.* (2014) found that the results for their humerus (MNHN-ZA-AC 2010-2) suggested an amphibious lifestyle. There were, however, a number of deviations within the juvenile samples. Juvenile humerus MVD-R 12a suggested an amphibious lifestyle whereas juvenile tibii MVD-R 11d and MVD-R 11e, suggested a terrestrial lifestyle. However, sections from MVD-R 11d and MVD-R 11e were taken closer to the epiphyses, resulting in incorrect lifestyle readings. However, once again, this has to be explained with a larger sample size looking at various parts of the bone.

A Wilcoxon rank sum test with continuity correction was completed for the global compactness and K values (ratio of the internal diameter to the external diameter) (Currey & Alexander 1985) for all of the elements to determine the similarity between the bones.

H_0: There is no difference between elements

H_a: There is a difference between elements

Significance = 0.05

After the tests had been completed, all of the p-values were greater than 0.05, thus the null hypothesis is accepted and it can be concluded that there is no significant

difference between samples in terms of their compactness or k values (See appendix 6 for complete list of p-values after completion of the test).

Table 4: Compactness profiles for the specimens used in the study. Note the almost invariable lifestyle reading despite different values for Min (minimum compactness), Max (maximum compactness), P (transition area) and S (proportional value of the width transition zone) (0-aquatic; 1: amphibious; 2: terrestrial). See text for explanation of the variables.

Accession #	Element	Min	Max	S	P	Lifestyle reading
MVD-R 12b	Humerus	1.518	0.969	0.071	0.514	0
MVD-R 12a	Humerus	0.219	0.999	0.071	0.646	1
MVD-R 11b	Humerus	0.551	0.999	0.052	0.560	0
MVD-R 11a	Humerus	0.445	0.996	0.042	0.692	0
MVD-R 10a	Humerus	0.494	0.997	0.062	0.107	0
MVD-R 9	Humerus	0.872	0.999	0.042	0.441	0
MVD-R 8	Humerus	0.529	0.999	0.077	0.254	0
MVD-R 7	Humerus	0.764	0.999	0.038	0.397	0
MVD-R 6	Humerus	0.721	0.999	0.039	0.480	0
MVD-R 5	Humerus	0.573	0.999	0.051	0.436	0
MVD-R 4	Humerus	0.541	0.999	0.063	0.407	0
MVD-R 3	Humerus	0.492	0.999	0.076	0.570	0
MVD-R 2a	Humerus	0.634	0.999	0.041	0.638	0
MVD-R 1	Humerus	0.544	0.999	0.078	0.427	0
MNHN-ZA-AC 2010-2	Humerus	0.000	0.996	0.061	0.427	1
MVD-R 12c	Radius	1.131	0.999	0.022	0.754	0
MVD-R 18a	Radius	0.468	0.999	0.044	0.591	0
MVD-R 17	Radius	3.041	0.999	0.061	0.036	0
MVD-R 16	Radius	0.456	0.999	0.046	0.322	0
MVD-R 15	Radius	2.295	0.999	0.084	0.119	0
MVD-R 14	Radius	1.280	0.999	0.157	0.157	0
MVD-R 13	Radius	0.609	0.999	0.078	0.498	0
MVD-R 2b	Radius	0.531	0.999	0.074	0.452	0
MVD-R 12i	Tibia	7.270	0.999	0.020	0.706	0
MVD-R 12h	Tibia	1.312	0.974	0.016	0.442	0
MVD-R 11e	Tibia	0.183	0.999	0.039	0.729	2
MVD-R 11d	Tibia	0.528	0.999	0.023	0.754	2
MVD-R 33	Tibia	0.480	0.999	0.039	0.143	0
MVD-R 32	Tibia	0.359	0.999	0.039	0.403	0
MVD-R 31a	Tibia	1.160	0.999	0.132	0.187	0
MVD-R 30	Tibia	0.507	0.997	0.089	0.251	0
MVD-R 2e	Tibia	0.724	0.999	0.056	0.638	0
MVD-R 29	Tibia	0.750	0.999	0.055	0.596	0

5. DISCUSSION

5.1 Bone growth through ontogeny

Bone, like any biological system, changes through time. Bone microstructure undergoes numerous changes as a result of ontogeny, biomechanics, phylogeny, and environment (Francillion-Vieillot *et al*. 1990). The rate and type of change may even differ between taxa with different physiologies (e.g. between ecto- and endothermic see Kohler *et al*. 2012).

Stigmochelys pardalis exhibits some relatively rapid growth during the juvenile stage as seen by the patches of woven-fibred bone. The fibulae are an exception which grow a little more slowly as shown by the absence of woven-fibred bone and predominance of the slower growing parallel-fibred bone tissue. Parallel-fibred bone becomes the dominant bone tissue through early to mid-ontogeny. This represents relatively slow growth. However, radiating canals, indicating more rapid growth (de Margerie *et al*. 2004), were observed in the thickest areas of the cortex in the ulnae, tibiae and fibulae. These canals were found in both early and late sub-adults, but extended further towards the periphery in younger individuals and in certain cases appear to be associated with regions of muscle attachment to the bone. The presence of sub-reticular vascular canals deep in the cortex of the late sub-adult femur MVD-R 26 suggests that it grew more rapidly earlier in ontogeny (Stein *et al.* 2013). Primary osteons, indicating more rapid growth, are limited in most specimens and if present, are usually longitudinally-orientated and randomly distributed throughout the cortex. However, these primary osteons were found in circular rows in the inner and mid cortices in a number of specimens, but particularly in the sub-adult humeri and ulnae. According to Rieppel (2000) the presence of vascular tissue is expected in testudines. Although generally absent in lepidosaurs, vascular bone tissues are present in varanid lizards (de Buffrenil *et al*. 2008). They are also generally present in archosaurs (including extant crocodilians) (Padian *et al*. 2004). The presence of primary osteons in *S. pardalis*, indicates similar growth rates to these taxa.

Growth marks were observed in all sub-adult individuals. The deposition of growth marks within the cortex indicates that the growth of this species is affected by a number of factors that either result in a cessation of growth (LAG) or drastic decrease in the

growth rate of an individual (annuli). The type of growth mark (i.e. annuli or LAG) differs between element and ontogenetic stage.

The transition from parallel-fibred to relatively slower forming lamellar-zonal bone is typically found in older individuals and, together with a considerable decrease in vascularisation towards the periphery and increase in number and predominance of LAGs, indicates a decrease in growth later in life (Chinsamy 1990) and could possibly indicate that sexual maturity had been reached (Hutton 1986; Castanet 2004; Cerda & Chinsamy 2012; Kohler *et al.* 2012). The forelimb of early sub-adults display mostly annuli within their cortices whereas late sub-adults displayed LAGs. This, together with the transition from parallel-fibred to lamellar-zonal bone, suggests that growth dramatically decreased later in development because annuli indicate a decrease in the rate of bone growth whereas LAGs are a complete cessation of bone growth (Steyer *et al*. 2004).

An EFS was also observed in a number of different elements all of the same approximate ontogenetic stage. These are humerus MVD-R 5, radius MVD-R 14 and the fibulae MVD-R 2f and MVD-R 35, which are between 56% and 60% adult size suggesting that at this stage, growth decreased dramatically. An EFS indicates a mature ontogenetic stage and often the onset of sexual maturity (e.g. Horner *et al.* 2000 in dinosaurs; de Ricqlès *et al.* 2001 in basal birds; Straehl *et al.* 2013 in Xenathran mammals and Klein *et al.* 2009 in *Alligator mississippiensis*). The reproductive age of *S. pardalis* is 15 years (Orenstein 2012) so to test if the EFS in this species indicated the onset of sexual maturity, the age of individuals displaying an EFS was determined. This was done by counting the number of growth marks up to the EFS by overlaying smaller (younger) images of sections over larger (older) ones to account for the resorption of earlier growth marks. Approximately 10 growth marks are present prior to the EFS suggesting that growth reached an asymptote before sexual maturity was reached. However, it should be noted that given the difficulty in observing unclear growth marks and extensive resorption, this observation should be confirmed with a larger sample size in future studies.

Lamellar-zonal bone was more prevalent in the bones of the hind limb than the forelimb. These bones were considerably less vascularised than the forelimb, indicating relatively slower growth (Table 3). Their vascular canals were small, mainly limited to the inner and mid cortices and decreased considerably in size and number

towards the periphery, particularly in the tibiae and fibulae. As vascularisation is closely linked to growth rate, the lower vascularisation in the bones of the hind limb suggests that they grow more slowly than those of the forelimb. The humeri, radii and ulnae typically display annuli, indicating that growth did not cease completely during the unfavourable growing season, whereas the femur, tibia and fibula generally exhibit LAGs and even double LAGs, indicating that these bones stopped growing completely during the unfavourable growing season. This, together with a lower overall vascularisation and predominance of lamellar-zonal bone in the hind limb elements, suggests that the hind limb grew more slowly than those of the forelimb, possibly due to the method of locomotion seen in testudines. In chelonians, the humerus is longer than the femur (Gans 1973) indicating that the humerus has to grow faster to reach full size in relation to the size of the other fully grown bones.

Sharpey's fibres are filamentous structures indicating areas where tendons or ligaments attach to bone (Chen *et al.* 2006). They are present in a number of specimens, but the extent and depth to which the fibres penetrate the bone tissues differs between different elements and ontogenetic age. There is almost no evidence for attachment in the juveniles except in the femur MVD-R 11f where Sharpey's fibres are present. Interestingly, this is the same bone that contains a growth mark. These features suggest that despite its similar size to the other juveniles it may have been slightly more developed. Sharpey's fibres were observed less frequently in the humerus compared to other elements, possibly because this element tends to undergo more extensive resorption, thus destroying any evidence of soft tissue attachment.

5.2 Microanatomy and lifestyle

One of the most noticeable changes through the various developmental stages is the variation in cortical thickness and size of the medullary cavity. The cortices of juveniles are relatively thin and the bones contain open medullary cavities. During the early sub-adult stage the compact cortex thickens substantially while the medullary region becomes infilled with bony trabeculae and the actual main cavity occupies an even smaller portion of the bone. Relatively few resorption cavities surround the medullary cavity at this stage in most elements, but in the humerus there are a number of cavities particularly in the older early sub-adults. During the late sub-adult stage the thick cortex becomes extensively resorbed and the medullary cavity expands resulting in a large infilled medullary cavity surrounded by numerous resorption cavities and

secondary osteons in the peri-medullary region. Larger cavities are concentrated towards the centre of the medullary region and smaller cavities at the periphery resulting in a gradual transition zone between spongy and compact bone. Typically, larger animals display thicker cortices and smaller medullary regions (Canoville & Laurin 2009), but this is not the case here. The extensive resorption seen in *S. pardalis* has been previously observed in other testudines (Scheyer & Sander 2007; Nakajima *et al*. (2014). A large infilled medullary cavity has also been observed in testudine shell microstructure (Scheyer *et al*. 2014). Generally, a spongy infilled medullary cavity is found in aquatic species (such as cetaceans) where compact bone has been resorbed (de Buffrènil & Schoevaert 1988), but this feature has been observed in terrestrial turtle species as well. (Germain & Laurin 2005; Kriloff *et al.* 2008; Nakajima *et al*. 2014). The medullary cavities of turtles are never free of bony trabeculae, irrespective of lifestyle as seen in Scheyer *et al.* (2014). Houssaye (2014) also mentioned that this is particularly strange in terrestrial species whereas Nakajima *et al.* (2014) suggested it could be a result of their slow movement through an asymmetric gait used in locomotion. This asymmetric gate is seen in a number of species where the right and left limb display different patterns during movement. Alternatively, the trabecular infilling may be an attempt to provide extra support to the bones, which must support the extra weight of a shell during terrestrial locomotion.

Compactness has been used to infer the lifestyle of a variety of species through the use of Bone Profiler software to measure compactness (Germain & Laurin 2005; Canoville & Laurin 2010; Quemeneur *et al.* 2013; Amson *et al.* 2014). However, the use of compactness profiles to exemplify lifestyle in testudines seems to be relatively inaccurate as noted by Scheyer *et al*. (2014). This observation is supported by the results in this study (Table 5, 6) where all elements (apart from a few juveniles) indicate that *Stigmochelys pardalis* is an aquatic species when in fact, it is purely terrestrial. Nakajima *et al.* (2014) analysed the humeral microanatomy of several aquatic and terrestrial turtle species (MNHN-ZA-AC 2010-2 in Table 5) and found that the growth centre (and thickest part of the compact cortex) was often situated towards the proximal end of the bone and not at the mid-diaphysis level. They suggested that using a cross-section from the growth centre would result in a different lifestyle reading to that shown in Canoville & Laurin (2010) and Germain & Laurin (2005). This is indeed the case as the humeral lifestyle inference model from Canoville & Laurin (2010)

provides an amphibious and not an aquatic lifestyle reading for the *S. pardalis* humerus from the Nakajima *et al.* (2014) study.

However, the humeri of aquatic species appear to grow more asymmetrically than terrestrial species as the growth centre of many of the terrestrial species in the Nakajima *et al.* (2014) study was generally in the same region of the thickest cortex located in the mid-diaphysis. This is particularly the case in *Stigmochelys pardalis*. In this study, the thickest part of the compact cortex was found at the mid-diaphyseal level, the same region where Canoville & Laurin (2010) and Germain & Laurin (2005) would have analysed the *S. pardalis* specimen in their study. Thus, at least for this species, the mid-diaphyseal level does represent the area of thickest compact cortex and thus, the most accurate region for inferring lifestyle in Bone Profiler.

6. CONCLUSIONS

This is the first study to examine the inter-elemental and intra-elemental variation in the bone histology and microanatomy in a single species of testudine through ontogeny. The bone microstructure of *Stigmochelys pardalis* is indicative of a slow growing species with either parallel-fibred bone or even slower growing lamellar-zonal bone being the predominant bone tissues from fairly early on in ontogeny. An External Fundamental System, indicating a substantial decrease in growth rate, was observed in individuals of between 56-60% of the maximum known size for this species. Growth appears to asymptote several years prior to the onset of sexual maturity, but requires further confirmation due to the difficulty of counting unclear growth marks and the extensive resorption in the older individuals. If correct, however, the appearance of an EFS cannot be used as an indicator of sexual maturity as it is deposited approximately five years prior the onset of the active reproductive period.

Notable inter-elemental histovariation is present between the forelimb and hind limb bones of *S. pardalis*. The bone tissues of the forelimb elements are predominantly parallel-fibred with slightly higher vascularisation and interrupted by annuli, whereas the hind limb elements are less vascularised and reveal more lamellar-zonal bone interrupted by LAGs. These features indicate that the forelimb grew more quickly than the hind limb possibly as a result of the chelonian type of locomotion where the forelimb is slightly longer than the hind limb and thus, must grow more quickly to reach adult size.

Bone microanatomy revealed substantial primary bone deposition during early ontogeny with an onset of bone resorption and medullary cavity infilling during mid to late ontogeny. This caused the lifestyle inferences using traditional bone histological techniques to be inaccurate, as seen in previous studies. This shows that ontogeny and biomechanics do destroy the ecological signal in the bone microstructure of *S. pardalis* as there are major differences in the microanatomy between different age classes.

REFERENCES

Amprino R. 1947. La structure du tissue osseux envisage comme expression de differences dans a vitesse de l'accroissement. *Archives of Biology* 56: 315-330.

Amson E, De muizon C, Laurin M, Argot C, De buffrènil V. 2014. Gradual adaptation of bone structure to aquatic lifestyle in extinct sloths from Peru. *Proceedings of the Royal Society* 281: 20140192.

An YH, Martin KL. 2003. *Handbook of histology methods for bone and cartilage*. Humana Press, New Jersey, USA.

Aresco MJ, C Guyer. 1998. Efficacy of using scute annuli to determine growth histories and age of *Gopherus polyphemus* in southern Alabama. *Copeia* 1998:1094–1100.

Boycott RC, Bourquin O. 2000. *The South African tortoise book: A guide to Southern African tortoises, terrapins and turtles*. Southern Book publishers, Johannesburg, South Africa.

Branch B. *Field guide to snakes and other reptiles of southern Africa*. 1998. Struik Publishers (Pty) Ltd, Cape Town, South Africa.

Branch WR 1984. Preliminary observations on the ecology of the angulate tortoise (*Chersina angulata*) in the Eastern Cape Province, South Africa. *Amphibia-Reptilia* 5: 43-55.

Brown TK, Nagy KA, Morafka DJ. 2005. Costs of growth in tortoises. *Journal of herpetology* 39: 19-23.

Butcher MT, Blob RW. 2008. Mechanics of limb bone loading during terrestrial locomotion in river cooter turtles (*Pseudemys concinna*). *Journal of Experimental Biology* 211: 1187–1202.

Canoville A, Laurin M. 2009. Microstructural diversity of the humerus and lifestyle in lissamphibians. *Acta Zoologica* 90: 110-122.

Canoville A, Laurin M. 2010. Evolution of humeral microanatomy and lifestyle in amniotes, and some comments on palaeobiological inferences. *Biological Journal of the Linnean Society* 100: 384-406.

Carter D, Van der meulen M, Beaupre D. 1996. Mechanical factors in bone growth and development. *Bone* 18: 5-10.

Castanet J. 1994. Age estimation and longevity in reptiles. *Gerontology* 40: 174-192.

Cerda I, Chinsamy A. 2012. Biological implications of the bone microstructure of the Late Cretaceous Ornithopod dinosaur *Gasparinisaura cincosaltensis. Journal of Vertebrate Paleontology* 32: 355-368.

Chen H, Yao XF, Emura S, Shoumura S. 2006. Morphological changes of skeletal muscle, tendon and periosteum in the senescence-accelerated mouse (SAMP6): A murine model for senile osteoporosis. *Tissue and Cell* 38: 325-335.

Chinsamy A. 1990. Physiological implications of the bone histology of *Syntarsus rhodesiensis* (Saurischia: Theraposa). *Palaeontologica Africana* 27: 77-82.

Chinsamy A, Hurum JH. 2006. Bone microstructure and growth patterns of early mammals. *Acta Palaeontologica Polonica* 51: 325-338.

Chinsamy A, Valenzuela N. 2008. Skeletochronology of the endangered side neck turtle, *Podocnemis expansa*. *South African Journal of Science* 104: 311-314.

Crawford NG, Faircloth BC, Mccormack JE, Brumfield RT, Winker K, Glenn TC. 2012. More than 1000 ultra-conversed elements provide evidence that turtles are the sister group of archosaurs. *Biological Letters* 8: 783-786.

Currey JD. 1984. What should bones be designed to do? *Calcified Tissue International* 36: 7-10.

Currey JF. 2003. The many adaptations of bone. *Journal of Biomechanics* 36: 1487-1495.

Currey JD, Alexander RM. 1985. The thickness of tubular bones. *Journal of Zoology* 206:453–468.

Daniels SR, Hofmeyr ND, Henen BT, Baard EHW. 2010. Systematics and phylogeography of a threatened tortoise, the speckled padloper. *Animal conservation* 13: 237-246.

de Boef M, Larsson HCE. 2007. Bone microstructure: quantifying bone vascular orientation. *Canadian Journal of Zoology* 85: 63-70.

de Buffrènil V, Castanet J. 2000. Age estimation by skeletochronology in the Nile monitor (*Varanus niloticus*), a highly exploited species. *Journal of Herpetology* 34: 414-424.

de Buffrenil V, Schoevaert D. 1988. On how the periosteal bone of the Delphinid humerus becomes cancellous: Ontogeny of a histological specialisation. *Journal of morphology* 198: 149-164.

de Margerie E, Cubo J, Castanet, J. 2002. Bone typology and growth rate: testing and quantifying 'Amprinos rule' in the mallard (*Anas platyrhynchos*). *Comptes Rendus Biologies* 325: 221-230.

de Margerie E, Robin JP, Verrier D, Cubo J, Groscolas R, Castanet J. 2004. Assessing a relationship between bone microstructure and growth rate: a fluorescent study in the king penguin chick (*Aptenodytes patagonicus*). *The Journal of Experimental Biology* 207: 869-879.

de Ricqlès A. 1983. Cyclical growth in the long limb bones of a sauropod dinosaur. *Acta Palaeontologica Polonica* 28: 225–232

de Ricqlès AJ. 1976. On bone histology of fossil and living reptiles, with comments on its functional and evolutionary significance. In D'A. BELLAIRS, A. & COX, C. B. *Morphology and Biology of Reptiles*. London: Academic Press (pp. 123–150).

de Ricqlès A, Padian K, Horner JR. 2001. The bone histology of basal birds in phylogenetic and ontogenetic perspectives. In: GAUTHIER, J. & GALL, L.F. *New perspectives on the origin and early evolution of birds: Proceedings of the international symposium in honour of John H. Ostrum*. Peabody Museum of Natural History, Yale University, USA.

Erickson GM, Catanese III J, Keaveny TM. 2002. Evolution of the biomechanical properties of the femur. *The anatomical record* 268: 115-124.

Francillon-Vieillot H, de Buffrènil V, Castanet J, Geraudie J, Meunier FJ, Sire JY, Zylberberg, L, De ricqlès A. Microstructure and mineralisation of vertebrate skeletal tissues. In: CARTER, J.G. 1990. *Skeletal biomineralisation: Patterns, processes and evolutionary trends*. Van Nostrand Reinhold, New York. (Appendix 1)

Fritz U, Daniels SR, Hofmeyr MD, Gonzalez, J, Barrio-amoros, CL Siroky, P, Hundsdorfer, AK, Stuckas, H. 2010. *Journal of zoological systematics and evolutionary research* 48: 348-359.

Furrer SC, Hatt JM, Snell H, Marquez C, Honegger RE, Rübel A. 2004. Comparative study on the growth of juvenile Galapagos giant tortoises (*Geochelone nigra*) at the

Charles Darwin Research Station (Galapagos Islands, Ecuador) and Zoo Zurich (Zurich, Switzerland). *Zoo Biology* 23: 177-183.

Gans C. 1973. *Biology of the Reptilia*: 4 Morphology. Academic press Incorporated, London, UK.

Germain D, Laurin M. 2005. Microanatomy of the radius and lifestyle in amniotes (Vertebrata, Tetrapoda). *Zoologica Scripta* 34: 335-350.

Girondot M, Laurin M. 2003. Bone profiler: A tool to quantify, model and statistically compare bone section compactness profiles. *Journal of Vertebrate Paleontology* 23: 458-461.

Guarino FM, Lunardi S, Carlomagno M, Mazzotti S. 2003. A skeletochronological study of growth, longevity, and age at sexual maturity in a population of *Rana latastei* (Amphibia, Anura). *Journal of Biological Sciences* 28: 775-782.

Hill RV. 2005. Integration of morphological data sets for phylogenetic analysis of Amniota: the importance of integumentary characters and increased taxonomic sampling. *Systematic Biology* 54: 530–547.

Horner J, De ricqlès A, Padian K. 2000. Long bone histology of the Hadrosaurid dinosaur *Maiasaura peeblesorum*: Growth dynamics and physiology based on an ontogenetic series of skeletal elements. *Journal of Vertebrate Paleontology* 20: 115-129.

Houssaye A. 2012. Bone histology of aquatic reptiles: what does it tell us about secondary adaptation to an aquatic life? *Biological Journal of the Linnean Society* 108: 3-21.

Houssaye A. 2014. Advances in vertebrate palaeohistology: Recent progress, discoveries and new approaches. *Biological Journal of the Linnean Society* 112: 645-648.

Huttenlocker AK, Rega E. 2011. The paleobiology and bone microstructure of pelcosaurian-grade synapsids. In: CHINSAMY-TURAN, A. *The forerunners of mammals: radiation, histology and biology*. Indiana University Press, USA (pp 90-119).

Hutton JM. 1986. Age determination of living Nile crocodiles from the cortical stratification of bone. *Copeia* 2: 332–341.

Klein N, Scheyer T, Tutken T. 2009. Skeletochronology and isotopic analysis of a captive individual of *Alligator mississippiensis* Daudin, 1802. *Fossil Record* 12: 121-131.

Kriloff A, Germain D, Canoville A, Vincent P, Sache M, Laurin M. 2008. Evolution of bone microanatomy of the tetrapod tibia and its use in palaeobiological inference. *Journal of Evolutionary Biology* 21: 807–826.

Kohler M, Moratalla NM, Jordana X, Aanes R. 2012. Seasonal bone growth and physiology in endotherms shed light on dinosaur physiology. *Nature* 487: 358-361.

Laurin M, Canoville A, Germain D. 2011. Bone microanatomy and lifestyle: A descriptive approach. *Comptes Rendus Palevol* 10: 381-402.

Lee MSY. 1997. Pareiasaur phylogeny and the origin of turtles. *Zoological Journal of the Linnean Society* 120: 197-280.

Lee MSY. 2013. Turtle origins: insights from phylogenetic retrofitting and molecular scaffolds. *Journal of Evolutionary Biology* 26: 2729–2738.

Lyson TR, Bever GS, Bhullar BAS, Joyce WG, Gauthier JA. 2010. Transitional fossils and the origin of turtles. *Biology Letters* 6: 830–833.

Lyson TR, Bever GS, Scheyer TM, Hsiang A, Gauthier JA. 2013. Evolutionary origin of turtle shell. *Current Biology* 23: 1–7.

Lyson TR, Schachner ER, Botha-brink J, Scheyer TM, Lambertz M, BEVER GS, RUBIDGE BS, DEQUEIRNOZ K. 2014. Origin of the unique ventilatory apparatus of turtles. *Nature communications* 5: 1-11.

Lyson TR, Sperling EA, Heimberg AM, Gauthier JA, King BL, Peterson KJ. 2011. MicroRNAs support a turtle and lizard clade. *Biology Letters* 8: 104–107.

Mason MC, Weatherby CA. 1995. Home Range of *Geochelone pardalis* and *Chersina angulata*: 2 Sympatric Genera in the Eastern Cape, South Africa. Fourth HAA Symposium on African Herpetology, St. Lucia. Kwa Zulu-Natal (taken from McMaster and Downs 2009).

McMaster MK. 2001. The Status and Ecology of the Leopard Tortoise *Geochelone pardalis* on Farmland in the Nama-Karoo. M.Sc. Thesis, University of Natal, Pietermaritzburg, South Africa.

Mcmaster MK, Downs CT. 2006. Does seasonal and behavioural differences in the use of refuges by the leopard tortoise (*Geochelone pardalis*) favour passive thermoregulation? *Herpetologica* 62: 37-46.

Mcmaster MK, Downs CT. 2009. Home range and daily movement of leopard tortoises (*Stigmochelys pardalis*) in the Nama-Karoo, South Africa. *Journal of Herpetology* 43: 561-569.

Miller E, Fowler ME. 2015. *Fowler's zoo and wild animal medicine*. Volume 8. Elsevier Saunders, Missouri, USA.

Misawa Y, Matsui M. 2009. Age determination by skeletochronology of the Japanese salamander *Hynobius kimurae* (Amphibia, Urodela). *Zoological Science* **16**: 845-851.

Nagashima H, Kuraku S, Uchida K, Ohya YK, Narita Y, Kuratani S. 2007. On the carapacial ridge in turtle embryos: its developmental origin, function and the Testudines n body plan. *Development* 134: 2219–2226.

Nakajima Y, Hirayama R, Endo H. 2014. Turtle microanatomy and its relationship to lifestyle. *Biological Journal of the Linnean Society* 112: 719-734.

Orenstein R. 2012. *Turtles, tortoises and terrapins*: *A natural history*. Firefly Books Ltd, USA.

Padian K, de Ricqlès A, J Horner. 2001 Dinosaurian growth rates and bird origins. *Nature* 412: 405-408.

Padian K, Horner JR, de Ricqlès A. 2004. Growth in small dinosaurs and pterosaurs: the evolution of archosaurian growth strategies. *Journal of Vertebrate Paleontology* 24: 555-571.

Patterson RW, Boycott RC, Morgan DR. 1989. Reproduction and husbandry of the leopard tortoise (*Geochelone pardalis*) in an alien habitat. The *Journal of Herpetological Association* 36: 75-75.

Quemeneur S, de Buffrènil V, Laurin M. 2013. Microanatomy of the amniote femur and inference of lifestyle in limbed vertebrates. *Biological Journal of the Linnean Society* 109: 644-655.

Ray S, Chinsamy A. 2004. *Diictodon feliceps* (Therapsida, Dicynodontia); bone histology, growth and biomechanics. *Journal of vertebrate Paleontology* 24: 180-194.

Reisz RR, Laurin M. 1991. Owenetta and the origin of turtles. *Nature* 349: 324–326.

Rieppel O. 2000. Turtles as diapsid reptiles. *Zoologica Scripta* 29: 199-212.

Rieppel O, Debraga M. 1996. Turtles as diapsid reptiles. *Nature* 384: 453–455.

Rose W. 1950. *The reptiles and amphibians of southern Africa*. Maskew Miller, Cape Town, South Africa.

Ross MH, Pawlina W. 2011. *Histology: A text and atlas*, 6th edition. Lippincott Williams and Wilkins, Baltimore.

Scheyer TM, Sander PM. 2007. Shell bone histology indicates terrestrial paleoecology of basal turtles. *Proceedings of the royal society* 274: 1885-1893.

Scheyer TM, Sander PM, Joyce WG, Bohme W, Witzel U. 2007. A plywood structure in the shell of fossil and living soft shelled turtles (Trionychidae) and its evolutionary implications. *Organisms, Diversity and Evolution* 7: 136-144.

Scheyer TM, Danilov IG, Sukhanov VB, Syromyatnikova EV. 2014. The shell bone histology of fossil and extant marine turtles revisited. *Biological Journal of the Linnean Society* 112: 701–718.

Schmidt KP, Inger RF. 1957. *Living reptiles of the world*. Hamish Hamilton Ltd, London, United Kingdom.

Seebacher F, Sparrow J, Thompson MB. 2004. Turtles (*Chelodina longicollis*) regulate muscle metabolic enzyme activity in response to seasonal variation in body temperature. *Journal of Comparative Physiology B* 174: 205–210.

Shaffer HB, Minx P, Warren DE, Shedlock AM, Rhomson RC, Valenzuela N, Abramyan J, Amemiya CT, Badenhorst D, Biggar KK, Borchert GM, Botka CW, Bowden RMM, Baun ELL Bronikowski AM, Bruneau BG, Buck LT, Capel B, Castoe TA, Czerwinski M, Delehaunty KD, Edwards SV, Fronick CC, Fujita MK, Fulton L, Graves TA, Green RE, Haerty W, Hariharan R, Hernandez O, Hillier LW, Hollowat AK, Janes D, Janzen FJ, Kandoth C, Kong L, De koning APJ, Li Y, LIterman R, Mcgaugh SE, Mork L, O'laughlin M, Paitz RT, Pollock DD, Ponting P, Radhakrishnan R, Raney BJ, Richman JM, St john J, Schwartz T, Sethuraman A, Spinks PQ, Storey KB, Thane N, Vinar T, Zimmerman LM, Warren WC, Mardis ER, Wilson RK. 2013. The western painted turtle genome, a model for the evolution of extreme physiological adaptations in a slowly evolving lineage. *Genome Biology* 14: 1-22.

Shearman RM, Burke AC. 2009. The lateral somatic frontier in ontogeny and phylogeny. *Journal of experimental zoology Part B: Molecular and developmental evolution* 312: 603-612.

Simang A, Cunningham PL, Henen BT. 2010. Colour selection by juvenile leopard tortoises (*Stigmochelys pardalis*) in Namibia. *Journal of herpetology* 44: 327-331.

Stein, M Hayashi S, Sander MP. 2013. Long bone histology and growth patterns in Ankylosaurs: Implications for life history and evolution. *Plos one* 8: 1-13.

Steyer JS, Laurin M, Castanet J, De Ricqlès A. 2004. First histological and skeletochronological data on temnospondyl growth: palaeoecological and palaeoclimatological implications. *Palaeogeography, Palaeoclimatology, Palaeoecology* 206: 193-201.

Straehl FR, Scheyer TM, Forasiepi AM, Macphee RD, Sanchez-villagra MR. 2013. Evolutionary patterns of bone histology and bone compactness in Xenarthran mammal long bones. *Plos one* 8: 1-19.

Taylor M. 2000. Functional significance of bone ballast in the evolution of buoyancy control strategies by aquatic tetrapods. *Historical Biology* 14: 15–31.

Tucker AD. 1997. Validation of skeletochronology to determine age of freshwater crocodiles (*Crocodylus johnst*oni). *Marine and Freshwater Research* 48: 343-351.

Wall WP. 1983. The correlation between high-limb density and aquatic habitats in recent mammals. *Journal of Paleontology* 57: 197-207.

Zardoya R, Meyer, A. 2001. The evolutionary position of turtles revised. *Naturwissenschaften* 88: 193-200.

APPENDICES

Appendix 1: The complete growth mark count and corresponding age class for all forelimb elements (J: juvenile; ESA: early sub-adult; LSA: late sub-adult); (LAG: line of arrested growth; EFS: external fundamental system).

Accession #	Element	Age Class	Growth marks
MVD-R 12b	Humerus	J	-
MVD-R 12a	Humerus	J	-
MVD-R 11b	Humerus	J	-
MVD-R 11a	Humerus	J	-
MVD-R 10a	Humerus	ESA	3 single annuli
MVD-R 9	Humerus	ESA	3 single annuli
MVD-R 8	Humerus	ESA	4 single annuli
MVD-R 7	Humerus	ESA	Double lag, 4 single annuli
MVD-R 6	Humerus	ESA	2 annuli
MVD-R 5	Humerus	LSA	9 single annuli, 1 single LAG
MVD-R 4	Humerus	LSA	5 annuli
MVD-R 3	Humerus	LSA	5 single LAGs (EFS)
MVD-R 2a	Humerus	LSA	5 single annuli
MVD-R 1	Humerus	LSA	6 single LAGs
MNHN-ZA-AC 2010-2	Humerus	A	-
MVD-R 12c	Radius	J	-
MVD-R 18a	Radius	J	-
MVD-R 17	Radius	ESA	5 single LAGS
MVD-R 16	Radius	LSA	5 single LAGS
MVD-R 15	Radius	LSA	4 single annuli with single LAG within
MVD-R 14	Radius	LSA	4 single LAGs (EFS)
MVD-R 13	Radius	LSA	3 single LAGs
MVD-R 2b	Radius	LSA	1 single LAG,1 double annuli and 2 single annuli
MVD-R 12e	Ulna	J	-
MVD-R 12d	Ulna	J	-
MVD-R 18b	Ulna	J	-
MVD-R 10b	Ulna	ESA	1 single annuli
MVD-R 23	Ulna	ESA	5 single annuli
MVD-R 22	Ulna	ESA	3 single annuli, 2 single LAGs
MVD-R 21	Ulna	LSA	2 single LAGs
MVD-R 20	Ulna	LSA	7 single annuli
MVD-R 19	Ulna	LSA	3 single LAGs, 1 double lag,
MVD-R 2c	Ulna	LSA	2 single annuli, 1 single LAG

Appendix 1 continued: The complete growth mark count and corresponding age class for all hind limb elements (J: juvenile; ESA: early sub-adult; LSA: late sub-adult); (LAG: line of arrested growth; EFS: external fundamental system).

Accession #	Element	Age Class	Growth marks
MVD-R 12g	Femur	J	-
MVD-R 12f	Femur	J	-
MVD-R 11c	Femur	J	hatchling line
MVD-R 10c	Femur	ESA	2 single LAGs
MVD-R 28	Femur	ESA	6 double LAGs
MVD-R 27	Femur	LSA	2 single LAGs, one double LAG
MVD-R 26	Femur	LSA	4 single annuli
MVD-R 25	Femur	LSA	1 double LAG, 2 single LAGs
MVD-R 24	Femur	LSA	4 single LAGs, 2 double LAGs
MVD-R 2d	Femur	LSA	2 single LAGs
MVD-R 12i	Tibia	J	-
MVD-R 12h	Tibia	J	-
MVD-R 11e	Tibia	J	-
MVD-R 11d	Tibia	J	-
MVD-R 33	Tibia	ESA	5 single LAGs
MVD-R 32	Tibia	LSA	5 single annuli
MVD-R 31a	Tibia	LSA	triple annulus, two single annuli and 2 double LAGs
MVD-R 30	Tibia	LSA	double annuli, 1 single LAG, and 2 double LAGs
MVD-R 2e	Tibia	LSA	1 double LAG, 5 single LAGs
MVD-R 29	Tibia	LSA	6 single LAGs
MVD-R 12k	Fibula	J	-
MVD-R 12j	Fibula	J	-
MVD-R 11f	Fibula	J	-
MVD-R 36	Fibula	ESA	6 single LAGs
MVD-R 31b	Fibula	LSA	double annuli, single LAG and double LAG
MVD-R 35	Fibula	LSA	8-10 single LAGs
MVD-R 34	Fibula	LSA	4 single LAGs, (EFS)
MVD-R 2f	Fibula	LSA	8 single LAGs (EFS)

Appendix 2: The evidence of muscle attachment for the forelimb elements.

Accession #	Element	Evidence of attachment
MVD-R 12b	Humerus	-
MVD-R 12a	Humerus	-
MVD-R 11b	Humerus	-
MVD-R 11a	Humerus	-
MVD-R 10a	Humerus	-
MVD-R 9	Humerus	-
MVD-R 8	Humerus	Sharpey's fibres
MVD-R 7	Humerus	-
MVD-R 6	Humerus	-
MVD-R 5	Humerus	-
MVD-R 4	Humerus	-
MVD-R 3	Humerus	-
MVD-R 2a	Humerus	-
MVD-R 1	Humerus	Sharpey's fibres
MNHN-ZA-AC 2010-2	Humerus	-
MVD-R 12c	Radius	-
MVD-R 18a	Radius	-
MVD-R 17	Radius	Sharpey's fibres
MVD-R 16	Radius	Sharpey's fibres
MVD-R 15	Radius	Sharpey's fibres
MVD-R 14	Radius	-
MVD-R 13	Radius	-
MVD-R 2b	Radius	Sharpey's fibres
MVD-R 12e	Ulna	-
MVD-R 12d	Ulna	-
MVD-R 18b	Ulna	-
MVD-R 10b	Ulna	Sharpey's fibres
MVD-R 23	Ulna	Sharpey's fibres
MVD-R 22	Ulna	-
MVD-R 21	Ulna	Sharpey's fibres
MVD-R 20	Ulna	Sharpey's fibres
MVD-R 19	Ulna	Sharpey's fibres
MVD-R 2c	Ulna	Sharpey's fibres

Appendix 2 continued: The evidence of muscle attachment of all hind limb elements.

Accession #	Element	Evidence of attachment
MVD-R 12g	Femur	-
MVD-R 12f	Femur	-
MVD-R 11c	Femur	Sharpey's fibres
MVD-R 10c	Femur	Sharpey's fibres
MVD-R 28	Femur	Sharpey's fibres
MVD-R 27	Femur	-
MVD-R 26	Femur	Sharpey's fibres
MVD-R 25	Femur	Sharpey's fibres
MVD-R 24	Femur	-
MVD-R 2d	Femur	-
MVD-R 12i	Tibia	-
MVD-R 12h	Tibia	-
MVD-R 11e	Tibia	-
MVD-R 11d	Tibia	-
MVD-R 33	Tibia	-
MVD-R 32	Tibia	Sharpey's fibres
MVD-R 31a	Tibia	Sharpey's fibres
MVD-R 30	Tibia	Sharpey's fibres
MVD-R 2e	Tibia	-
MVD-R 29	Tibia	Sharpey's fibres
MVD-R 12k	Fibula	-
MVD-R 12j	Fibula	-
MVD-R 11f	Fibula	Sharpey's fibres
MVD-R 36	Fibula	-
MVD-R 31b	Fibula	Sharpey's fibres
MVD-R 35	Fibula	Sharpey's fibres
MVD-R 34	Fibula	Sharpey's fibres
MVD-R 2f	Fibula	Sharpey's fibres

Appendix 3: A few of the selected compactness profiles highlighting the changes through ontogeny. 1: Juvenile; 2: Early sub-adult; 3: Late sub-adult. A: Humeri; B: Radii; C: Ulnae; D: Femuri; E: Tibiae; F: Fibulae.

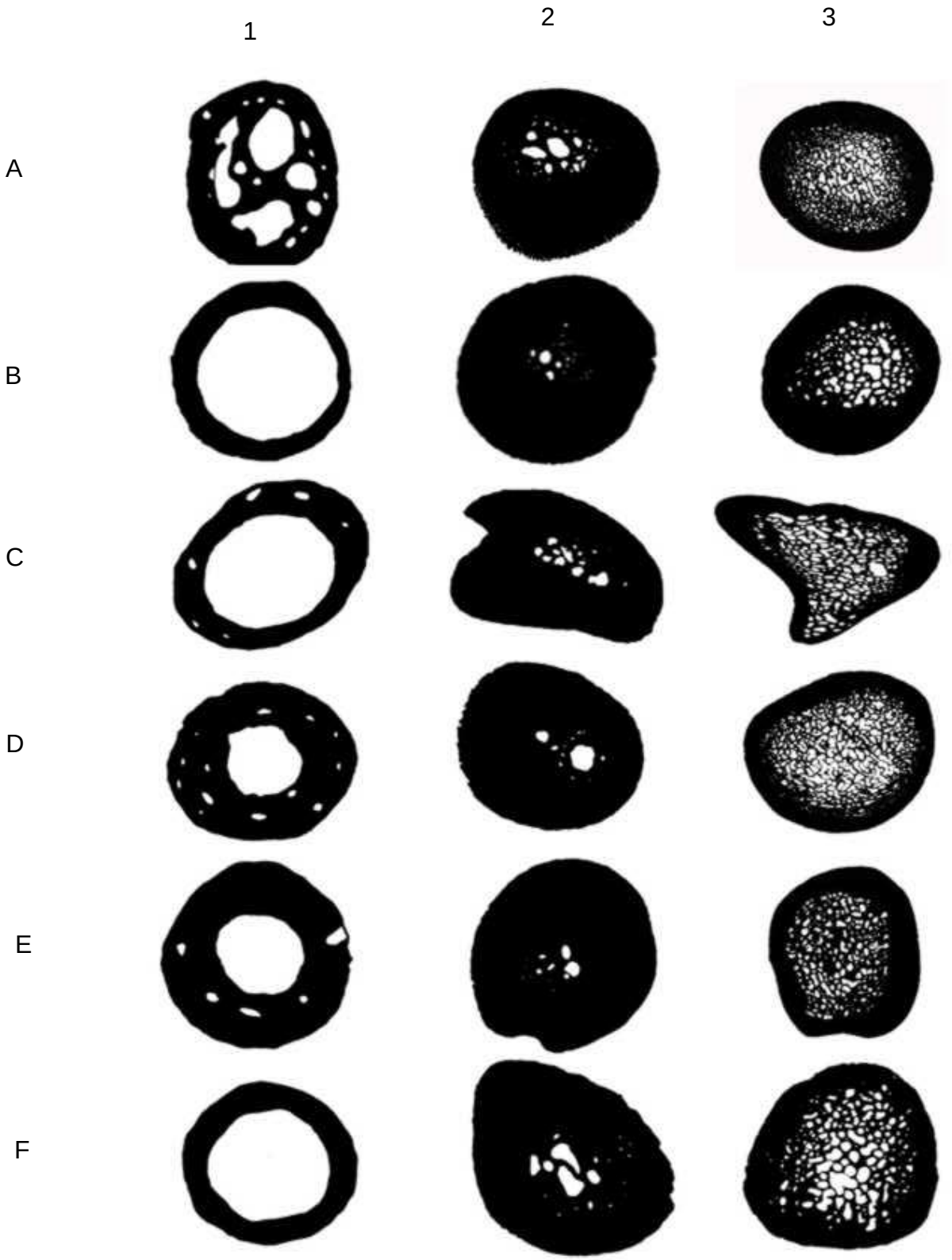

Appendix 4: The p-values for the compactness profiles comparison (A) together with the p-values for the K value (B) resulting in the null hypothesis being accepted and indicating almost no differences between the elements. Matching colours indicate the same test that was run twice (For example: Ulna vs Femur and Femur vs Ulna; both have p values of 0.2).

A

	Humeri	Radii	Ulnae	Femora	Tibiae	Fibulae
Humeri	x	0.5	0.66	0.24	0.53	0.73
Radii	0.72	x	0.5	0.2	0.64	0.64
Ulnae	0.66	0.5	x	0.48	0.8	1
Femora	0.24	0.2	0.48	x	0.94	0.59
Tibiae	0.53	0.4	0.8	0.94	x	0.66
Fibulae	0.73	0.64	1	0.59	0.66	x

B

	Humeri	Radii	Ulnae	Femora	Tibiae	Fibulae
Humeri	x	0.97	0.64	0.26	0.46	0.83
Radii	0.97	x	0.57	0.27	0.57	0.96
Ulnae	0.64	0.57	x	0.63	0.8	0.63
Femora	0.26	0.27	0.63	x	0.94	0.27
Tibiae	0.46	0.57	0.8	0.94	x	0.46
Fibulae	0.83	0.96	0.63	0.27	0.46	x